

**STUDIES ON SURFACE MODIFICATIONS OF MATERIALS FOR TISSUE
ENGINEERING APPLICATIONS**

by

Chung-Jen Hsieh

B.S. in Chemical Engineering, National Taiwan University of Science and Technology,
Taiwan, 2000

M.S. in Chemical Engineering, National Tsing Hua University, Taiwan, 2002

Submitted to the Graduate Faculty of
School of Engineering in partial fulfillment
of the requirements for the degree of
Master of Science

University of Pittsburgh

2006

UNIVERSITY OF PITTSBURGH

SCHOOL OF ENGINEERING

This thesis was presented

by

Chung-Jen Hsieh

It was defended on

March 28, 2006

and approved by

Dr. Kacey G. Marra, Professor, University of Pittsburgh Medical Center

Dr. Ian Nettleship, Associate Professor, Materials Science and Engineering Department

Thesis Advisor: Dr. Pradeep P. Fulay, Professor, Materials Science and Engineering

Department

Copyright © by Chung-Jen Hsieh

2006

STUDIES ON SURFACE MODIFICATIONS OF MATERIALS FOR TISSUE ENGINEERING APPLICATIONS

Chung-Jen Hsieh, M.S.

University of Pittsburgh, 2006

Peripheral nerve injury (PNI) is a serious health problem for the society today. It affects 2.8% of trauma patients, many of whom acquire life-long disability. Approximately 360,000 people in the United States suffer from upper extremity paralytic syndromes yearly. Two current clinical approaches: end-to-end surgical reconnection and autologous nerve graft are used to cure the patients suffered PNI. However, both approaches have some disadvantages such as loss functions of donor site and two surgeries, at least, are needed. Therefore, various synthetic materials for bridging the injured nerve gap and surface modifications for enhancing the outgrowth of nerve cells have been reported. The objectives of this research were: 1) To investigate ways of modifying the surface of some biomaterials; 2) To investigate the influence of surface properties, such as the types of functional groups, wettability, and surface morphology on the cell culture; 3) To investigate the possibility of differentiating between male and female stem cells in the cells via surface modification.

Three materials, mica, glass, and polycaprolactone (PCL) were used as substrates in this study. Mica substrates were prepared and modified using PAMAM dendrimer polymers. The optical microscopy images showed that neurites started to sprout and considerable neuron cell adhesion on the mica substrates coated with multilayer PAMAM dendrimers but uncoated and monolayer coated mica substrates showed no cell adhesion after a 12 hr cell culture. Similarly, the surfaces of gold and titanium coated glass substrates were modified so that the surface was terminated with different functional groups. Atomic force microscopy (AFM) measurements showed that the average surfaces roughness increased from 4.663 to 5.328 nm after gold-coated surface reacted with 1-dodecanethiol. The average surface roughness (R_a) increased after gold-coated surface reacted with 11-mercaptoundecanoic acid ($R_a = 0.190$ nm) and 11- mercapto-1-undecanol($R_a = 0.394$ nm). The contact angle (θ) increased from $76.56 \pm 4.6^\circ$ to $107.43 \pm 4.6^\circ$

after gold-coated surface reacted with 1-dodecanethiol. The surfaces became more hydrophilic after gold-reaction with 11-mercaptoundecanoic acid ($\theta=37.24 \pm 2.2^\circ$) and 11-mercapto-1-undecanol ($\theta= 28.42 \pm 2.0^\circ$). Based on the cell culture data on PCL, the carboxyl terminated surface showed more cell attachment than methyl and hydroxyl terminated surface. The numbers of cells adhering to each modified surface after a 12 hr cell culture in an ascending order is as follow: $\text{NH}_2 < \text{COOH} < \text{CH}_3$, Control PCL. In the surface modifications we investigated, the behavior of male and female adult fat derived stem cells was essentially identical.

DESCRIPTORS

| | |
|----------------------------|-------------------------|
| Adipose-derived stem cells | Advancing contact angle |
| Cell attachments | Cell culture |
| Contact angles | Glass coverslips |
| Hysteresis | Mica |
| Neuron | PC12 cells |
| Polycaprolactone | Receding Contact angle |

ACKNOWLEDGEMENTS

I wish to thank my thesis advisor, Dr. Pradeep P. Fulay, for his patience, guidance, and encouragement throughout this thesis. I am grateful Dr. Kacey G. Marra and Dr. John A. Barnard for all their help, interest and discussions. This thesis was made possible with all their help. I would like to thank Dr. Nettleship for his interest and discussions.

I am thankful to Mr. Albert Stewart, Candace Brayfield, Fengting (Frank) Xu for and Renee all their help, support, assistance and friendship.

The University of Pittsburgh, Department of Mechanical Engineering and the University of Pittsburgh Medical Center are also acknowledged for letting us use their sputtering machine and cell culture equipment, respectively.

I want to dedicate this work to my mother Sue-Gi, Yung and my father Ming-Yung Hsieh and my sister Huai-Yuang Hsieh and Huai-Jin Hsieh for their inspiration, patience, and encouragement throughout my graduate study.

TABLE OF CONTENTS

| | |
|--|-----------|
| 1.0 INTRODUCTION..... | 1 |
| 1.1 INTRODUCTION..... | 1 |
| 1.2 CELL INTRECTIONS WITH FOREIGN SURFACES | 5 |
| 2.0 BACKGROUND | 8 |
| 2.1 SYNTHETIC MATERIALS | 8 |
| 2.1.1 Poly (Glycolic Acid) (PGA) | 9 |
| 2.1.2 Poly (Lactic Acid) (PLA) | 10 |
| 2.1.3 Poly (Latic-co-Glycolic Acid) (PLGA) | 10 |
| 2.1.4 Poly (caprolactone) (PCL)..... | 13 |
| 2.1.5 Polyvinylidene fluoride (PVDF) | 14 |
| 2.2 SURFACE MODIFICATIONS..... | 16 |
| 2.2.1 Gradient-guided neurite outgrowth | 18 |
| 2.2.2 Surface modulation by self-assembled monolayers (SAMs) of alkanethiols . | 21 |
| 2.2.3 Surface modification via aminolysis..... | 21 |
| 2.2.4 Plasma surface modification | 23 |
| 2.2.5 Laser surface modification..... | 26 |
| 2.3 SCAFFOLD FABRICATION TECHNIQUES | 27 |

| | |
|--|-----------|
| 3.0 EXPERIMENTAL PROCEDURES | 30 |
| 3.1 RESEARCH OBJECTIVES..... | 30 |
| 3.2 PAMAM DENDRIMERS ON MICA SUBSTRATES..... | 31 |
| 3.2.1 Preparing mica substrates coated with monolayer/multilayer dendrimers .. | 34 |
| 3.3 SURFACE MODIFICATION OF GLASS SUBSTRATES | 34 |
| 3.4 POLYCAPROLACTONE(PCL) SUBSTRATES | 38 |
| 3.4.1 Aminolysis of poly(caprolactone) | 38 |
| 3.4.2 Attachment of dodecanedicarboxylic acid/ tetradecanoic acid to the aminolyzed PCL surface | 39 |
| 3-5 CELL CULTURE EXPERIMENTS | 40 |
| 3-6 CONTACT ANGLE MEASUREMENT..... | 41 |
| 4.0 RESULTS AND DISCUSSIONS..... | 47 |
| 4.1 NEURON CELL OUTGROWTH ON MODIFIED MICA SURFACE | 47 |
| 4.2 CELL CULTURE ON SURFACE OF MODIFIED GLASS SUBSTRATES | 50 |
| 4.2.1 Atomic force microscopy (AFM) analysis..... | 50 |
| 4.2.2 Scanning electron microscopy | 56 |
| 4.2.3 Wettability of modified glass surfaces | 59 |
| 4.2.4 Cell culture analysis on modified surfaces | 62 |
| 4.2.5 Discussion of results on cell culture on modified glass surface..... | 65 |

| | |
|--|------------|
| 4.3 CELL CULTURE ON MODIFIED POLYCAROLACTONE (PCL) | |
| SUBSTRATES | 66 |
| 4.3.1 Scanning electron microscopy analysis..... | 66 |
| 4.3.2 Surface energy analysis | 78 |
| 4.3.3 Cell culture analysis..... | 84 |
| 5.0 SUMMARY AND CONCLUSIONS | 90 |
| 6.0 SUGGESTION FOR FUTURE WORK..... | 93 |
| APPENDIX A GLOSSARY | 94 |
| APPENDIX B FUNDAMENTAL PROCEDURES AND KNOWLEDGE FOR | |
| CELL CULTURE | 100 |
| APPENDIX C FORMULAS AND PARAMETERS APPEARED IN AFM | |
| IMAGES | 107 |
| BIIBLIOGRAPHY..... | 108 |

LIST OF TABLES

| Table Number | Page |
|---|-------------|
| Table 1-1 Nerve grafts and nerve conduit materials..... | 3 |
| Table 1-2 Requirements of materials used as a nerve guide..... | 4 |
| Table 2-1 Surface modification methods | 18 |
| Table 4-1 Contact angle and the image of water drops (the volume of each water drop is $0.3 \mu\text{l}$) on the..... | 60 |
| Table 4-2 The image of water drops(the volume of each water drop is $0.3 \mu\text{l}$) on the modified gold-coated surface after dipping in PBS for 12 hr | 61 |

LIST OF FIGURES

| Figure Number | Page |
|---|------|
| Figure 1-1 Cell interactions with foreign surfaces are mediated by integrin receptors with adsorbed adhesion proteins that sometimes change their biological activity when they adsorb..... | 6 |
| Figure 1-2 Progression of anchorage-dependent mammalian cell adhesion. | 7 |
| Figure 2-1 Properties of the ideal nerve guidance channel | 9 |
| Figure 2-2 Structures of (a) PGA, (b) PLA, (c) PLGA and (d) PCL | 12 |
| Figure 2-3 Schematic view of operative procedure. (A) The mesh is placed underneath the nerve and secured with sutures. (B) The nerve is resected. (C) The mesh is shaped like a tube around the nerve. (D) The tube is closed by sutures | 12 |
| Figure 2-4 Schematic of corona poling system | 15 |
| Figure 2-5 The closed looking of corona tip and sample | 16 |
| Figure 2-6 Schematic illustration of two-step grafting of PAA onto polymeric substrates..... | 20 |
| Figure 2-7 (a) Microscopic image of C17.2 cells on a –COOH gradient surface after Ar plasma treatment. (b) Schematic illustration of a cell on a gradient substrate surface | 20 |
| Figure 2-8 The schematic representation of aminolysis and further immobilization of biomolecules on polycaprolactone membrane | 22 |
| Figure 2-9 Schematic of plasma surface modification within the plasma reactor | 24 |

| | |
|--|----|
| Figure 2-10 Schematic of the reaction mechanisms of plasma surface modifications. | 25 |
| Figure 2-11 Schematic diagram of the petri dish arrangement used to cast the polymer films. SA denotes surface–air interface; SG denotes surface-glass interface | 29 |
| Figure 3-1 Schematic illustration of the expected charge state of the mica surface and dendrimer domains. | 32 |
| Figure 3-2 The Chemical structure and molecular structure of PAMAM from generation zero to generation four. | 33 |
| Figure 3-3 Sputtering system schematic. | 35 |
| Figure3-4 The image of sputtering system (ISE-OE-PVD-3000 DC AND RF MAGNETRON SPUTTERING MN 500 SYSTEM)..... | 36 |
| Figure 3-5 Schematic of surface modification of glass coverslips. | 37 |
| Figure 3-6 Schematic of surface modification of PCL disk. | 40 |
| Figure 3-7 The OM image of the PCL substrate after 12 hr cell culture. | 41 |
| Figure 3-8 The image of contact angle measurement system, DSA100 (KRÜSS GmbH). | 42 |
| Figure 3-9 Contact angle formation on a solid surface according to Yung’s theory. | 43 |
| Figure 4-1 Optical microscopy image of 12 hr neuron cell culture on mica substrate coated with multi-layers of PAMAMA dendrimers..... | 48 |
| Figure 4-2 Optical microscopy image of 12 hr neuron cell culture on mica substrate coated with multi-layers of PAMAMA dendrimers..... | 49 |
| Figure 4-3 AFM image of glass coverslip coated with 10 nm titanium (bottom layer) and 20 nm gold (upper layer) (a) the cross-section image; (b) 2-D image; (c) the related data of surface roughness and (d) 3-D image. | 52 |
| Figure 4-4 AFM image of gold-coated glass coverslip after surface has been passivated with 1-dodecanethiol. (a) the cross-section image; (b) 2-D image; (c) the related data of surface roughness and (d) 3-D image. | 53 |

| | |
|--|-----------|
| Figure 4-5 AFM image of gold-coated glass coverslip after surface has been passivated with 11-mercaptoundecanoic acid. (a) the cross-section image; (b) 2-D image; (c) the related data of surface roughness and (d) 3-D image. | 54 |
| Figure 4-6 AFM image of gold-coated glass coverslip after surface has been passivated with 11-mercapto-1-undecanol. (a) the cross-section image; (b) 2-D image; (c) the related data of surface roughness and (d) 3-D image. | 55 |
| Figure 4-7 SEM images of gold-coated glass coverslips (A) non-modified surface and surface modified by (B) 1- dodecanethiol, (C) 11-mercaptoundecanoic acid and (D) 11-mercapto-1-undecanol at lower magnification..... | 57 |
| Figure 4-8 SEM images of gold-coated glass coverslips (A) non-modified surface and surface modified by (B) 1- dodecanethiol, (C) 11-mercaptoundecanoic acid and (D) 11-mercapto-1-undecanol at higher magnification. | 58 |
| Figure 4-9 Female (age 35) adipose-derived stem cells (ASC) cultured on modified gold-coated glass coverslips for 12 hr. | 63 |
| Figure 4-10 Male (age 33) adipose-derived stem cells (ASC) cultured on modified gold-coated glass coverslips for 12 hr. | 64 |
| Figure 4-11 SEM images of modified PCL substrates using THF as the solvent (A) non-modified PCL surface; (B) PCL surface after aminolization and PCL surface further reacted with (C) tetradecanoic acid and (D) dodecanedicarboxylic acid at lower magnification.. | 71 |
| Figure 4-12 SEM images of modified PCL substrates using THF as the solvent (A) non-modified PCL surface; (B) PCL surface after aminolization and PCL surface further reacted with (C) tetradecanoic acid and (D) dodecanedicarboxylic acid at higher magnification. | 72 |
| Figure 4-13 SEM images of modified PCL substrates using acetone as the solvent (A) non-modified PCL surface; (B) PCL surface after aminolization and PCL surface further reacted with (C) tetradecanoic acid and (D) dodecanedicarboxylic acid at lower magnification. | 73 |
| Figure 4-14 SEM images of modified PCL substrates using acetone as the solvent (A) non-modified PCL surface; (B) PCL surface after aminolization and PCL surface further reacted with (C) tetradecanoic acid and (D) dodecanedicarboxylic acid at higher magnification. | 74 |

| | |
|--|-----|
| Figure 4-15 SEM images of modified PCL substrates using dichloromethane as the solvent (A) non-modified PCL surface; (B) PCL surface after aminolization and PCL surface further reacted with (C) tetradecanoic acid and (D) dodecanedicarboxylic acid at lower magnification. | 75 |
| Figure 4-16 SEM images of modified PCL substrates using dichloromethane as the solvent (A) non-modified PCL surface; (B) PCL surface after aminolization and PCL surface further reacted with (C) tetradecanoic acid and (D) dodecanedicarboxylic acid at higher magnification. | 76 |
| Figure 4-17 SEM images of modified PCL/Dichloromethane surface after the surface aminolization and further react with tetradecanoic acid. | 77 |
| Figure 4-18 The surface advancing contact angle (ACA) of PCL/THF, PCL/ Acetone and PCL/Dichloromethane substrates..... | 80 |
| Figure 4-19 The surface receding contact angle (RCA) of PCL/THF, PCL/ Acetone and PCL/Dichloromethane substrates..... | 81 |
| Figure 4-20 The contact angle hystereses (ACA-RCA) of PCL/THF, PCL/ Acetone and PCL/Dichloromethane substrates..... | 82 |
| Figure 4-21 Schematic illustration of the possible structure of the PCL surface after the surface reacted with (A) 0.01 M tetradecanoic acid and (B) 0.01 M dodecanedicarboxylic acid | 83 |
| Figure 4-22 PC12 cells attached onto modified PCL/THF substrates for 12 hr. | 87 |
| Figure 4-23 PC12 cells attached onto modified PCL/Acetone substrates after 12 hr cell culture. | 88 |
| Figure 4-24 PC12 cells attached onto modified PCL/Dichloromethane substrates after 12 hr cell culture. | 89 |
| Figure 4-25 PC12 cells attached onto modified PCL substrates after 12 hr cell culture. | 90 |
| Figure B-1 Hemacytometer method..... | 102 |
| Figure B-2 Counting chamber | 103 |

1.0 INTRODUCTION

1.1 INTRODUCTION

The central nervous system (CNS) represents the largest part of the nervous system and together with the peripheral nervous system (PNS). The CNS has a fundamental role in the control of behavior. The central nervous system is composed of the brain and spinal cord and is surrounded by bone-skull and vertebrae. Fluid and tissue also insulate the brain and spinal cord. The peripheral nervous system contains only nerves and connects the brain and spinal cord to the rest of the body. The central nervous system cannot regenerate; therefore regeneration only occurs when the peripheral nervous system is injured. Peripheral nerve injury (PNI) is a serious health problem for society today [1]*. It affects 2.8% of trauma patients, many of whom acquire life-long disability. Approximately 360,000 people in the United States suffer from upper extremity paralytic syndromes yearly, resulting in 8,648,000 and 4,916,000 restricted activity days and bed/disability days, respectively. Furthermore, 44,000 upper extremity inpatient procedures involved the nervous system in the United States from 1989–1991[1].

Peripheral nerve injuries remain a difficult and challenging problem in reconstructive surgery [2]. Direct end-to-end surgical reconnection of the damaged nerve ends or the use of an autologous nerve graft are the current clinical approaches for the repair of peripheral nerve defects. However, the reconnection of the damaged nerve ends is not desired for larger nerve defects because any tension introduced into the nerve cable would inhibit nerve regeneration [2]. Thus, for longer nerve defects, the only approach is autologous nerve graft that is harvested from

* Parenthetical references superior to the line of text to the bibliography.

another site in the body. Several disadvantages of this approach includes loss of function at the donor site , the need for multiple surgeries, the limited availability of donor sites for nerve grafts and the suboptimal functional status restored following nerve grafting. Therefore, much effort has been focused on the development of alternative techniques for bridging the nerve gaps. In the past few decades, various synthetic materials for bridging the nerve gap and surface modifications for enhancing the outgrowth of nerve cells have been reported [3-12, 15-17]. Since that electrical charges play an important role in simulating proliferation and differentiation for several cell types has been proved, polymers such as poly (Lactic acid) (PLA)[2,3], poly (D,L-lactic-co-glycolide acid) (PLGA)[4], poly(caprolactone)[6,7], and polyvinylidene fluoride (PVDF)[8] have been used in an attempt to develop scaffold that can physically guide axonal growth. **Table 1-1** provides the materials are in use or under investigation for nerve repair applications [19]. **Table 1-2** shows requirements of materials used as a nerve guide (the information in **Table 1-2** is collected from Dr. Marra's lecture: Biomaterials for Nerve Regeneration, Biomaterials and biocompatibility).

Table 1-1 Nerve grafts and nerve conduit materials [19]

Autologous tissue grafts

1. Nerve Grafts (gold standard)
2. Vein grafts
3. Muscle grafts
4. Epineurial sheaths
5. Tendon grafts

Nonautologous/ acellular grafts

1. Immunosuppression with allografts
2. Acellular allografts and xenografts
 - Thermal decellularization
 - Radiation treatment
 - Chemical decellularization
3. Small intestinal submucosa (SIS)
4. Human amnion

Natural-based materials

1. ECM protein-based materials
 - Fibronectin
 - Laminin
 - Collagen
2. Hyaluronic acid-based materials
3. Fibrin/fibrinogen
4. Other materials (alginate, agarose...)

Synthetic materials

1. Biodegradable synthetic materials
 - Poly(lactic acid) (PLA)
 - Poly(lactic-co-glycolic acid) (PLGA)
 - Poly(caprolactone)
 - Poly(urethane)
 - Poly(organo) phosphazene
 - Poly(3- hydroxybutyrate)
 - Poly(ethylene glycol) “glue”
 - Biodegradable glass
2. Electrically active materials
 - Piezoelectric
 - Electrically conducting
3. Nonbiodegradable synthetic materials
 - Silicone
 - Gore-Tex or ePTFE

Table 1-2 Requirements of materials used as a nerve guide

| Nerve Guide Properties | Requirements of a nerve guide | Additional nerve guide properties |
|---|--|---|
| <ul style="list-style-type: none"> -Permeability (Porosity) -Length -Material(Polymeric) -Adhesion properties -Mechanical properties (Pliable) -Degradation properties (at least 4 weeks) | <ul style="list-style-type: none"> -Tube must have diameter similar to nerve. -Tube must be surgically compliant. -Permanent materials are not desired due to risk of infection or dislodgement. -Tube must be sterilizable. -Tube must not be too rigid, yet not be easily compressed. | <ul style="list-style-type: none"> -Surface of biomaterial (which can provide strong adhesiveness between the protein layer and the substrate) -Porosity -Electrical properties -Incorporation of neurotrophic factors -Incorporation of cells |

1.2 CELL INTERACTIONS WITH FOREIGN SURFACES

Cell interactions with foreign surface include four steps: 1) protein adsorptions; 2) cells anchored to adsorbed protein via cell integrins; 3) cell differentiate, multiply, communicate with other cell types and organize themselves; 4) cells and tissues (implant materials) respond to mechanical forces [64].

First, when the biomaterials implant into the body, proteins are immediately adsorbed (<1 second) onto the surface of implanted materials. In seconds to minutes, a monolayer of protein adsorbs to most surface. The protein adsorption event occurs well before cells arrive at the surface. Therefore, cells see primarily a protein layer, rather than actual surface of biomaterial. Since cells respond specifically to proteins, this interfacial protein film may be the event that controls subsequent bioreaction to implants [64].

Second, cells arrive at an implant surface propelled by diffusive, convective or active mechanisms after protein adsorb as shown in **Figure 1-1**. The cells can adhere, release active compounds, recruit other cells, grow in size, replicate and die. These processes often occur in response to the proteins on the surface [64].

Third, cells may differentiate, multiply, communicate with other cell types and organize themselves into tissues comprised of one or more cell types after cells arrive and interact at implant surfaces as shown in **Figure 1-2**. Cells secrete extracellular matrix (ECM) molecules that fill the spaces between cells and serve as attachment structures for proteins and cells [64].

Finally, cells and tissues respond to mechanical forces. Two samples made of the same material, one a triangle shape and the other a disk, implanted in soft tissue, will show different healing reactions with considerably more fibrous reaction at the asperities of the triangle than along the circumference of the circle [64].

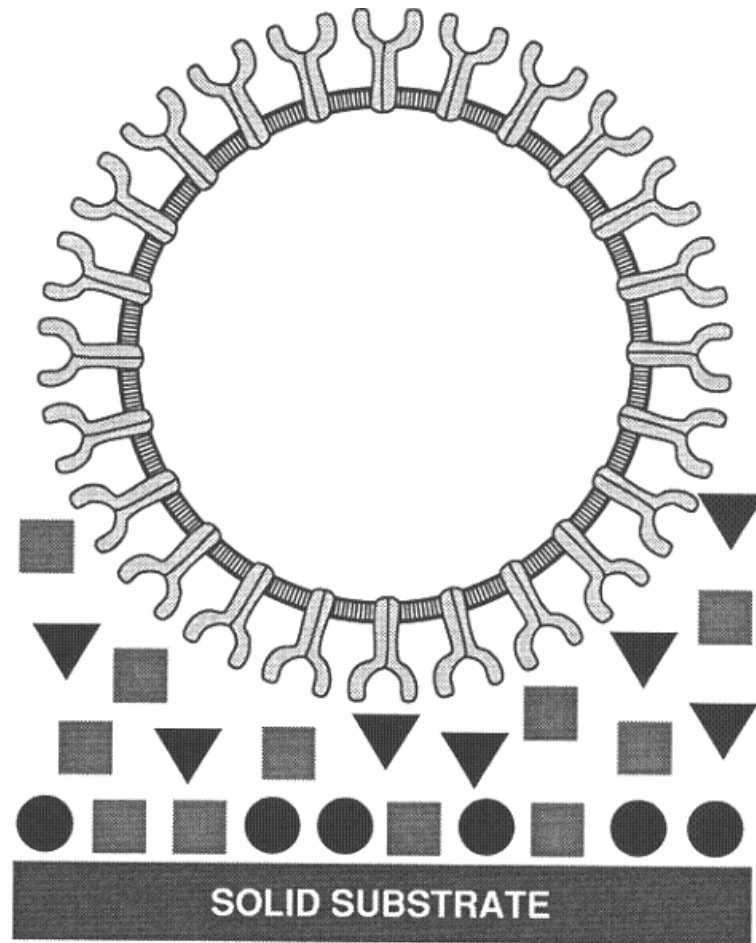


Figure 1-1 Cell interactions with foreign surfaces are mediated by integrin receptors with adsorbed adhesion proteins that sometimes change their biological activity when they adsorb.

The cell is shown as a circular space with a bilayer membrane in which the adhesion receptor protein molecules (the slingshot-shaped objects) are partly embedded. The proteins in the extracellular fluid are represented by circles, squares, and triangles. The receptor proteins recognize and cause the cell to adhere only to the surface-bound form of one protein, the one represented by a solid circle. The bulk phase of this same adhesion protein is represented by a triangle, indicating that the solution and solid phase forms of this same protein have a different biological activity. The figure is schematic and not to scale (From Horbett, 1996.) [64]

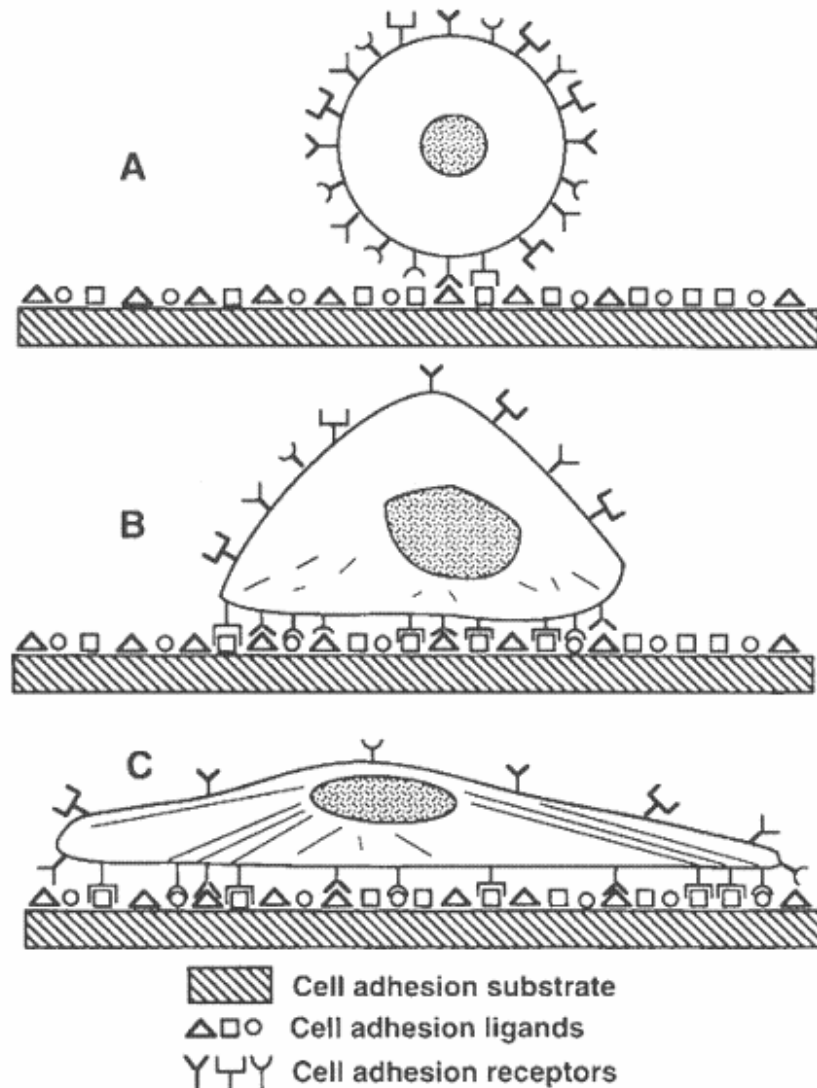


Figure 1-2 Progression of anchorage-dependent mammalian cell adhesion.

(A) Initial contact of cell with solid substrate. (B) Formation of bonds between cell surface receptors and cell adhesion ligands. (C) Cytoskeletal reorganization with progressive spreading of the cell on the substrate for increased attachment strength. (Reproduced by permission from Massia, S.P., 1999. Cell-extracellular matrix interactions relevant to vascular tissue engineering. In *Tissue Engineering of Prosthetic Vascular Grafts*, P. Zilla and H. P. Greisler, eds., RG Landes Co.) [64]

2.0 BACKGROUND

2.1 SYNTHETIC MATERIALS

To select an appropriate synthetic material as a scaffold, there are several properties that are desired: (a) we should be able to fabricate the material in form of hollow tubes with diameters (from 4 to 100 μm) similar to that of nerves [65]; (b) the material should be sterilizable and (c) surgically compliant. In general, permanent materials are not desired since they pose a higher risk for infection and are more likely to provoke a chronic inflammatory response. They also have the potential to compress the nerve over time. Thus, a nerve guide material that degrades as the nerve regenerates is preferred. Additionally, guidance channels should be pliable, but should maintain their shape and resist collapse during implantation and over the time course for regeneration. Research has also shown that guidance channels should be semi-permeable and should have a smooth inner wall. **Figure 2-1** shows the desired physical properties of the nerve guidance channel. Following is a description of different synthetic materials which have been explored for use in aiding nerve regeneration.

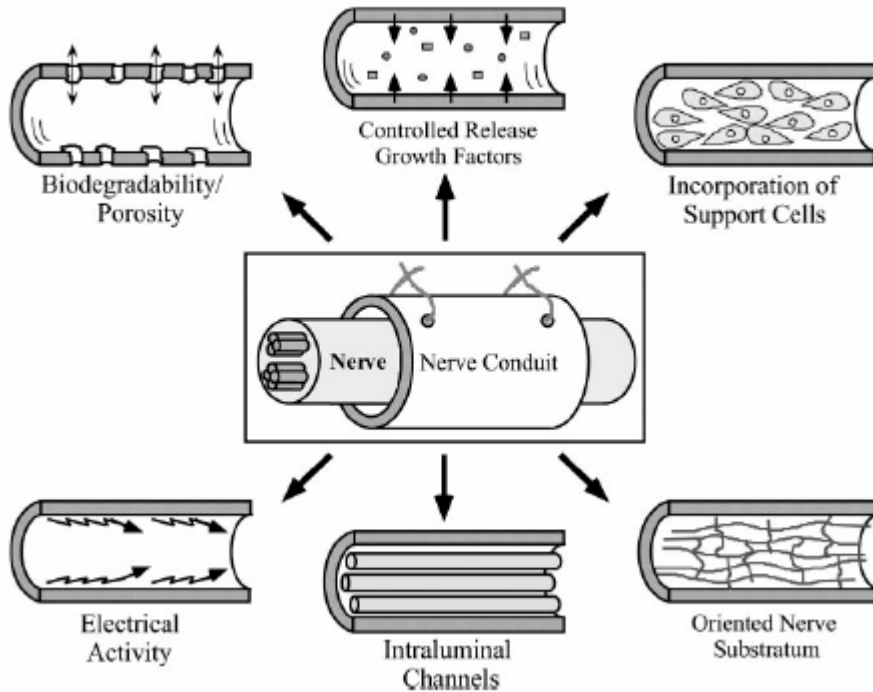


Figure 2-1 Properties of the ideal nerve guidance channel [19]

2.1.1 Poly (Glycolic Acid) (PGA)

PGA is a biocompatible material. However, hexafluoroisopropanol ($((\text{CF}_3)_2\text{OH})$) is one of PGA's only solvents and this solvent is highly toxic. Therefore, PGA is more commonly utilized as a copolymer with PLA (**Figure 2-2 b**). PGA can be extruded into fibers, which can then be braided into woven structures. PGA degrades to glycolic acid, which is then metabolized in the body.

2.1.2 Poly (Lactic Acid) (PLA)

PLA (**Figure 2-2 b**) has two enantiomeric isomers** of lactide exist. One is poly (L-lactic acid) (PLLA); the other is poly (D-lactic acid) (PDLA). The key difference between PLLA and PDLA is the orientation of CH₃ and C=O groups. Both PLLA and PDLA have been examined as biocompatible materials. PLLA is more crystalline, and degrades more slowly than PDLA. PLA's degradation product is lactic acid which is also biocompatible, yielding CO₂ and water [15].

Evans et al. [4] used PLLA as a potential conduit for bridging nerve gaps, because of several advantages including biodegradability, porous structure for vascularization and consistency in design requirements. The goal of the work by Evans et al. [4] was to demonstrate that allogeneic Schwann cells (SCs) injected into the PLLA conduits can enhance nerve regeneration. Their study showed that SCs appear to play a unique and dynamic role in nerve repair and offer a highly preferred substrate for axon migration, SCs can release bioactive factors that further enhance nerve migration. However, they were unable to demonstrate a significant difference in the functional outcome between PLLA conduits implanted with SC and isograft controls.

2.1.3 Poly (Latic-co-Glycolic Acid) (PLGA)

The copolymer of PLA and PGA, poly (lactic-co-glycolic acid) (PLGA), (**Figure 2-2.c**) has been extensively studied in a variety of tissue engineering applications. The PLGA copolymer that consists of 82% PLLA and 18%PGA is referred to as LactoSorb^(TM). LactoSorb^(TM) was introduced in 1996 and is being sold by Lorenz Surgical Inc. LactoSorb^(TM) was shown to

** Technical terms are explained in Appendix A.

completely resorb in 12 months, and has been used clinically in pediatric craniofacial reconstruction for six years [15].

Molendar et al. [5] used PLGA suture mesh as guidance around nerve defects. The operative procedure is shown in **Figure 2-3**. In their experiments, PLGA tube bridging the nerve defect served as a framework for the proliferating cells. This technique had three advantages: (a) the nerve defect created was small; (b) axons were able to cross the defect in the limited space, and (c) PLGA tube was permeable so that nutrients could pass through into the tube. They concluded that comparing to the control and the spreading of the regenerating axons, PLGA tube offered a suitable space for regenerating axons, growing Schwann cells, fibroblasts, and endothelial cells.

The concept that electrical fields can influence cell behavior is long-standing. For example, Bryan et al. proved that PLGA guides prepared with electrical poling enhanced peripheral nerve regeneration [16]. The polymer, Poly (lactic-co-glycolic acid)-85:15 (PLGA), dissolved in methylene chloride, was poled at 20kV for 10 min (piezo group 1) and 24kV for 45 min (piezo group 2). The control group was unpoled PLGA. The result showed only group 2 produced statistically significant increases in total axon number, in the number of myelinated axons and the compound potential of the nerve regeneration. Although they have proved that poled PLGA could enhance neurons outgrowth, the precise mechanism for the observed effect is unclear. In the *in vitro* experiments performed with mouse neuroblastoma (Nb2a) cells, one proposed explanation for the growth of neuritis on poled PLGA film has been the presence of a field-induced gradient of ions in the tissue culture medium; the other explanation is that electrical stimulation of PC12 cells can increase protein adsorption.

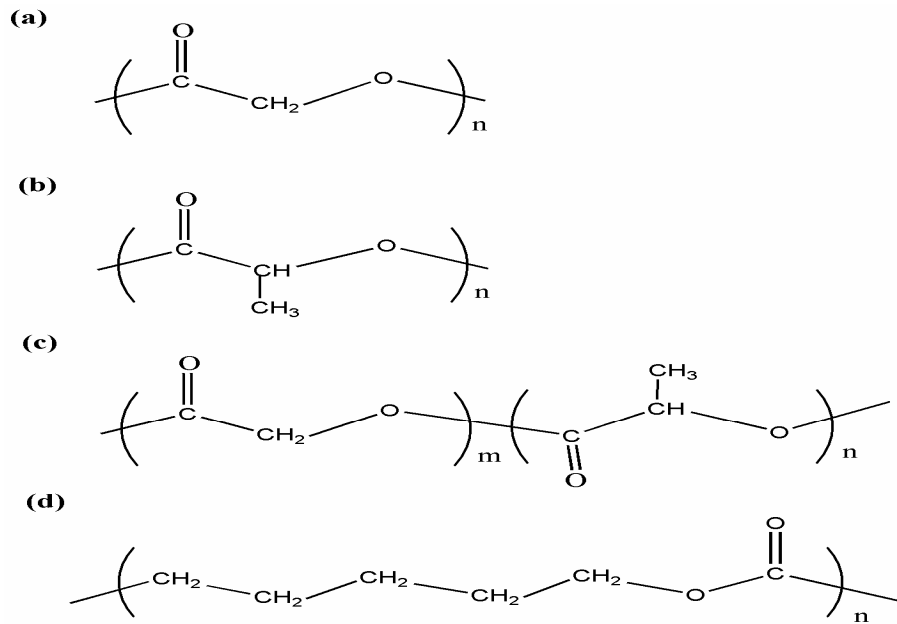


Figure 2-2 Structures of (a) PGA, (b) PLA, (c) PLGA and (d) PCL

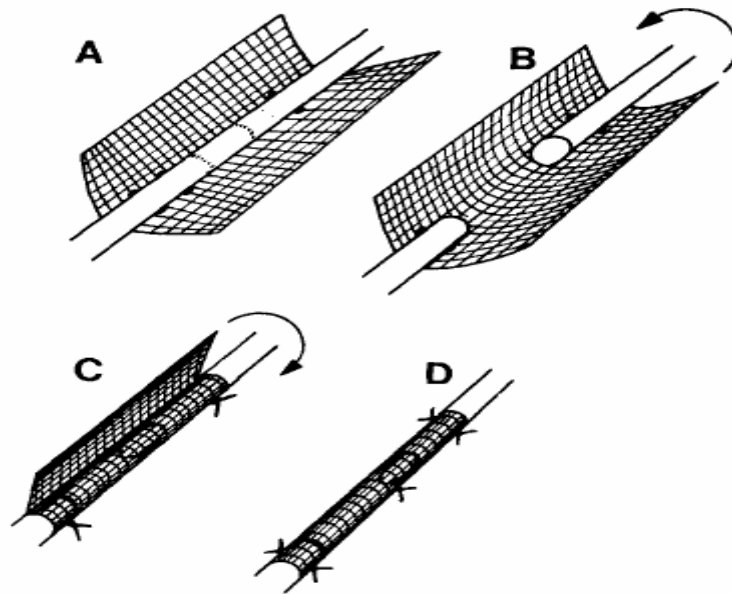


Figure 2-3 Schematic view of operative procedure. (A) The mesh is placed underneath the nerve and secured with sutures. (B) The nerve is resected. (C) The mesh is shaped like a tube around the nerve. (D) The tube is closed by sutures [5].

2.1.4 Poly (caprolactone) (PCL)

Poly (caprolactone) (**Figure 2-2 d**) is a biodegradable thermoplastic polymer derived from the chemical synthesis of crude oil or ring opening polymerization of lactone. Although not produced from renewable raw materials, it is fully biodegradable. Poly (caprolactone) has good water, oil, solvent and chlorine resistance. It has a low melting-point (58-60 °C) and low viscosity, and is easy to process.

The biodegradable copolymer consists of 50% PLA (85% L-lactide and 15%D- lactide) and 50% poly (ϵ -caprolactone) is used to be the nerve guidance by Dunnen et al [6]. The copolymer has a weight-average molecular weight (M_w) of 1.1×10^6 kg/kmol, a polydispersity index of 2.5, and a glass transition temperature (T_g) of -12 °C. The shape of the guidance channel was tube-like with a diameter of 1.5 mm, a wall thickness of 0.30 mm, and a length of 14 mm. In their paper, they report that after reconstruction of a 1-cm gap in the sciatic nerve of the rat with a 12-mm poly[50/50(85/15L/D)LA/ ϵ -CL] nerve guide, axon regeneration starts after a few days and is quite fast. After 10 weeks, the regenerating nerve inside the nerve guide has almost matured and the weight-average molecular weight (M_w) decreases *in vitro* from 6.5×10^5 kg/kmol to 1.0×10^5 kg/kmol. They concluded that a nerve guide constructed of poly[50/50(85/15L/D)LA/ ϵ -CL] could be used in the case of 1-cm gap in the sciatic nerve of the rat, and was even better than autologous nerve grafts. The nerve guide degrades completely within 1 year; this period is long enough to assure both the outgrowth and maturation of the nerve fibers through a 1-cm gap. However, p[50/50(85/15L/D)LA/ ϵ -CL] nerve guides could only be used in the small nerves and peripheral nerve regeneration in humans which is slower than that in rat [6]. Therefore, refinements of the poly[50/50(85/15L/D)LA/ ϵ -CL] nerve guide are necessary. Refinements can be obtained as follows: (a) in the polymer itself, (b) changing the composition

of the nerve guide wall, and (c) the addition of growth factors, extracellular matrix molecules and/ or Schwann cells inside the nerve guide [6].

Valero-Cabre et al. [7] compared autograft, tubulization with impermeable silicone tubes and permeable tubes of poly-L-lactide- ϵ - caprolactone in the compound muscle action potential (CMAP) from gastrocnemius(mGC), tibialis anterior(mTA) and plantar(mPL). The CMAP amplitude achieved in mGC, mTA and mPL was similar after nerve autograft (39%, 42%, 22% of control values) and PLC tube implantation (37%, 36%, 24%) but lower with silicone tube (29%, 30%, 14%). The total number of labeled motoneurons for the three muscles did not differ in autograftd rats (1186 ± 56 ; mean \pm SEM) with respect to controls (1238 ± 82), but was reduced with PLC tube (802 ± 101) and silicone tube (935 ± 213). According to the result, PLC nerve conduits seem superior to SIL tubes and a suitable alternative to autografts for the repair of long gaps [7].

2.1.5 Polyvinylidene fluoride (PVDF)

Polyvinylidene fluoride (PVDF) is a biocompatible and semi-crystalline homopolymer formed by the head-to-tail addition of $[CF_2-CH_2]_n$. A homopolymer is a polymer in a mixture of crystalline and amorphous states. PVDF is a well known piezoelectric material which can create electrical charge when mechanically stressed. One of the crystal states for PVDF is ferroelectric and thus responsible for PVDF's piezoelectric properties. Piezoelectric PVDF is prepared by uniaxial (anisotropic) or biaxial (isotropic) mechanical stretching followed by exposure to a high intensity corona poling process. The fluorine and hydrogen atoms lie on opposite sides of the carbon backbone creating a strong molecular dipole [64].

Since PVDF can generate transient surface charges under minute mechanical strain, Valentini et al. [25] cultured Nb2a cells on electrically poled and unpoled PVDF substrates in serum-free and serum-containing media to analyze the influence of electric charge on Nb2a cells outgrowth [22]. PVDF is poled by the corona poling process, a non-discharge technique which permanently orients molecular dipoles parallel to the intense electric field, endowing the material with a strong, net-dipole moment. The schematic of corona poling system was shown in **Figure 2-4** and **2-5**. After they were poled, PVDF substrates generate 2-3mV at 1200Hz when placed on standard incubator shelves and unpoled PVDF substrates showed no electrical output. Valentini et al. concluded enhanced cell differentiation on poled PVDF was better than that on unpoled PVDF in both serum-free and serum-containing media.

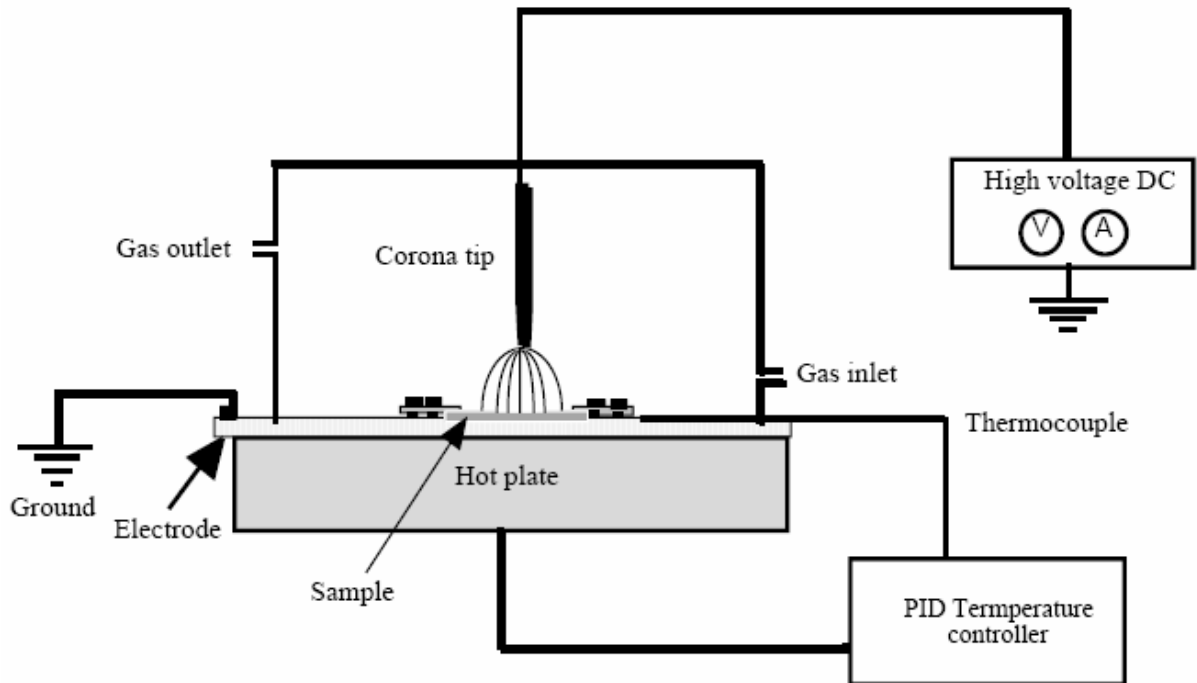


Figure 2-4 Schematic of corona poling system [66]

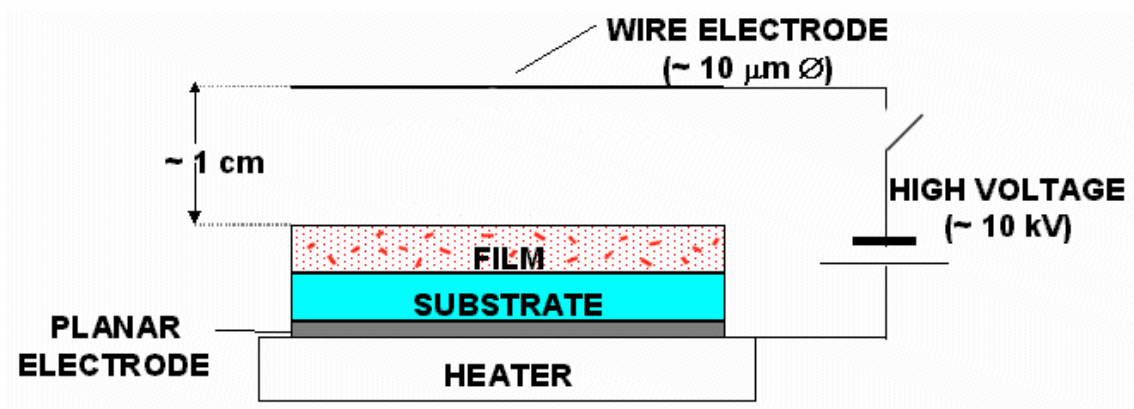


Figure 2-5 The closed looking of corona tip and sample [66]

2.1.6 Other polymers

Other than the polymers mentioned previously, biodegradable polymers such as poly (urethane) [26], poly (pyrrole) [8], poly (organo phosphazene)[27], methacrylate- based hydrogels [28], and poly (3- hydroxybutyrate)[29], have shown a capacity for guiding regeneration. Also, many advancing materials processing techniques creating three- dimensional channels and porous surface with a specific pore size have been adopted to make more efficiency polymeric channels [30-41].

2.2 SURFACE MODIFICATIONS

Surface modifications also attracted many researchers' attention because cell behavior on synthetic polymer substrates are often governed by substratum properties, especially the surface characteristics, such as chemical composition, wettability, ionic charge, texture and topography [9, 10]. Ideal biomaterials encourage good cell-substrate interaction and stimulate the cells by

substrate-bound chemical, biological, electrical, and mechanical signals. Recent investigations [9, 10] have demonstrated that precisely controlled surface chemistries such as patterns or gradients of surface-bound molecules can be used to regulate the cell-surface interaction and control cellular activity. For example, it has been shown that neurite outgrowth is enhanced on electrets such as poled polyvinylidene fluoride (PVDF) [21, 22] and poled polytetrafluoroethylene [23]. This work has shown that electrical charges play an important role in stimulating either the proliferation or differentiation of various cell types has been demonstrated. Furthermore, Li et al. [11, 12] showed that protein gradients and carboxyl group density could affect cells extension and regeneration of transected nerve ends. Keselowsky et al. [13, 14] used self-assembled monolayers (SAMs) as a model biomaterial surface presenting well defined chemistries to demonstrate that surface chemistry modulates osteoblastic differentiation and matrix mineralization independently from alternations in cell proliferation.

In most circumstances, the polymer materials are subjected to surface modification or functionalization in order to give them the necessary surface characteristics, or to introduce functional groups, allowing other biomolecules to be attached to the surface. Following are some examples of polymeric surface modifications in order to enhance cell proliferation and differentiation. **Table 2-1** shows the methods of surface modifications.

Table 2-1 Surface modification methods (*Information is from www.astp.com*)

| <u>Physical</u> | <u>Chemical</u> | <u>Radiation</u> |
|---|--|---|
| <ul style="list-style-type: none"> - Physical adsorption - Langmuir Blodgett film | <ul style="list-style-type: none"> - Oxidation by strong acids - Ozone treatment - Chemisorption - Flame treatment | <ul style="list-style-type: none"> - Plasma (glow discharge) - Corona discharge - Photo-activation (UV) - Laser - Ion beam - Electron beam - γ - irradiation |

2.2.1 Gradient-guided neurite outgrowth

Li et al. grafted poly (acrylic acid) onto PET surfaces as shown in **Figure 2-6** [11, 12]. The substrate was pre-irradiated with UV under a chrome-coated quartz photo mask. The movement of the substrates was controlled by the stage that is computer controlled and has a resolution of 100 nm. After pretreatment, the substrate was exposed to air for at least 2 minutes before being put into a 10wt% acrylic acid (AA) and 0.01M ammonium iron (II) sulfate heptahydrate (AISH) aqueous solution in a glass photoreactor and then purged with argon for 10 minutes. The photoreactor was placed under a UV lamp at a distance of 18 cm. A PET film (0.25mm thick) was used as a filter to cut off UV light with a wavelength below 310nm. After 10 minutes UV irradiation, the substrate was soaked in 70 °C deionized water for 24 h to remove the AA

monomer and non-grafted PAA homopolymer on the surface. The use of this technique can control the gradient of carboxyl group on PET substrates.

Li et al. [11, 12] demonstrated that both the attachment and differentiation behaviors of C17.2 cells were significantly affected by -COOH group density. Furthermore, neurites grew from high -COOH density toward lower -COOH density were longer than those from lower -COOH density toward high -COOH density as shown in **Figure 2-7**.



Figure 2-6 Schematic illustration of two-step grafting of PAA onto polymeric substrates [12].

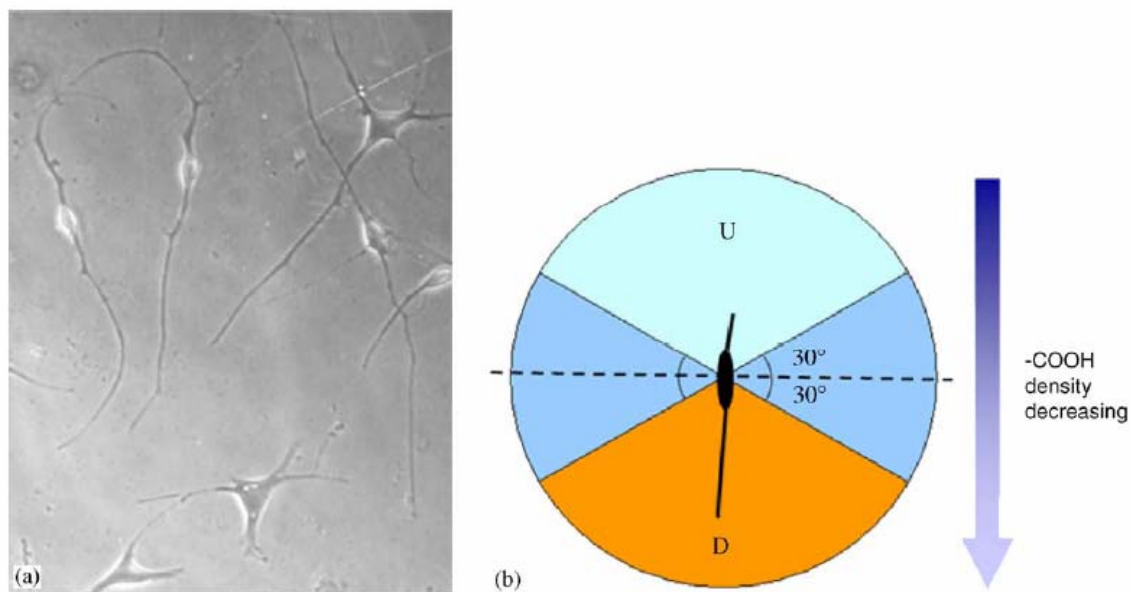


Figure 2-7 (a) Microscopic image of C17.2 cells on a $-\text{COOH}$ gradient surface after Ar plasma treatment. (b) Schematic illustration of a cell on a gradient substrate surface [12].

2.2.2 Surface modulation by self-assembled monolayers (SAMs) of alkanethiols

The function of fibronectin (Fn) is to mediate cell attachment by interacting with cell surface receptors and extracellular matrix components. Fibronectin absorption onto substrates of varying properties alters its conformation/structure and its ability to support cell adhesion was researched by Keselowsky et al.[13, 14]. In their reports, alkanethiols including 1-dodecanethiol ($\text{HS}-(\text{CH}_2)_{11}-\text{CH}_3$), 11-mercapto-1-undecanol ($\text{HS}-(\text{CH}_2)_{11}-\text{OH}$), 11-mercaptoundecanoic acid ($\text{HS}-(\text{CH}_2)_{10}-\text{COOH}$), and 12-amino-1-mercaptododecane ($\text{HS}-(\text{CH}_2)_{12}-\text{NH}_2$) were, respectively, self-assembled onto glass cover slips coated by titanium(10 nm) and gold(20 nm). After SAMs (12 hours reaction) are formed on the surface, SAMs were coated with Fn diluted in Dulbecco's phosphate-buffered saline (DPBS: 137 mM NaCl, 2.7 mM KCl, 4.3 mM $\text{Na}_2\text{HPO}_4 \cdot 7\text{H}_2\text{O}$, 1.5 mM KH_2PO_4 , 0.9 mM $\text{CaCl}_2 \cdot 2\text{H}_2\text{O}$, 1 mM $\text{MgCl}_2 \cdot 6\text{H}_2\text{O}$, pH=7.4) for 30 minutes. They concluded that different surface chemistry modulated Fn structure to alter integrin adhesion receptor binding; the result showed that more Fn absorbed on the NH_2 SAMs surface than COOH , CH_3 and OH SAM surface at high Fn coating concentration but there were no differences at low Fn coating concentration. In their further research [14], Keselowsky et al. reported that the immature osteoblast-like cell (MC3T3-E1) had better differentiation and mineralization results on $-\text{NH}_2$ and $-\text{OH}$ SAMs surface than $-\text{CH}_3$ and $-\text{COOH}$ SAMs surface at equivalent Fn surface density (40 ng/cm^2) and 14 analyzed days.

2.2.3 Surface modification via aminolysis

Zhu et al. proved that amino groups were covalently introduced onto a polycaprolactone (PCL) surface [18] and poly (L- lactic acid) (PLLA) surface [24], by the reaction between 1,6-

hexanediamine and -C=O group on the polymeric surfaces. After the surface aminolization (PCL for 1 hr and PLLA for 20 min), the surface NH_2 density is $2 \times 10^{-7} \text{ mol/cm}^2$ on PCL surface and $1.6 \times 10^{-7} \text{ mol/cm}^2$ on PLLA surface which was identified by UV-vis spectrophotometer at the absorbance wavelength of 538 nm. The aminolyzed substrates were used to immobilize gelatin, chitosan or collagen as shown in **Figure 2-8**. That the introduction of the biocompatible macromolecules had a positive effect on modifying the cytocompatibility of PCL can be proven by their cell culture research on the modified surfaces. They concluded that the cell attachment and proliferation ratios were obviously improved and the cells spread well and lived comfortably from the cell morphology observed under SEM.

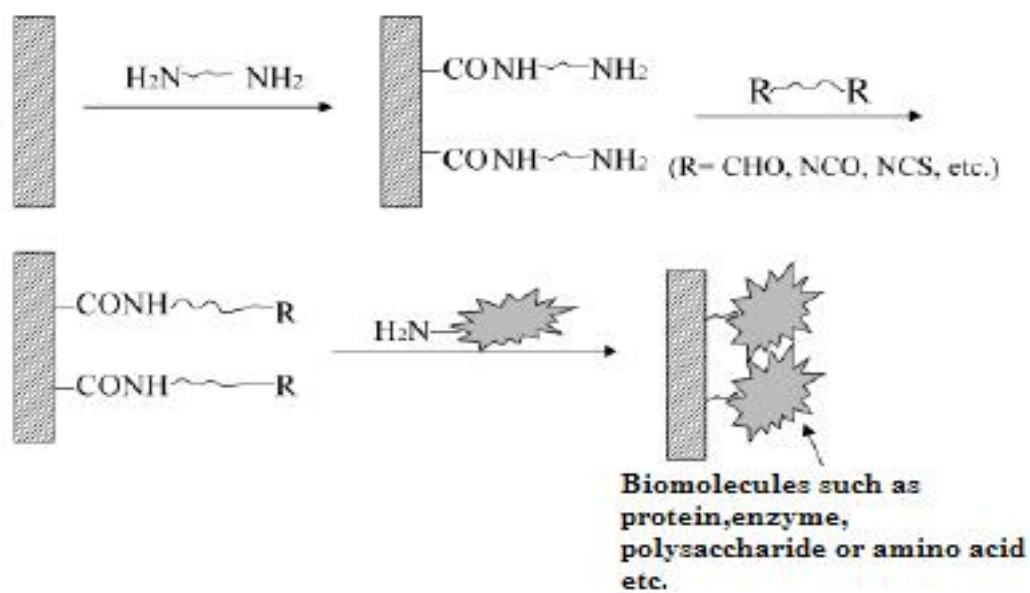


Figure 2-8 The schematic representation of aminolysis and further immobilization of biomolecules on polycaprolactone membrane [18].

2.2.4 Plasma surface modification

Many researchers are using gas plasma to modify polymeric surfaces because the plasma surface modification process has many advantages including (a) adhesion promotion, (b) enhanced surface wettability and spreading, (c) biocompatibility improvement, (d) surface functionalization, (e) reduced surface friction and tackiness, (f) molecular immobilization, (g) non-fouling coating, and (h) barrier surface coating [42-45]. According to the information published on the website of AST Product Inc. (www.astp.com), the plasma surface modification process can be briefly described as follow: in the plasma surface modification process, glow discharge plasma is created by evacuating a vessel, usually quartz because of its inertness, and then refilling it with a low-pressure gas. The gas is then energized using techniques such as radio-frequency energy, microwaves, alternating current or direct current. The energetic species in a gas plasma include ions, electrons, radicals, metastables, and photons in the short-wave ultraviolet (UV) range. Surfaces in contact with gas plasmas are bombarded by these energetic species and their energy is transferred from the plasma to the solid as shown in **Figure 2-9**. These energy transfers are dissipated within the solid by a variety of chemical and physical processes as schematically illustrated in **Figure 2-10**, to result in the surface modification. The unique surface modification that can be achieved using the plasma process results from the effects of the photons and active species in the plasma. These react with surfaces in depths from several hundred angstroms to 10 μm without changing the bulk properties of the biomaterial. A wide variety of parameters can directly affect the chemical and physical characteristics of a plasma and subsequently affect the surface chemistry obtained by plasma modification. Processing parameters, such as gas types, treatment power, treatment time and operating pressure, can be varied by the user; and system parameters, such as electrode location, reactor design, gas

inlets and vacuum, are set by the design of the plasma equipment. This wide range of parameters offers greater control over the plasma process than that offered by most high-energy radiation processes. Other advantages of this technology include low environmental impact; no line-of-sight problem compared with electron-beam, laser or UV radiation; and a pinhole-free coating. In addition, although gas plasma treatments are typically carried out in a batch process, continuous on-line treatment of fibres, tubing membranes, fabrics and films, is also common. In many cases, a custom-designed reactor is necessary to maintain a high level of throughput and maximize the economic feasibility of the process.

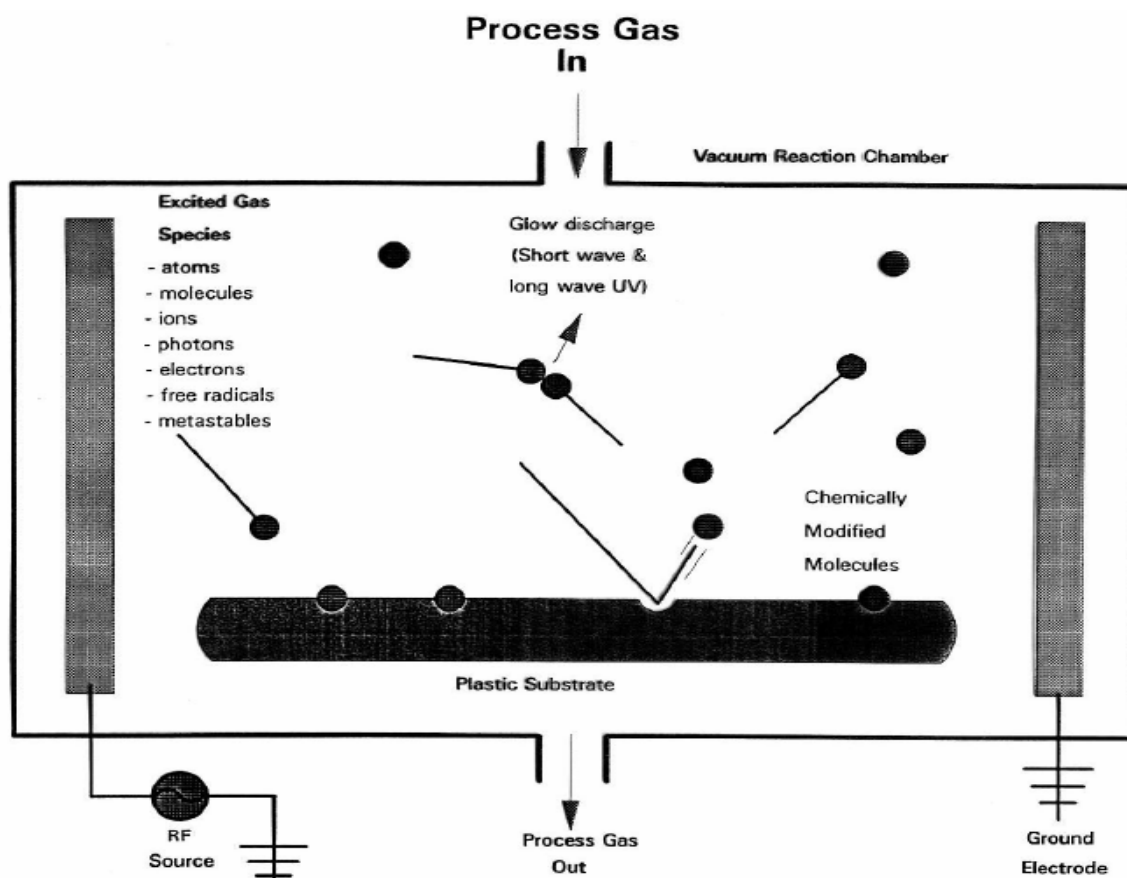


Figure 2-9 Schematic of plasma surface modification within the plasma reactor

(Information is collected from www.astp.com).

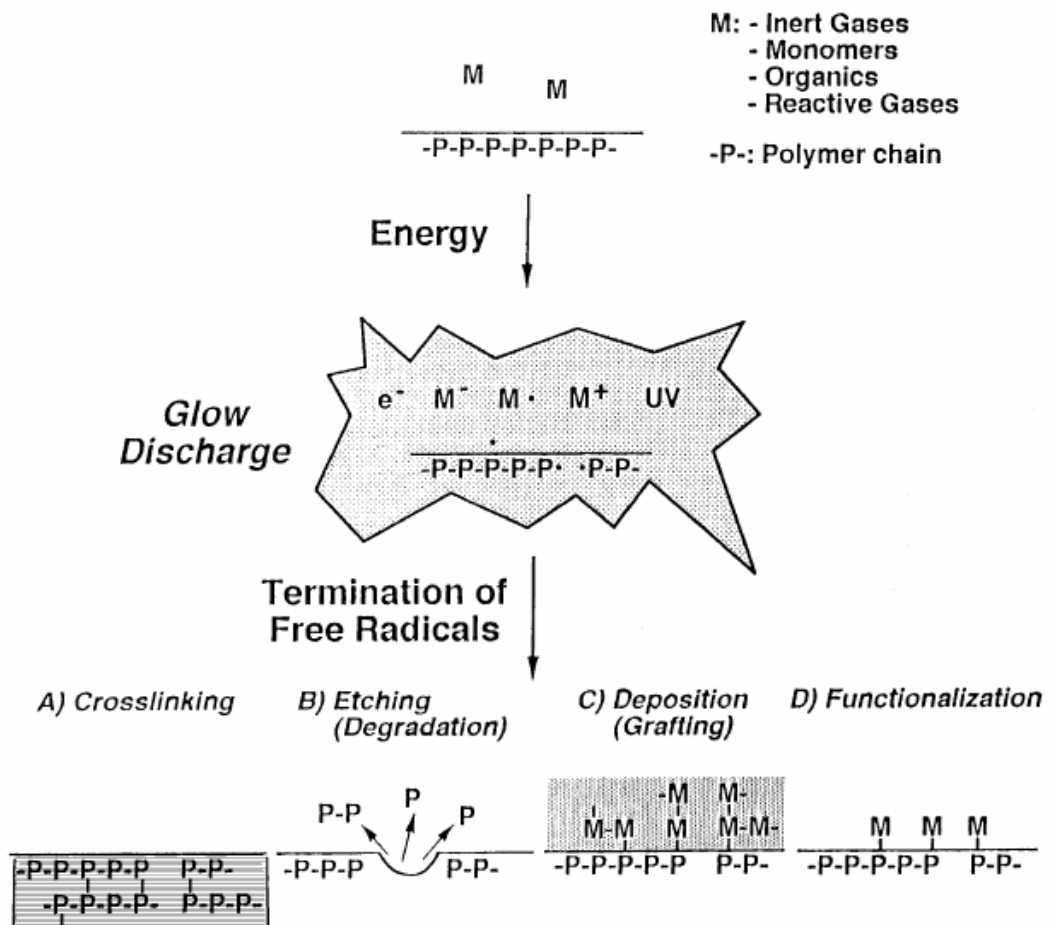


Figure 2-10 Schematic of the reaction mechanisms of plasma surface modifications

(Information is collected from www.astp.com).

2.2.5 Laser surface modification

Laser treatments of materials offer advantages over both chemical and physical methods. For example, they enable precise modification of certain surfaces that are difficult to treat with conventional chemical methods. The resulting modified surfaces are free from contaminant. Most importantly, the bulk properties of the material remain intact. The development of laser-assisted modification of polymer surfaces is a rapidly growing and developing field that has gained considerable interest among scientists in the past decade. Khorasani et al. [57] used pulsed CO₂ laser to modify the surface of polydimethylsiloxane (PDMS) membrane of 0.3 mm thickness. The super- hydrophobic surface has been created while the bulk properties of the substrates are kept intact. This laser treatment introduced peroxide groups onto the PDMS surface, which is capable of initiating graft polymerization of 2-hydroxyethylmethacrylate (HEMA) onto the PDMS [58]. The result shows that the modified surface can reduce platelet adhesion. Tiaw et al. [59] femtosecond and excimer lasers were used to perforate and modify the surface of PCL membranes. Both laser types enhanced the wettability of the PCL membrane. The wettability characteristics were directly dependent on pulse energies and pulse number. In the perforation of PCL membrane using femtosecond laser, the pulse energy of the femtosecond laser directly affected the size of the holes while the pulse number can affect the quality of the holes produced. For the KrF excimer laser, increasing the pulse number (corresponding to longer laser irradiation time), and the 5-10 degrees (depending on the power of the excimer laser and the exposure time) water contact angle dropped indicating an increased in the surface hydrophilicity of the PCL. Tiaw et al. demonstrated that laser surface modification on the PCL can be achieved with high degree of success and precision. This paved the way for further enhancement in membrane tissue engineering.

2.3 SCAFFOLD FABRICATION TECHNIQUES

Except surface modification, the scaffold fabrication technique is another way to make polymeric materials into a form that can provide the appropriate spatial and temporal scaffold for cell proliferation or tissue development. Because of these techniques the scaffold can be made with higher mechanical strength and surface area. Miller et al. [46], produced a solvent cast poly (D,L – lactic acid) (PDLA) films with a micro-patterned surface topology that was transferred from a silicon wafer. Pattern widths or spacings of 10-20 μm were found to be optimal for the alignment of Schwann cells (size 5-10 μm). Ishaug- Riley et al. [47] used spin casting for a series of degradable polymer films used in studies of human articular chondrocyte adhesion and proliferation. The chondrocytes attached and proliferated on all the biodegradable FDA-approved materials, including poly (ϵ -caprolactone), although chondrocyte adhesion was reduced on PCL and L-PLA films compared to PGA films. Calvert et al. [48] cast PCL, PLGA, and blends of the two polymers, onto glass microscope slides and studied the transplantation of osteoblasts. Of the two homopolymers, PLGA was found to be osteoconductive whereas PCL was less capable of retaining the osteoblast phenotype and while the polymer blends exhibited superior osteoconductive properties compared to homopolymers, blends of PCL and PLGA that incorporated 10% PCL were considered to be compatible whereas those with 40% PCL were not. Tang et al. [49] used four different solvents, chloroform, tetrahydrofuran, acetone and ethyl acetate, to respectively dissolve poly (ϵ - caprolactone), and then cast on to glass petri dishes to form a PCL film. **Figure 2-11** shows schematic diagram of the petri dish arrangement used to cast the PCL films. They concluded that the contact angles, surface morphology, surface

chemistry and biocompatibility of PCL films depended on the nature of the solvent used and the surface properties of the substrate on which the films were cast. With hydrophobic solvents (chloroform and ethyl acetate) the advancing contact angle(ACA) for the surface exposed to atmosphere during casting was higher than that for the surface in contact with the glass petri dish; in the case of hydrophilic solvent systems (tetrahydrofuran and acetone), the opposite was the case. The ATR-FTIR spectra for all surfaces in contact with glass were similar, regardless of the solvent used, the spectra for the exposed surfaces were all different. The two surfaces also showed morphological differences in terms of the aggregates that formed during phase separation of PCL powders (solid phase) and solvents (liquid phase), and the micro-porosity of the surface. While poor solvent systems which were tetrahydrofuran and acetone (partial dissolution at room temperature) yielded filamentous PCL structures, good solvent systems which are chloroform and ethyl acetate (complete dissolution at room temperature) produced particulate structures. Preliminary cell culture experiment [49] carried out with the PCL films showed that fibroblasts grew well on all surfaces regardless of the solvent used, although the rates of adhesion and proliferation were not as great as these on tissue culture plastic controls. Of all the surfaces examined in this study, the cells favored the SG aspect of ethyl acetate cast PCL films, the surface of which had the finest pore size(from few to 20 μ m) and relatively low advancing contact angle($88.78 \pm 0.57^\circ$).

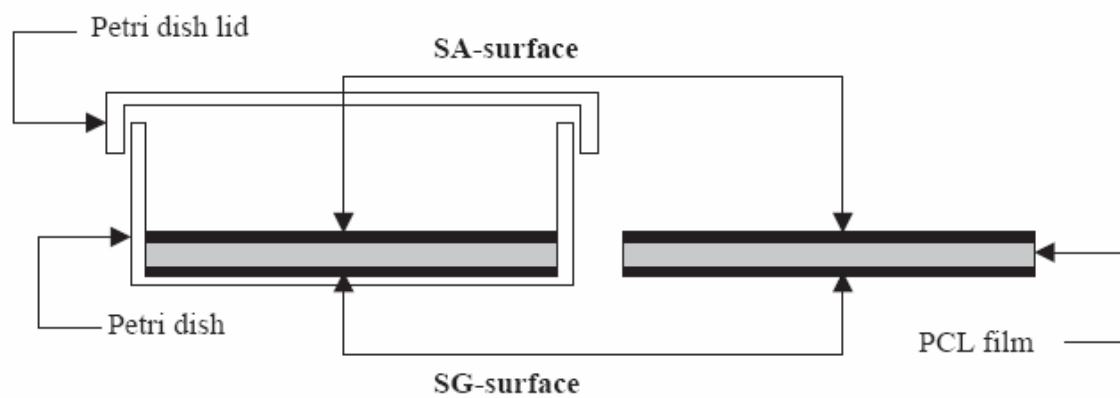


Figure 2-11 Schematic diagram of the petri dish arrangement used to cast the polymer films. SA denotes surface–air interface; SG denotes surface–glass interface [49].

3.0 EXPERIMENTAL PROCEDURES

3.1 RESEARCH OBJECTIVES

The overall of this research was to study the surface modifications of materials for tissue engineering applications. Although many materials and surface modification methods have been applied to investigate the possibility of being a nerve guide, very little research has been performed on investigating if the surface with different functional groups such as COOH(hydrophilic/negative charge surface), CH₃(hydrophobic/neutral surface), NH₂(hydrophilic/positive charge surface), and OH(hydrophilic/positive charge surface) are capable of affecting cell adhesion, cell outgrowth and cell proliferation. Three materials, micas, glass coverslips and polycaprolactone disks, were used as a substrate to do the surface modifications. Mica and glass coverslip provide smooth surface morphologies and non-porous surfaces; polycaprolactone disks made from different solvents such as THF, dichloromethane and acetone provide different surface morphologies and porosity. In this study, PC12 cells, female and male adipose-derived stem cells (ASCs) were used to investigate the influence of surface properties on the cell culture and the differentiate between female and male stem cells on the cell attachment. More specifically, the objectives of this research were:

- 1) To investigate the influence of surface properties, such as wettability, surface morphology and the surface composition, on the cell culture.
- 2) To investigate the role of surface charges on cell culture.

- 3) In an effort to develop a new surface modification method and/ or fabrication technique so that a suitable nerve guide can be made.
- 4) To investigate the differentiate between female and male stem cells on the cell attachment.

3.2 PAMAM DENDRIMERS ON MICA SUBSTRATES

Poly (amidoamine) (PAMAM) dendrimers of generation 4 (48 primary amino surface groups and 16 N-(2-hydroxydodecyl)) obtained as a 0.05 weight percent (wt %) pentanolic solution (Aldrich, Milwaukee, WI) [51, 52]. It was selected because the N-(2-hydroxydodecyl) chains which replace 25% of the terminal amine groups found in a standard G4 PAMAM dendrimer were expected to enhance the dendrimer molecule/substrate interaction, leading to stronger adhesion between dendrimers and mica substrates as showed in **Figure 3-1**. The structure of PAMAM dendrimers from generation 1 to generation 4 is shown in **Figure 3-2**.

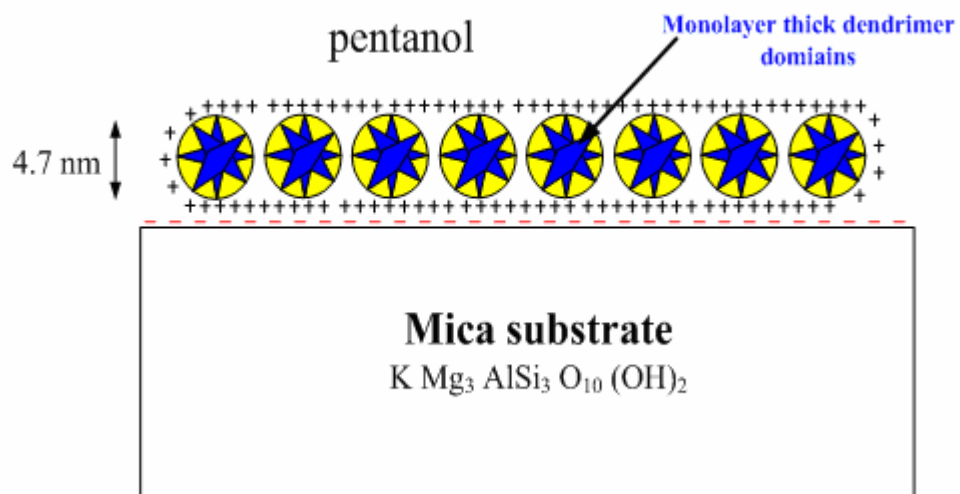
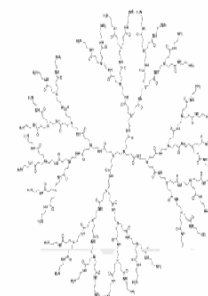
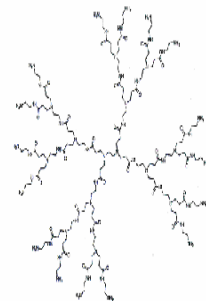
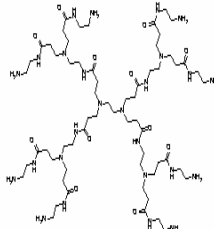
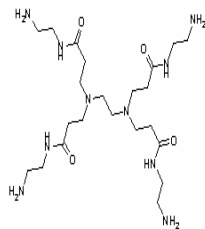


Figure 3-1 Schematic illustration of the expected charge state of the mica surface and dendrimer domains [51].

Chemical Structure



Generation 4

Generation

0

1

2

3

Molecular Structure

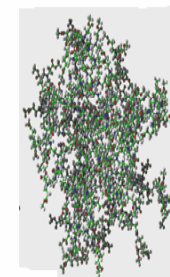
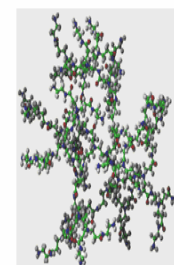
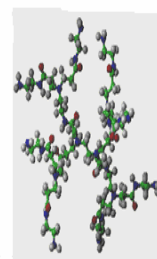
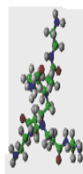


Figure 3-2 The Chemical structure and molecular structure of PAMAM from generation zero to generation four.

3.2.1 Preparing mica substrates coated with monolayer/multilayer dendrimers

Mica substrates were washed using 99.5 % ethanol (Pharmco^(TM), Brookfield, CT USA) and blown with N₂ gas until the surface was completely dry. The substrates were, then, immersed (dipped) into 0.05wt % (PAMAM dendrimers of G4/pentanol) solution for 24 hours. Multilayer dendrimers coated mica substrates were obtained by the solvent naturally evaporated from the mica surface. Monolayer dendrimers coated mica substrates were obtained by carefully rinsing the surface with R134a (1, 1, 1, 2- Tetrafluoro ethane) to remove the more loosely bound dendrimers which are not in direct contact with the substrate.

PC12 cells (neuron like cells) were directly cultured on the dendrimers bonded on mica surface without peptide deposition for 24 hours. Then, the optical microscopy (OM) was used to observe cells outgrowth.

3.3 SURFACE MODIFICATION OF GLASS SUBSTRATES

Alkanethiols 1-dodecanethiol (HS-(CH₂)₁₁-CH₃), 11-mercapto-1-undecanol (HS-(CH₂)₁₁-OH), and 11-mercaptoundecanoic acid (HS-(CH₂)₁₀-COOH) were purchased from Sigma-Aldrich Chemical (St. Louis, MO). Glass coverslips (Microscope Cover Glass, Fisher Scientific International, Fairlawn, NJ) were used as SAM substrates. The gold coated glass coverslips were prepared by sequential deposition of optically transparent films of titanium (10nm) and gold (20nm). The function of a 10 nm titanium layer deposited between glass coverslips and gold layer was to enhance the adhesion of gold layer on the substrates. A magnetron sputtering machine (ISE-OE-PVD-3000 DC AND RF MAGNETRON SPUTTERING MN 500 SYSTEM) as shown in **Figure 3-3** and **Figure 3-4** was used for Ti

and Au deposition at a chamber base-pressure 1.5×10^{-7} torr with a deposition rate 4 \AA/sec for Ti and 5 \AA/sec for Au. The gold coated glass coverslips were immersed in 0.001M ethanolic alkanethiol solutions (1 mM in absolute ethanol) and SAM were allowed to assemble for 12 hr. Before use, the substrates were rinsed in the solution of $\text{H}_2\text{O}:\text{C}_2\text{H}_5\text{OH}$ (volume ratio 1:1) and dried with N_2 . The procedure of surface modification of glass coverslips is presented in **Figure 3-5**.

The surface morphology was examined by AFM in tapping mode (Atomic Force Microscopy, Digital Instruments, Inc., model D-3100) and SEM in SE and BSE mode (Scanning Electron Microscopy, Philips XL30FEG). The surface composition was obtained by XRD (XRD, Philips Analytical Inc.). The surface wettability was measured by using DSA100 (KRÜSS GmbH) contact angle measurement system.

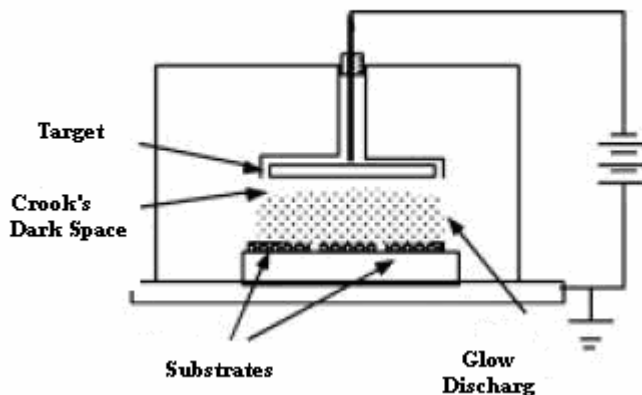


Figure 3-3 Sputtering system schematic (Information is from <http://cnx.rice.edu>).



Figure 3-4 The image of sputtering system (ISE-OE-PVD-3000 DC AND RF
MAGNETRON SPUTTERING MN 500 SYSTEM).

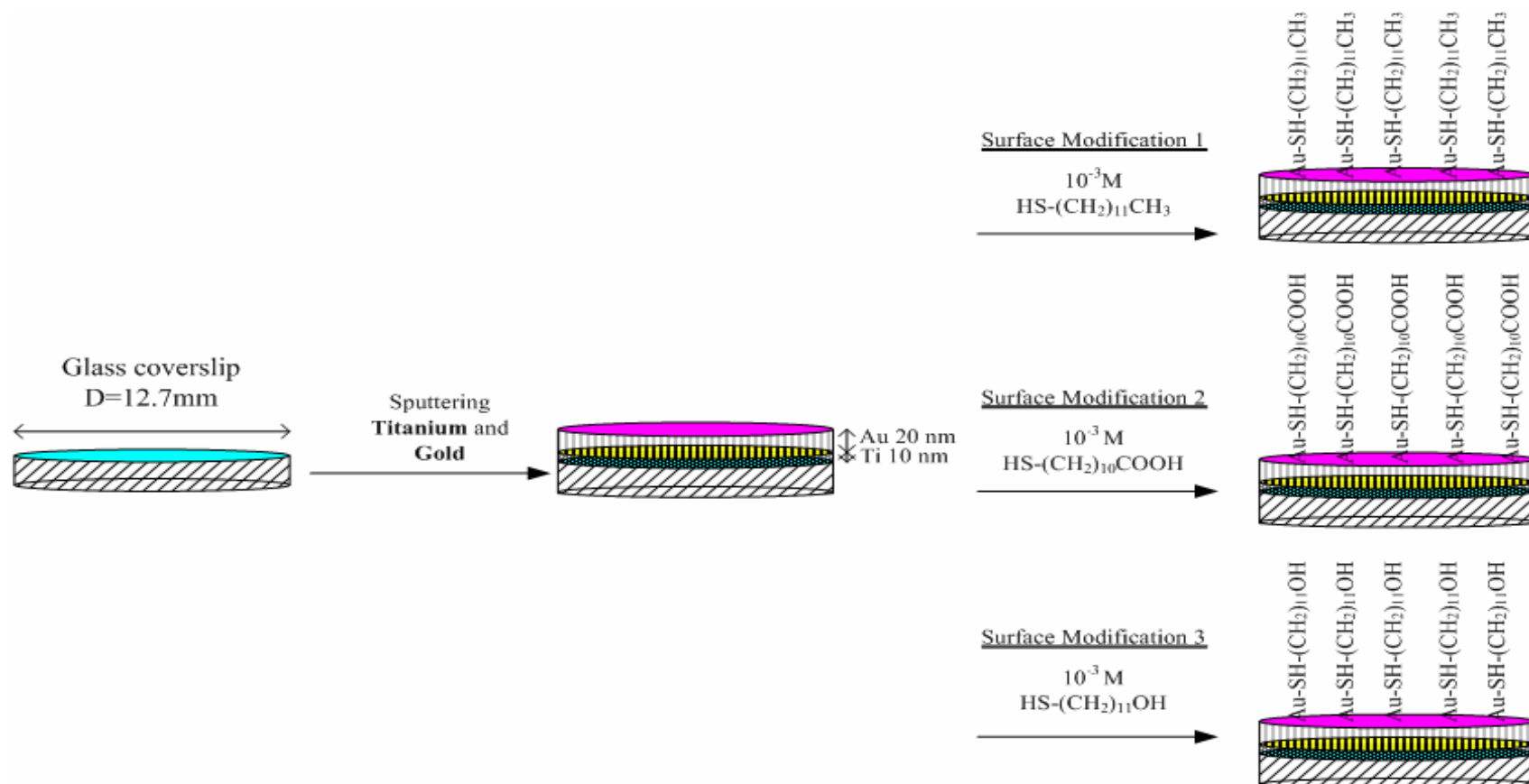


Figure 3-5 Schematic of surface modification of glass coverslips.

3.4 POLYCAPROLACTONE(PCL) SUBSTRATES

The polymer, 500g Poly (caprolactone) (PCL), was purchased from Sigma- Aldrich Chemical (St. Louis, MO). Solutions of PCL in tetrahydrofuran (THF) (0.8g/8ml) were mixed in the sealed beaker stirred for 24hours. In addition to THF, acetone (8 ml) and dichloromethane (8 ml) were, respectively, adopted to be the solvent to dissolve PCL (8 g). After 24 hours stirring, the transparent polymer solution was poured into a 2 inch circular Teflon mold dish. The culture dish had to be sealed and created 5-10 small pores on seal tape in order to control the evaporation rate of THF. High evaporation rates would lead to curved PCL films which are not desired. The films were placed in a flat culture dish in air bench hood until all the THF evaporated (5 to 8 hours). The PCL films were directly removed from the culture dish or soaking in a water bath at room temperature until the films could be peeled off. In order to fit the plastic cell culture plate, PCL films were cut to a circle form with 0.7 inch diameter. One film was cut to about 4-5 small substrates.

3.4.1 Aminolysis of poly(caprolactone)

A procedure reported by Zhu et al. [18] was used in order to incorporate amino groups onto the surface of PCL using 1, 6-hexanediamine. PCL substrates, 0.7 inch in diameter, were immersed into a 10 wt% solution of 1, 6-hexanediamine (10 g) prepared in isopropanol (90 g). The substrates were exposed to the chemical treatment at room temperature for 3 hr. After the exposure, the polymer substrates were thoroughly washed in deionized, distilled water and were dried at room temperature.

3.4.2 Attachment of dodecanedicarboxylic acid/ tetradecanoic acid to the aminolyzed PCL surface

0.258 g of dodecanedicarboxylic acid (or 0.228 g of tetradecanoic acid) was prepared in a 100 ml of deionized water to form a 0.01M solution. The dissolving procedure was processed in ultrasonic vibrator at 40 °C setting temperature until all the solutes were completely dissolved into the solvent. The solution was, then, pipetted over the surface of the aminolyzed poly(caprolactone) disks at a concentration of 0.8µg of dodecanedicarboxylic acid per mm² of surface area. The solution was maintained in the surface of the polymer for 3 hours at room temperature. Afterwards, the disks were washed in phosphate buffered saline (PBS) buffer and sterilized for the cell attachment studies, or thoroughly washed with ultra pure water and dried.

The overall procedure of surface modification of PCL disks is presented in **Figure 3-6**. The surface morphology was examined by SEM, (SEM, Philips XL30FEG) and the surface wettability was measured by using DSA100 (KRÜSS GmbH), after every surface treatment to observe the surface morphologic and wettability change.

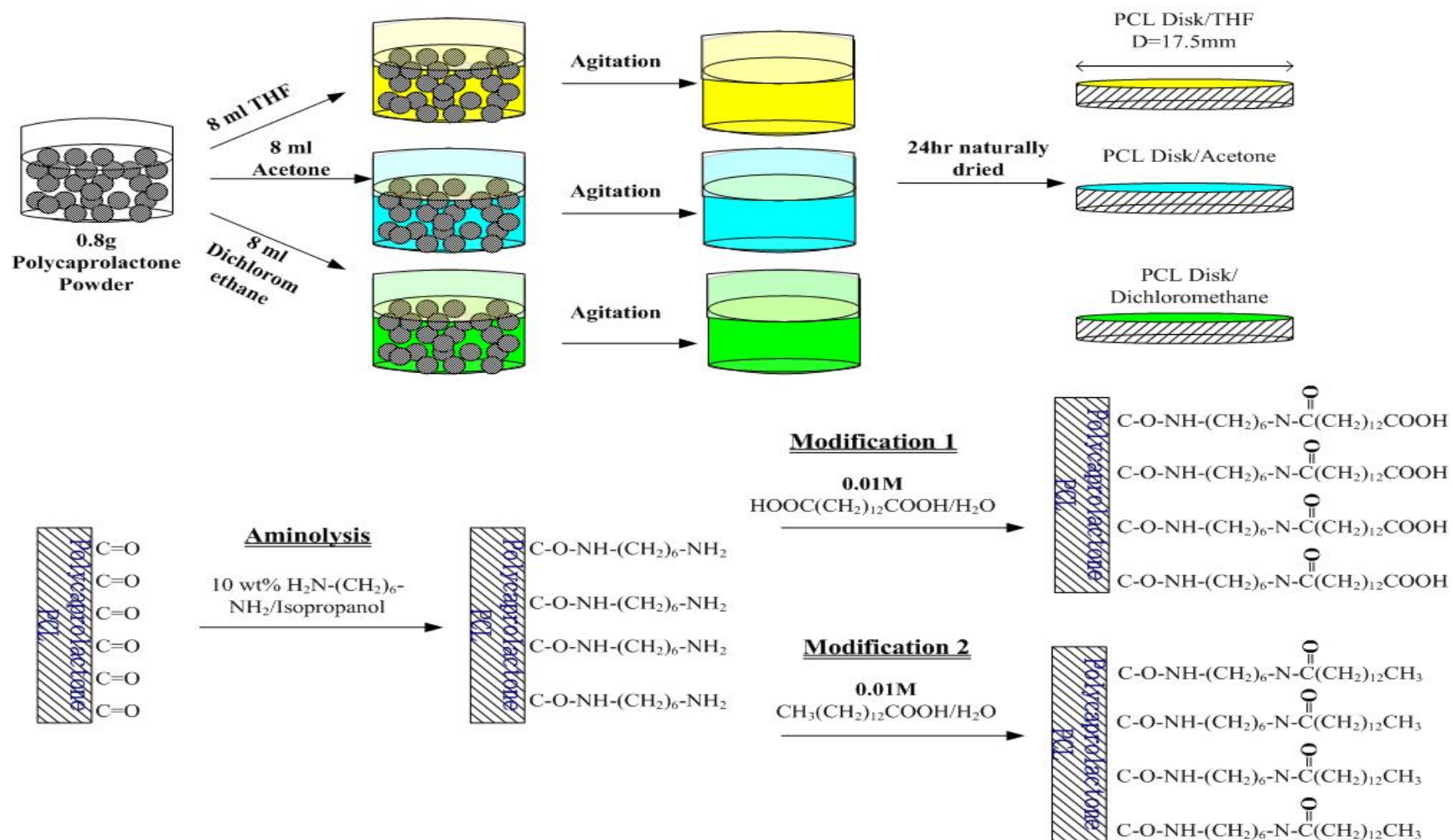


Figure 3-6 Schematic of surface modification of PCL disk.

3-5 CELL CULTURE EXPERIMENTS

The procedure^{***} used for the cell culture is listed in Appendix B. These procedures were provided and instructed by Dr. Kacey Marra and her graduate student Candace.

The data of cell differentiation are used to examine the outgrowth of neuron-like cells (PC12 cells) and the sprout of neurites. The optical microscopy is used to observe cell differentiation and the photo is taken using the SONY digital camera. Because of the limitation of optical microscopy, the substrates have to be transparent like mica or glass substrates. PCL substrates, which are not transparent, can only provide vague images as shown in **Figure 3-7**.

The data of cell proliferation are used to count the number of cells reproduced on the substrates after a specific time period such as 12, 24, 48 hours, and the data of cell attachment present that the number of cells attached onto the substrates. Both of them can be measured by hemacytometer method and histological assessment which are described in Appendix B. The cell attachment data showed in this thesis were using histological assessment.

^{***} The procedure of the cell culture is listed in Appendix B.

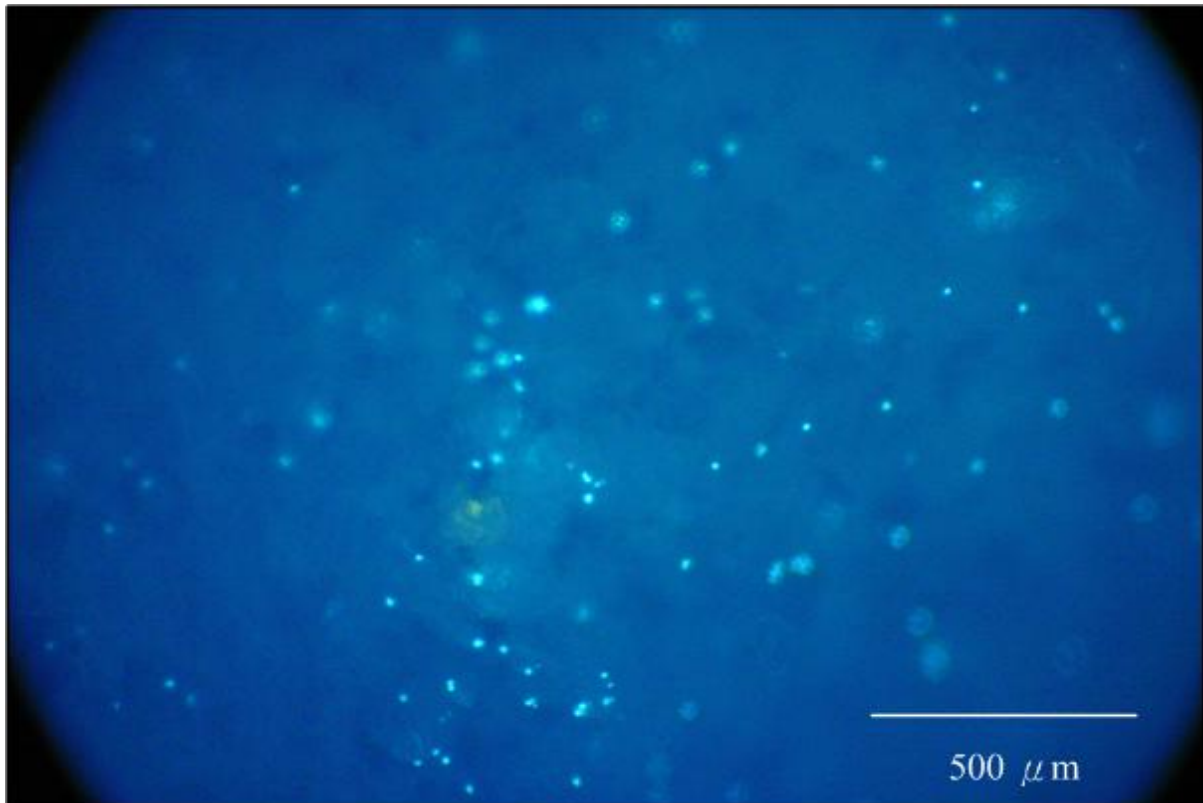


Figure 3-7 The OM image of the PCL substrate after 12 hr cell culture.

3-6 CONTACT ANGLE MEASUREMENT

The equipment, DSA100 (KRÜSS GmbH) as shown in **Figure 3-8**, was used to measure the contact angles between substrates and water drops. DSA 100 has a video system which can take pictures of drops on the substrates and provided 5 methods (Tangent methods 1, Tangent methods 2, Height- Width method, Circle Fitting method and Young-Laplace method (sessile drop fitting) to evaluate contact angles. In our system, Circle Fitting method

and Young- Laplace method were adopted since water drops on the substrates were approximately hemispherical.

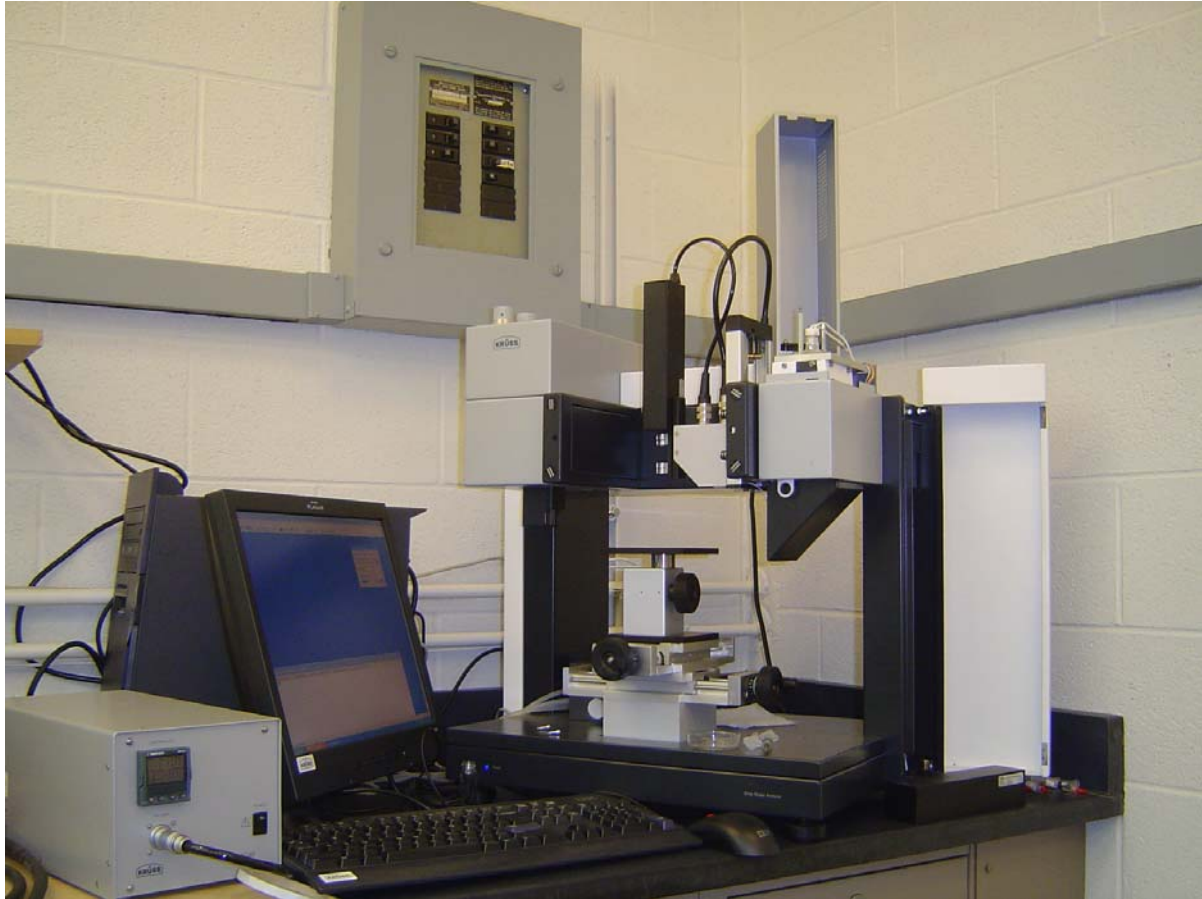


Figure 3-8 The image of contact angle measurement system, DSA100 (KRÜSS GmbH).

In 1805, Young [50] had already formulated a relationship between the interfacial tensions at a point on a 3-phase contact line as shown in **Figure 3-9**. Italic “s” and italic “l” stand for “solid” and “liquid”; the symbols σ_s and σ_l describe the surface tension of the liquid and the surface energy of the solid; symbol γ_{sl} represents the interfacial tension between the two

phases, and θ stands for the contact angle corresponding to the angle between vectors σ_l and γ_{sl} .

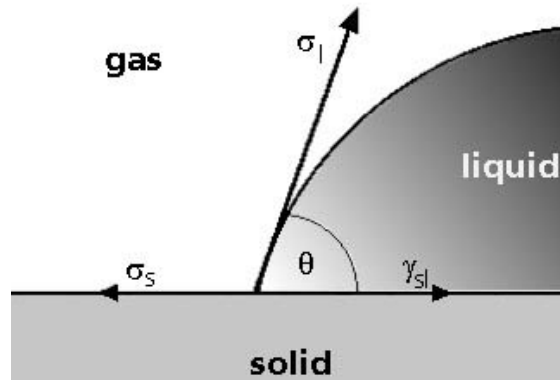


Figure 3-9 Contact angle formation on a solid surface according to Yung's theory.

Young formulated the following relationship between these quantities:

$$\sigma_s = \gamma_{sl} + \sigma_l \cos \theta$$

The methods implemented in the DSA100 program allow the determination of the surface energy of solids from contact angle data. They are mainly based on combining various starting equations for γ_{sl} with Young's equation to obtain equations of state in which $\cos \theta$ represents a function of the phase surface tensions and, if applicable, the (polar and disperse) tension components $\sigma_{l,D}$, $\sigma_{l,P}$, $\sigma_{s,D}$, $\sigma_{s,P}$.

As liquids with known surface tension data and known polar and disperse fractions are used it is possible to include $\sigma_{l,D}$ and $\sigma_{l,P}$ in the equations. All methods assume that the interactions

between the solid and the gas phase (or the liquid vapor phase) are so small as to be negligible. The methods are described in the following sections.

3.6.1 Methods of evaluating the drop shape

The basis for the determination of the contact angle is the image of the drop on the drop surface. In the DSA100 program the actual drop shape and the contact line (baseline) with the solid are first determined by the analysis of the grey level values of the image pixels. To describe this more accurately, the software calculates the root of the secondary derivative of the brightness levels to receive the point of greatest changes of brightness. The drop shape measured is adapted to fit a mathematical model which is then used to calculate the contact angle. The various methods of calculating the contact angle differ in the mathematical models used for analyzing the drop shape. Either the complete drop shape, part of the drop shape or only the area of phase contact are evaluated. All methods calculate the contact angle as tangent at the intersection of the drop contour line with the solid surface line (base line).

(A) Circle fitting method

As in the height-width method, in this method the drop contour is also fitted to a segment of a circle. However, the contact angle is not calculated by using the enclosing rectangle, but by fitting the contour to a circular segment function. The same conditions apply to the use of

this method as to the height-width method with the difference that a needle remaining in the drop disturbs the result far less.

(B) Young-Laplace (sessile drop fitting)

The most complicated, but also the theoretically most exact method for calculating the contact angle is the Young-Laplace fitting. In this method the complete drop contour is evaluated; the contour fitting includes a correction which takes into account the fact that it is not just interfacial effects which produce the drop shape, but that the drop is also distorted by the weight of the liquid it contains. After the successful fitting of the Young-Laplace Equation the contact angle is determined as the slope of the contour line at the 3-phase contact point.

If the magnification scale of the drop image is known (determined by using the syringe needle in the image) then the interfacial tension can also be determined; however, the calculation is only reliable for contact angles above 30° . Moreover, this model assumes a symmetric drop shape. Therefore, it cannot be used for dynamic contact angles where the needle remains in the drop.

3.6.2 Contact angle hysteresis

The contact angle hysteresis is simply calculated by subtracting the measured advancing (maximum) contact angle with the measured receding (minimum) contact angle i.e. $H = \theta_a - \theta_r$. One can thus say that the hysteresis is the range of stable *apparent* contact angles that can be measured for the system.

The hysteresis is mainly due to surface roughness, chemical contamination or heterogeneity of the solid substrate, and/or deposition of solutes (surfactants, polymers) from the liquid onto the solid surface.

4.0 RESULTS AND DISCUSSIONS

4.1 NEURON CELL OUTGROWTH ON MODIFIED MICA SURFACE

That generation 4 PAMAM dendrimers in pentanol solution can chemically bond (ionic bonding) to the mica surface due to the positive charge on dendrimer's amino groups and the negative charge on mica surface has been reported in Xu et al. [51, 52]. The permanent positive charge provided by dendrimer's amino groups was used to verify if surface charge could enhance PC12 cells outgrowth as well as cell proliferation. After a 12 hr cell culture with nerve growth factor (NGF), optical microscopy images, **Figure 4-1** and **Figure 4-2**, showed that neurites started to sprout and considerable neuron cell adhesion on mica substrates coated with multilayer dendrimers but uncoated and monolayer coated mica substrates showed no cell adhesion.

Preliminary attempts to measure quantitative data on mica substrates yielded inconclusive results. It is possible that part of the adsorbed dendrimer gets desorbed into the water based media containing cells. It is also possible that some of cells could bind to the dendrimer molecules in the liquid phase. Although no quantitative data were collected, the OM images showed a result which motivated further studies on surface modifications which could lead to enhance neuron cell outgrowth.

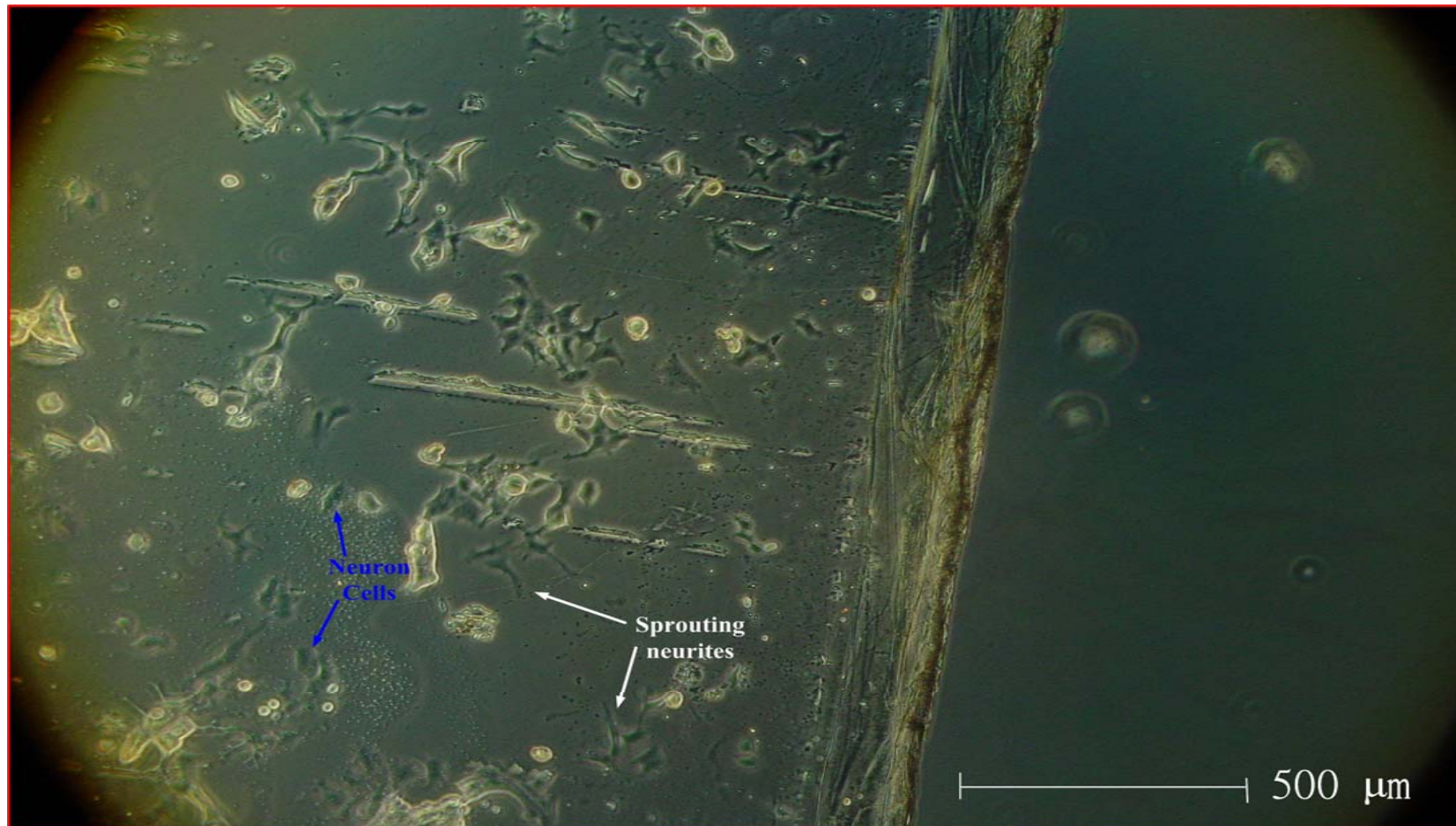


Figure 4-1 Optical microscopy image of 12 hr neuron cell culture on mica substrate coated with multi-layers of PAMAMA dendrimers

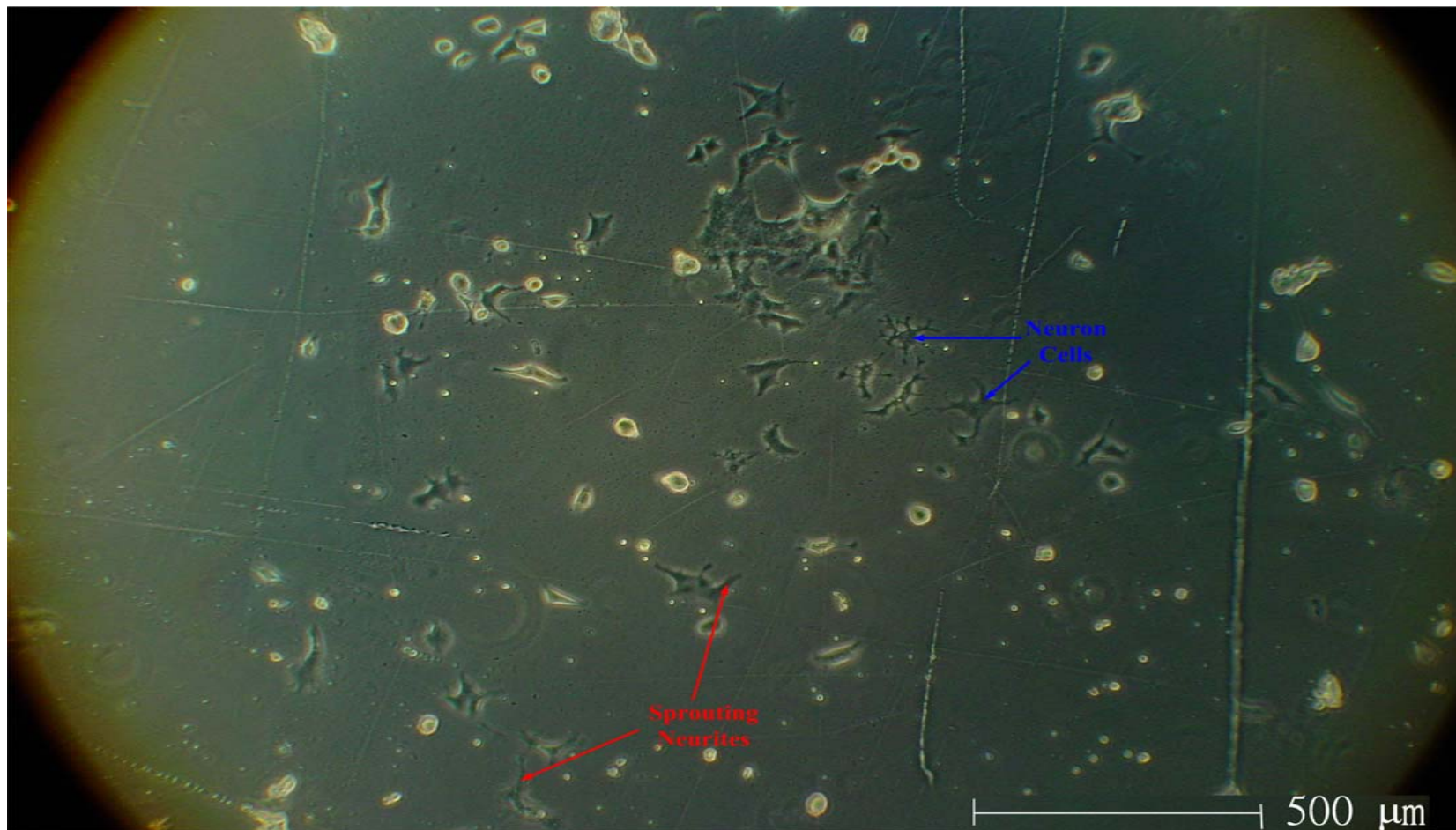


Figure 4-2 Optical microscopy image of 12 hr neuron cell culture on mica substrate coated with multi-layers of PAMAMA dendrimers

4.2 CELL CULTURE ON SURFACE OF MODIFIED GLASS SUBSTRATES

In this study, three functional end groups X (X= -CH₃, -OH, and -COOH) were used to examine the effect of surface properties on cell outgrowth and adhesion. Surface bonded with -CH₃ presents a nonpolar hydrophobic surface, whereas -OH provides a neutral hydrophilic surface, and the -COOH displays a negatively charged surface at pH=7.0[13].

4.2.1 Atomic force microscopy (AFM) analysis

As shown in **Figure 4-3**, the average plane roughness (Ra) of non-modified glass coverslips is 0.064 nm (Rmax=0.390 nm). After the glass surface was coated with titanium and gold, the average plane roughness considerably increased to as high as 4.663 nm (Rmax=21.040 nm), because gold deposited onto the glass surface and formed island shape surfaces as shown in **Figure 4-3**, and all formulas of parameters shown in the AFM images are listed in **Appendix C**.

The surface roughness increased slightly after 1- dodecanethiol bonded onto the gold-coated glass coverslips (Ra=5.328 nm and Rmax=19.659 nm) as shown in **Figure 4-4**. The surfaces have roughness, however, decreased after 11-mercaptoundecanoic acid and 11-mercapto-1-undecanol, respectively, bonded on to gold-coated surfaces. The average plane roughness of the gold-coated surface modified by 11-mercaptoundecanoic acid is 0.190 nm (Rmax= 1.020 nm), and Ra=0.394 nm (Rmax=1.829 nm) for the gold-coated surface modified by 11-mercapto-1-undecanol. **Figure 4-5** and **Figure 4-6** are AFM images of gold-coated glass surface modified by 11-mercaptoundecanoic acid and 11-mercapto-1-undecanol. The decrease in roughness of a gold surface via self-assembled

monolayers (SAMs) of thiol surfactants such as 16-mercaptohexadecanoic acid and 11-mercapto-1-undecanol is consistent with the work reported by Sergey et al. [53]. However, this passivation, the surface become smoother, was not obviously observed when gold-coated surface modified by 1- dodecanethiol. The reason is that hydrophobic terminated SAMs provides less passivating ability in polar solvents because polar solvents lead to poor intermixing and loosen the chain packing[54].

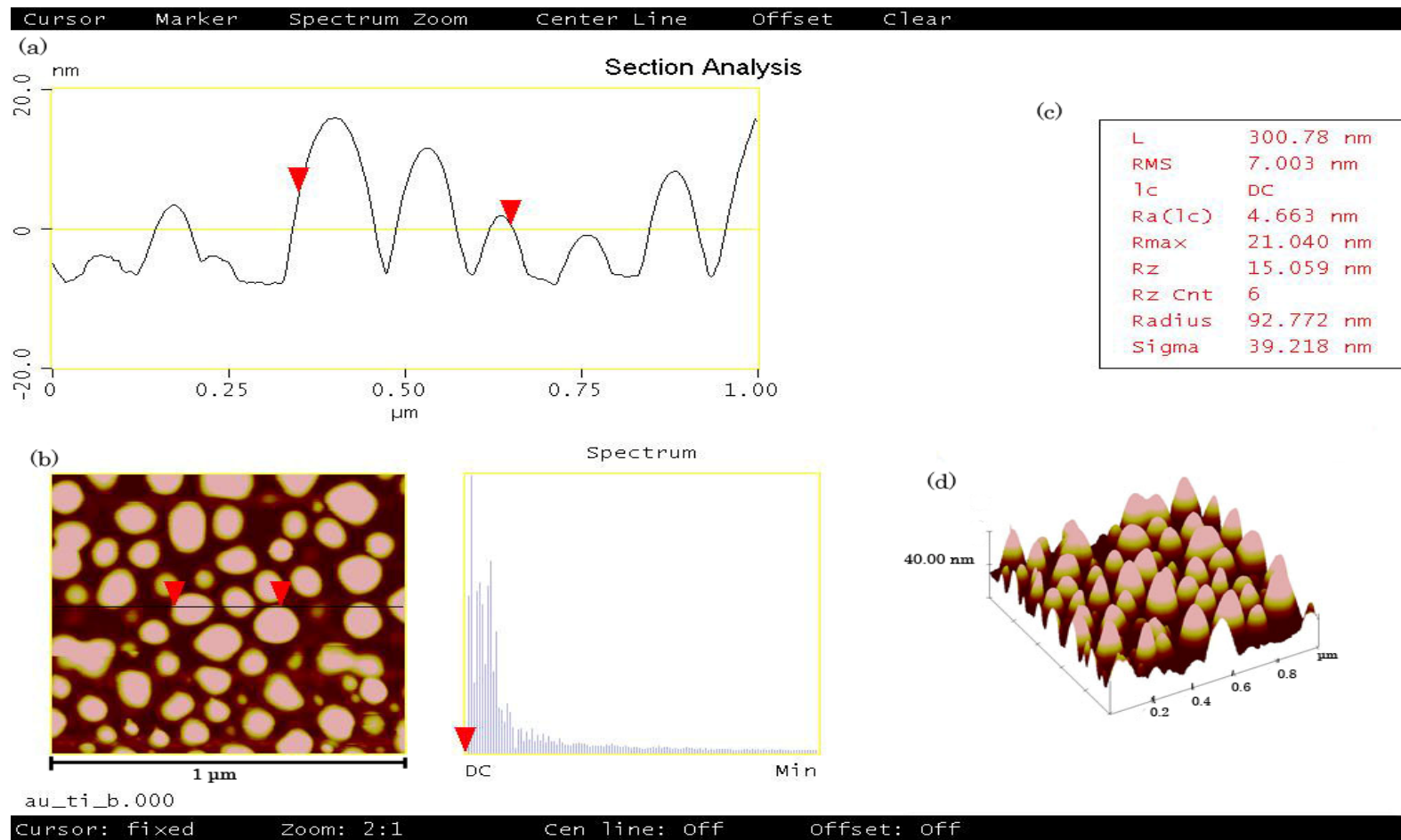


Figure 4-3 AFM image of glass coverslip coated with 10 nm titanium (bottom layer) and 20 nm gold (upper layer) (a) the cross-section image; (b) 2-D image; (c) the related data of surface roughness and (d) 3-D image.

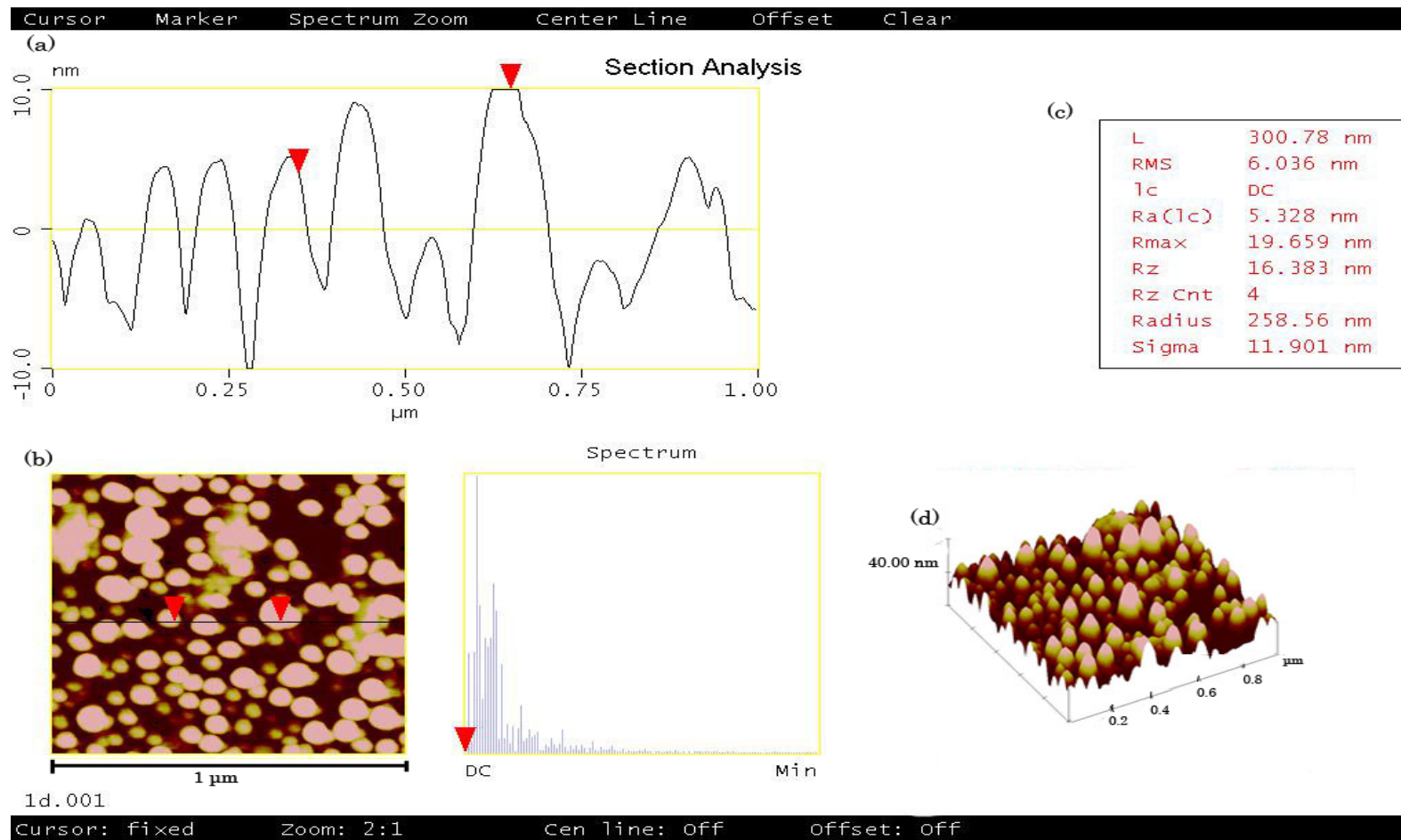


Figure 4-4 AFM image of gold-coated glass coverslip after surface has been passivated with 1- dodecanethiol. (a) the cross-section image; (b) 2-D image; (c) the related data of surface roughness and (d) 3-D image.

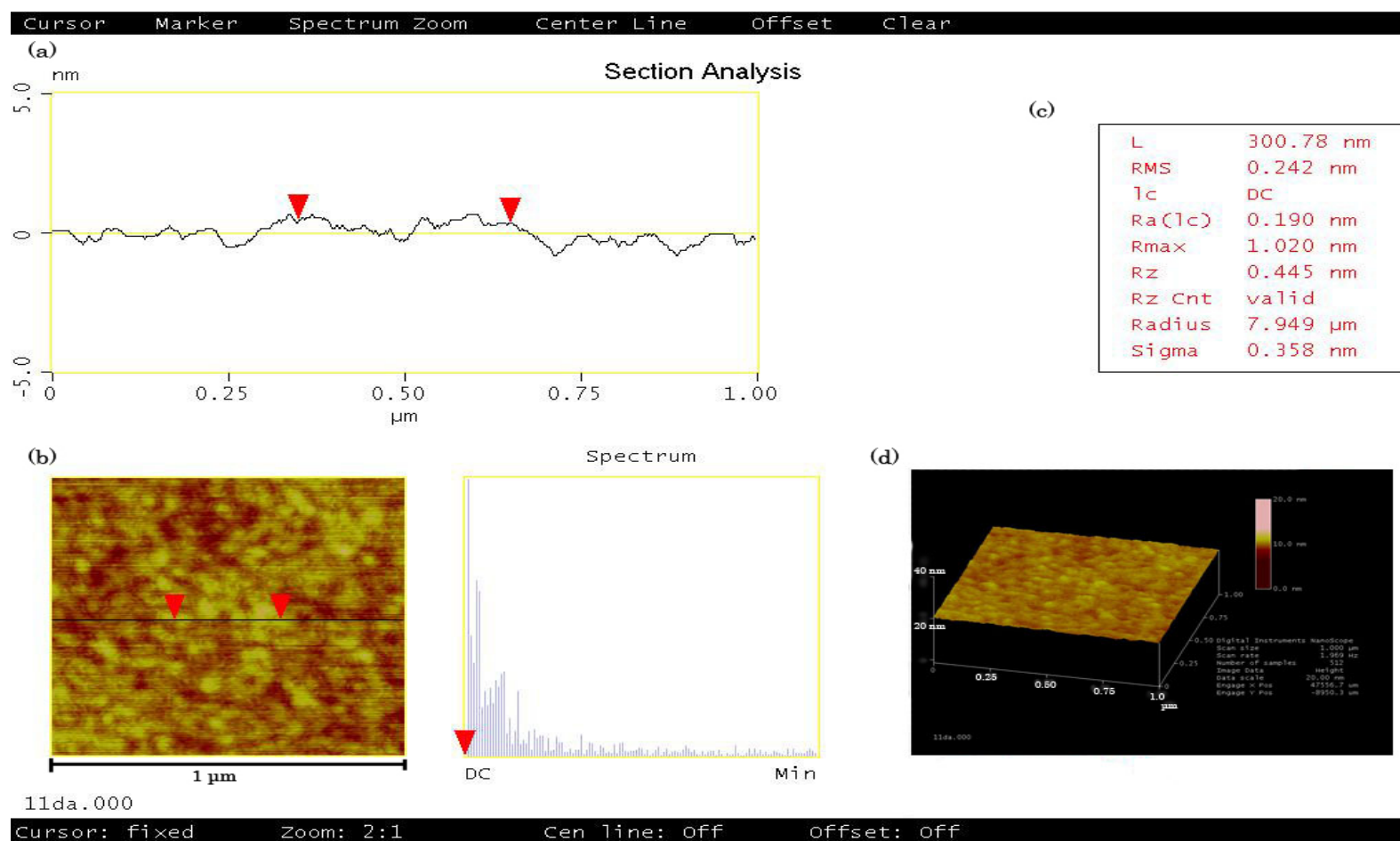


Figure 4-5 AFM image of gold-coated glass coverslip after surface has been passivated with 11-mercaptopundecanoic acid. (a) the cross-section image; (b) 2-D image; (c) the related data of surface roughness and (d) 3-D image.

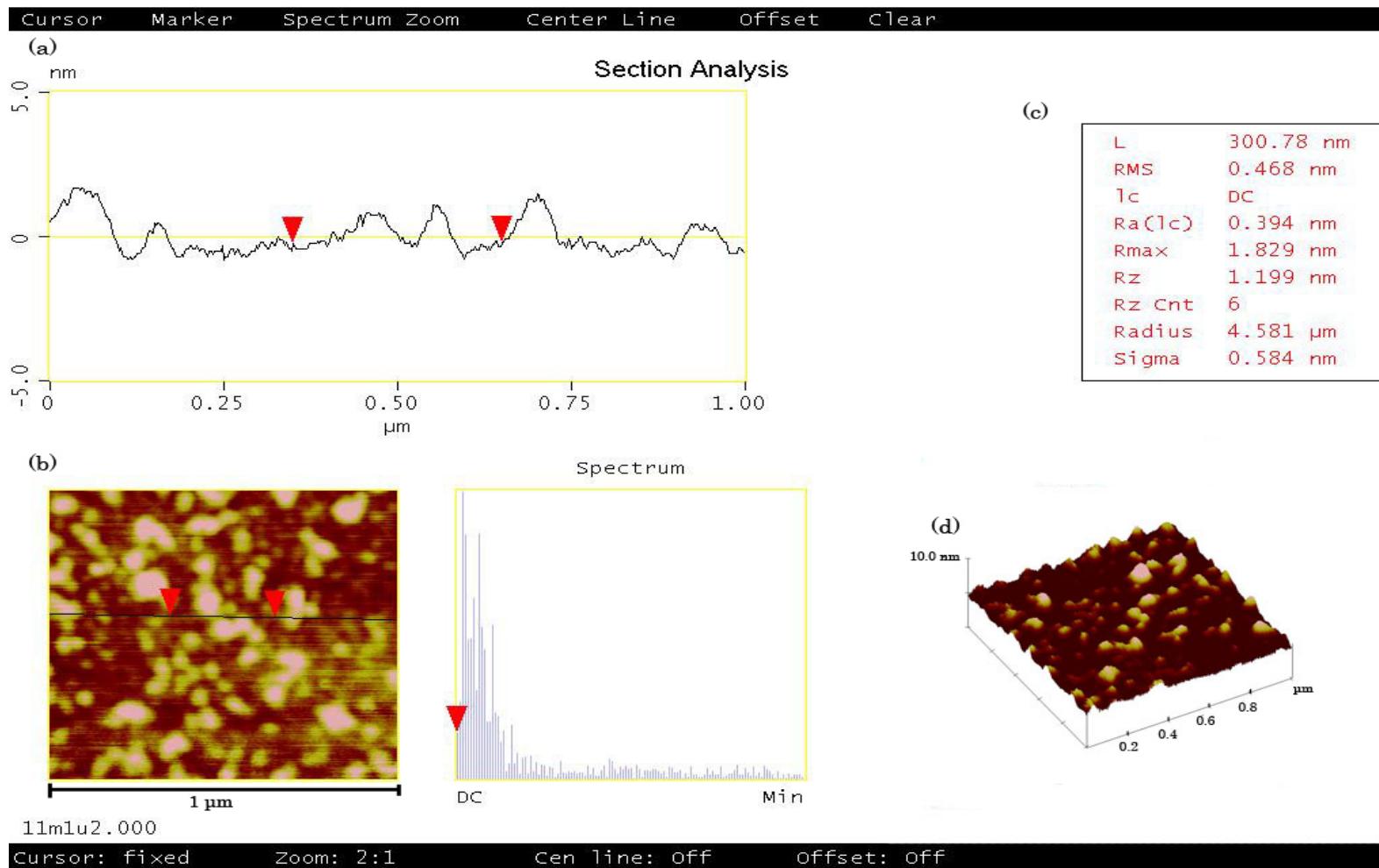


Figure 4-6 AFM image of gold-coated glass coverslip after surface has been passivated with 11-mercapto-1-undecanol. (a) the cross-section image; (b) 2-D image; (c) the related data of surface roughness and (d) 3-D image.

4.2.2 Scanning electron microscopy

Scanning electron micrographs which show the morphology of the modified gold-coated surface are given in **Figure 4-7** and **4-8**. In **Figure 4-7(B)**, some coagulation of thiol surfactants can be observed on 1- dodecanethiol and 11-mercapto-1-undecanol modified surfaces, but 11-mercaptoundecanoic acid modified surface shows very smooth morphology. The similar result is shown in **Figure 4-8**, where the SEM image has higher magnification. Due to the resolution limit of SEM, it is hard to say which surface is smoother. However, SEM images provide some useful information such as coagulation that occurred on 1- dodecanethiol surfactants and surface corrosion on gold-coated surface modified by 11-mercapto-1-undecanol.

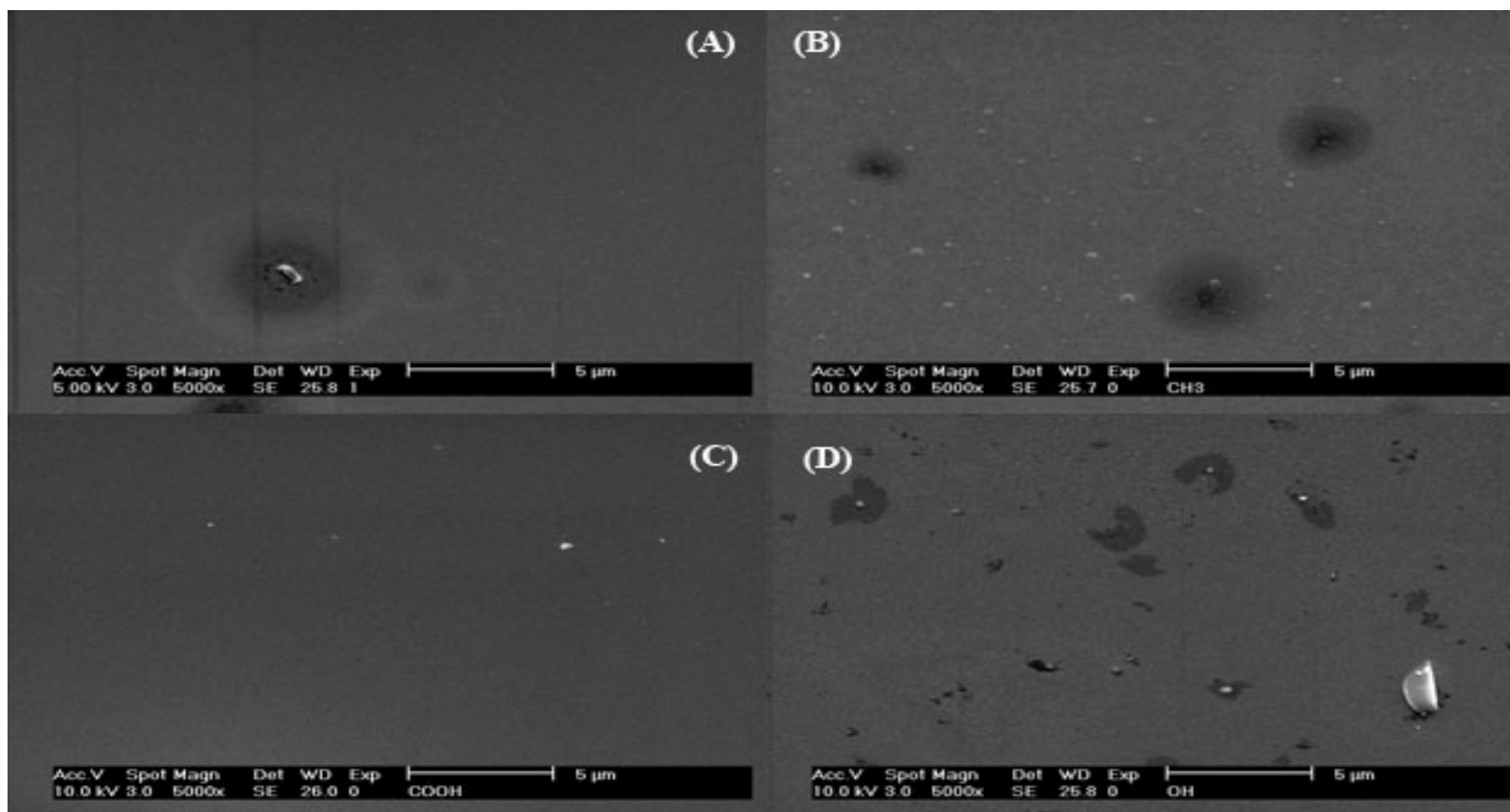


Figure 4-7 SEM images of gold-coated glass coverslips (A) non-modified surface and surface modified by (B) 1- dodecanethiol, (C) 11-mercaptopundecanoic acid and (D) 11-mercapto-1-undecanol at lower magnification.

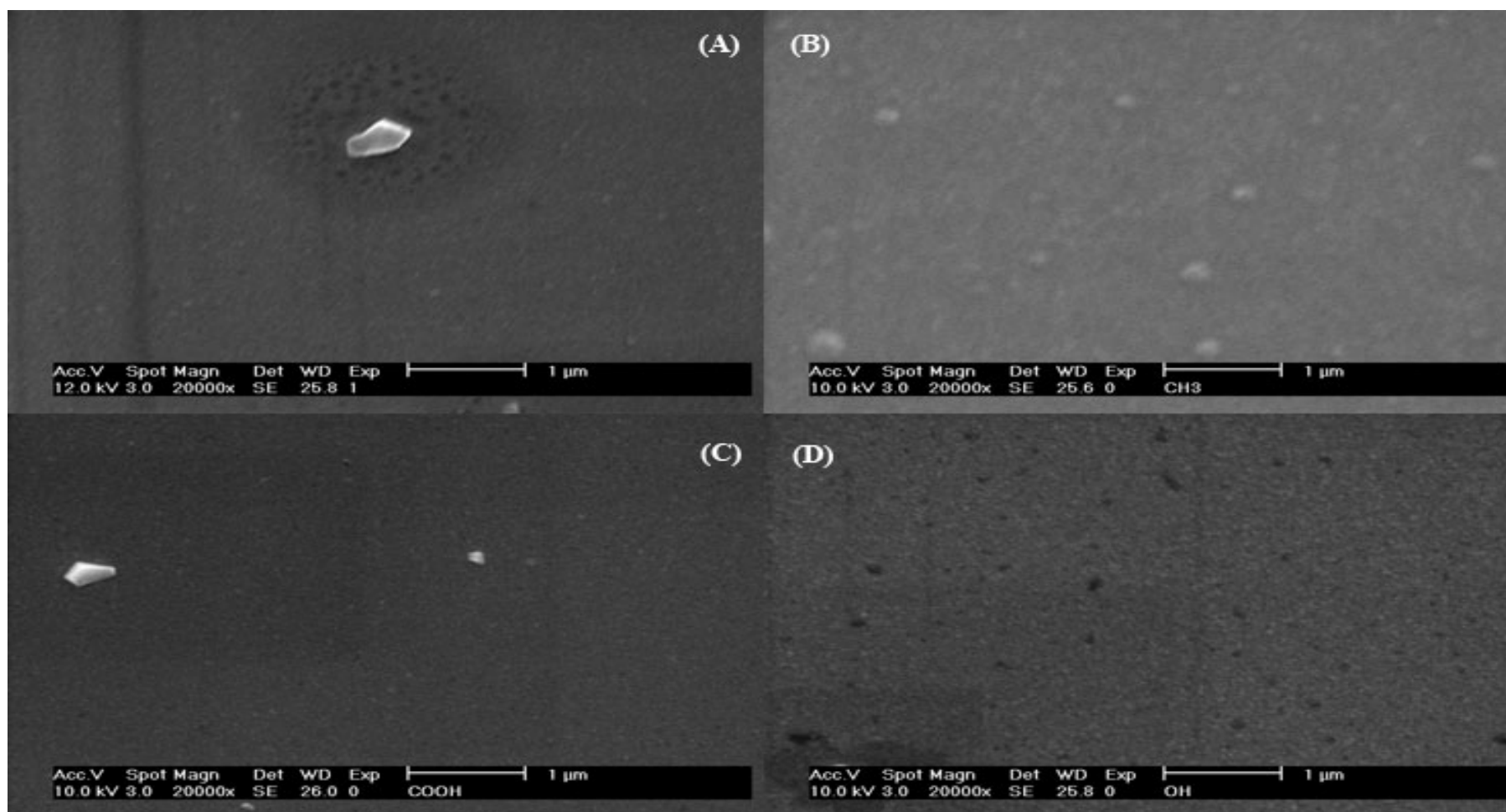


Figure 4-8 SEM images of gold-coated glass coverslips (A) non-modified surface and surface modified by (B) 1- dodecanethiol, (C) 11-mercaptopundecanoic acid and (D) 11-mercapto-1-undecanol at higher magnification.

4.2.3 Wettability of modified glass surfaces

The average contact angles of modified gold-coated surface are shown in **Table 4-1**. In **Table 4-1**, $-\text{CH}_3$ terminated SAMs on gold-coated substrate show hydrophobic surface on which the average contact angle(Θ) of 12 samples is $107.43 \pm 4.6^\circ$; $-\text{COOH}$ and $-\text{OH}$ terminated SAMs on gold-coated substrate are both hydrophilic surface on which the average contact angles (Θ) are $37.24 \pm 2.2^\circ$ and $28.42 \pm 2.0^\circ$ respectively. Comparing to the data in the works of Keselowsky[13, 14] and Hyo-Sok's [54], the average contact angles, in this study, are similar to the data they reported. Based on these results, it is clear that the SAMs terminated with $-\text{COOH}$ and $-\text{OH}$ functionalities yield much higher surface energy than those terminated with methyl($-\text{CH}_3$) group.

Since Phosphate-buffered saline (PBS) is commonly used in washing the disks for cell culture, it was important to know if the contact angle of the modified surface changes after exposure to PBS media. **Table 4-2** shows the images of water drops on the modified surface which have been exposed to PBS for 12 hours. As **Table 4-2** shows, it is difficult to measure contact angles after modified glass coverslip dipped in PBS media due to the irregular shapes of water drops. Although the values of contact angle cannot be measured, the images in **Tables 4-2** present that all modified surfaces become hydrophilic including the gold-coated surface modified with 1-dodecanethiol.

Table 4-1 Contact angle and the image of water drops (the volume of each water drop is 0.3 μ l) on the modified gold-coated surface

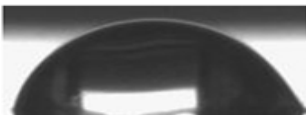

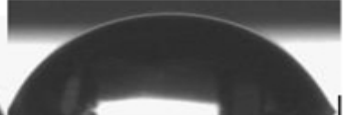








| | Contact angle (°) Water @ 24.5° C | Image of water drops on the modified surface | | |
|--|--|---|---|--|
| Gold-coated surface | 76.56 \pm 3.9 |  |  |  |
| 1-Dodecanethiol modified surface | 107.43 \pm 4.6 |  |  |  |
| 11-Mercaptoundecanoic acid modified surface | 37.24 \pm 2.2 |  |  |  |
| 11-Mercapto-1-undecanol modified surface | 28.42 \pm 2.0 |  |  | |

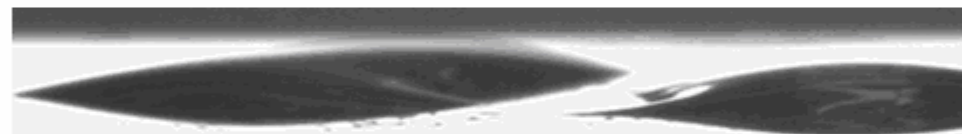
Table 4-2 The image of water drops(the volume of each water drop is 0.3 μ l) on the modified gold-coated surface after dipping in PBS for 12 hr

**1- dodecanethiol
modified gold-coated surface**

**Image of water drops on the modified surface
(After 12 hr dipping in PBS)**



**11-mercapto-1-undecanol
modified gold-coated surface**



**11-mercaptopundecanoic acid
modified gold-coated surface**



4.2.4 Cell culture analysis on modified surfaces

Figure 4-9 and **Figure 4-10** show that the extent of female and male adipose-derived stem cells (ASCs) outgrowth on modified gold coated surface for 12 hours. After the 12 hour cell culture, well plate has the largest amount of cells deposited on the surface, and the substrate coated with $-\text{CH}_3$ terminated SAMs has the fewest amount of deposited cells. The reason that less cells are adsorbed onto modified gold-coated substrates and blank gold-coated substrates is a result of the residual ethanol solvent which is usually used for sterilization. The sources of residual ethanol are the $\text{H}_2\text{O}:\text{C}_2\text{H}_5\text{OH}$ (1:1) solution used to clean the oil and chemicals on substrates before using and 0.001M ethanolic alkanethiol solutions which were prepared using pure ethanol as a solvent to dissolve solvent thiol surfactants. Because ethanol is usually used for medical sterilization, cells are killed and cell proliferation is prohibited when cells deposit onto the surface of modified gold coated substrates. Based on **Figure 4-9** and **Figure 4-10**, it appears cells prefer that the substrate coated with $-\text{COOH}$ terminated SAMs rather than the surface coated with $-\text{CH}_3$ terminated surface. Since the amount of residual ethanol on each substrate is unknown, it is hard to say whether or not the substrate coated with $-\text{COOH}$ terminated SAMs can enhance cell outgrowth and proliferation. Further research in the absence of ethanol environment is needed.

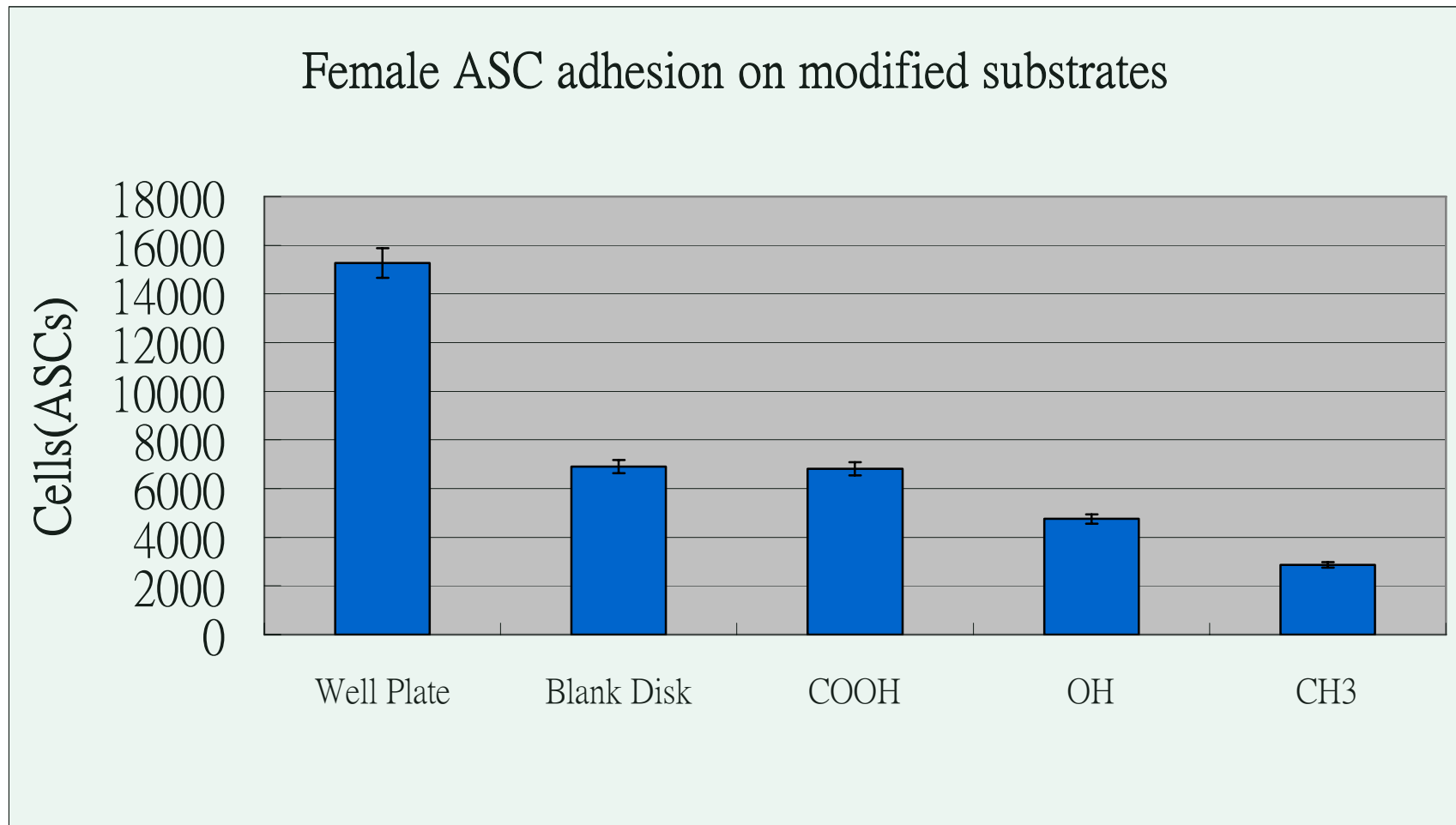


Figure 4-9 Female (age 35) adipose-derived stem cells (ASC) cultured on modified gold-coated glass coverslips for 12 hr.

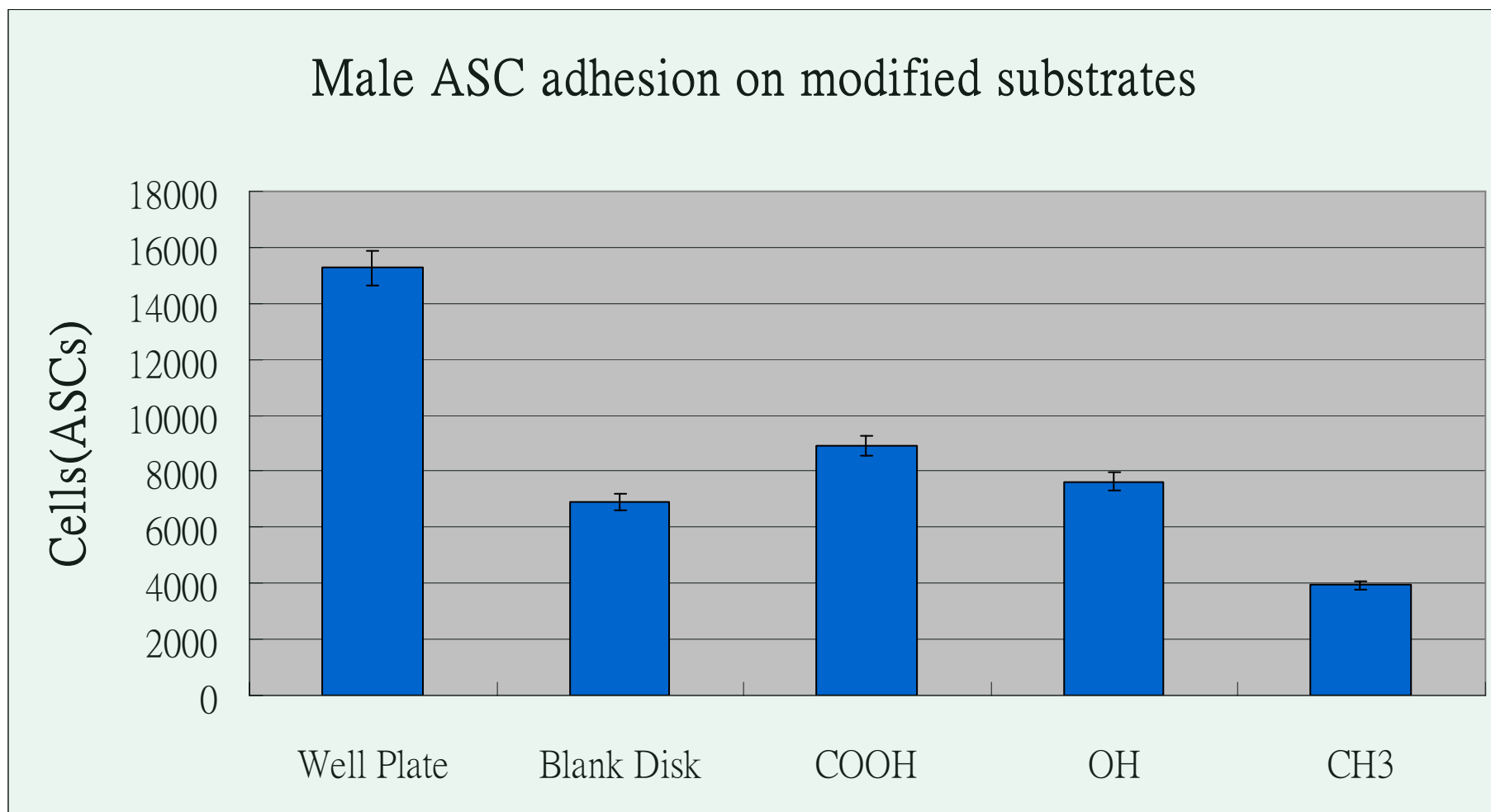


Figure 4-10 Male (age 33) adipose-derived stem cells (ASC) cultured on modified gold-coated glass coverslips for 12 hr.

4.2.5 Discussion of results on cell culture on modified glass surface

According to the data of AFM, SEM, XRD and contact angle measurement, gold-coated glass substrates have been successfully modified. The roughness of modified gold-coated glass substrates is CH_3 ($R_a=5.328$ nm) > OH ($R_a=0.394$ nm) > COOH ($R_a=0.190$ nm) (AFM). The coagulation size of thiol surfactants is CH_3 > OH, COOH (SEM). The surface wettability is OH > COOH > CH_3 (The average contact angles are $107.43^\circ \pm 4.6$, $37.42^\circ \pm 2.2$ and $28.42^\circ \pm 2.0$, respectively).

The number of cells deposited onto modified substrates is COOH > OH > CH_3 has been shown in both **Figure 4-9** and **Figure 4-10**. However, we cannot conclude that the substrate coated with -COOH terminated SAMs can enhance cells outgrowth and proliferation or the substrate coated with $-\text{CH}_3$ terminated SAMs can retard cells outgrowth and proliferation. This is because the residual ethanol has a detrimental effect on the culture.

This work was not pursued further since no ethanol environment is hard to be achieved. Polar solution, ethanol, is used to completely dissolve thiol surfactants which is barely dissolved in water and other polar solutions. In addition, other polar solutions might provide some more unpredictable factors for cell culture. Since gold-coated glass substrates are bio-incompatible, polycaprolactone substrates were used to instead of gold-coated glass coverslips for further study.

4.3 CELL CULTURE ON MODIFIED POLYCAROLACTONE (PCL)

SUBSTRATES

In this study, tetrahydrofuran (THF), acetone and dichloromethane, were used as a solvent to dissolve PCL powders. After the 0.8g/ 8ml PCL solution naturally dried on a Teflon plate, PCL substrates with different surface properties such as morphology and wettability, are formed and used for further surface modification. Then, three functional end groups, X (X=-NH₂, -CH₃, and -COOH) are chemically bonded to the surface of the PCL substrates to examine an effect of surface properties on cell culture. -NH₂ terminated PCL surfaces are formed via aminolization the reaction between 1, 6-hexanediamine and the ester groups of PCL; -CH₃ terminated PCL surfaces are formed from -NH₂ terminated PCL surfaces further reacted with tetradecanoic acid and -COOH terminated PCL surfaces are formed from -NH₂ terminated PCL surfaces further reacted with dodecanedicarboxylic acid.

4.3.1 Scanning electron microscopy analysis

(A) PCL/THF substrates

Figure 4-11 and **Figure 4-12** show the surface morphologies of the modified PCL/THF substrates at different magnifications. The surfaces of PCL/THF substrates exhibit rough surface morphologies compared to the surfaces of PCL/acetone substrates (rougher) and PCL/dichloromethane substrates (smoother). PCL/THF surface shows less porosity than PCL/Acetone surface, and seems to be fused forming many aggregates (diameter from 20 to 100 μ m). After the surface aminolization, many small crystal- like particles (diameter from few to 20 μ m) appear on the modified surface, although

surfaces have been ultrasonically vibrated in deionized water for 60 sec and then soaked for 1 hr. Cracks occur on the substrate surfaces if the sonication time is set for more than 10 minutes. **Figure 4-12** shows the image of modified surface with a higher magnification. Comparing **Figure 4.12 (A)** and **(B)**, two surface morphologies are totally different. The aminolized surface shows smoother morphology and is made up of fused aggregates (diameter less than $10\ \mu\text{m}$).

Figure 4-11 (C) and **Figure 4-12 (C)** show the surfaces of the aminolized PCL/THF substrates further reacted with 0.01 M tetradecanoic acid solution. After the surface modification, the aminolized surface seems to be covered by a thin film. Although we took the image with higher magnification, no pore or crack on the film-like surface can be observed but some crystal-like particles (diameter from few to $10\ \mu\text{m}$) bound to the modified surface can be seen as presented in **Figure 4-12 (C)**.

Figure 4-11 (D) and **Figure 4-12 (D)** show the surfaces of the aminolized PCL/THF substrates further reacted with 0.01 M dodecanedicarboxylic acid solution. The modified PCL/THF substrates exhibit an etched- like surface showing more surface porosity. Many cracks appear on fused aggregates and can be observed in **Figure 4.12 (D)**.

(B) PCL/Acetone substrates

Figure 4-13 and **Figure 4-14** show the surface morphologies of the modified PCL/Acetone substrates at different magnifications. The surfaces of PCL/Acetone substrates also exhibit rough surface morphologies; however, the surface, in this case, is composed of numerous filamentous PCL aggregations. PCL/Acetone substrates show the most porous surface among PCL substrates using THF, acetone and dichloromethane as the solvents. Again, the surface becomes smoother after the surface aminolization, as

shown in **Figure 4-13 (B)** and **Figure 4-14 (B)**. That the surface is made up of smaller filaments which have a diameter from few to 20 μ m can be observed at higher magnification.

Figure 4-13 (C) and **Figure 4-14 (C)** show the surfaces of the aminolized PCL/acetone substrates further reacted with 0.01 M tetradecanoic acid solution. The similar tendency that the aminolized surface is covered by a thin film has been observed. The modified PCL/acetone substrate shows less porosity because many small pores are covered by the thin film.

Figure 4-13 (D) and **Figure 4-14 (D)** show the surfaces of the aminolized PCL/Acetone substrates further reacted with 0.01 M dodecanedicarboxylic acid solution. Not like the surface modified by tetradecanoic acid solution, the surface modified by dodecanedicarboxylic acid solution exhibit more porous surface morphologies. A small amount of particles stuck on the porous surface can be observed in **Figure 4-14 (D)**.

(C) PCL/Dichloromethane substrates

Figure 4-15 and **Figure 4-16** show the surface morphologies of the modified PCL/Dichloromethane substrates at different magnifications. The surface of PCL/Dichloromethane substrates is composed of discrete, spherule-like aggregations (diameters form 50 to 200 μ m) and, therefore, exhibits smooth but uneven surface morphologies. Some tiny pores (diameter less than 5 μ m) on the PCL/Dichloromethane surface can be observed at higher magnification as shown in **Figure 4-16 (A)**. The surface also becomes smoother and the tiny pores disappear after the surface aminolization.

Figure 4-15 (C) and **Figure 4-16 (C)** show the surfaces of the aminolized PCL/Dichloromethane substrates further reacted with 0.01 M tetradecanoic acid solution. The modified PCL/Dichloromethane surface shows completely different morphologies from that of the modified PCL/Acetone and PCL/THF surface. In **Figure 4-15 (C)**, the irregular-shaped particles bond to the PCL/Dichloromethane surface and seem to fuse and spread out on the aminolized surface. This phenomenon occurs because the tetradecanoic acid surfactants have to react with the amino groups on the aminolized PCL surface to form a CONH bonding; meanwhile, they have to aggregate to reach a more stable state. **Figure 4-17** shows more details of particles fused and spread out on the surface. The similar phenomenon does not occur on PCL/Acetone and PCL/THF surfaces because the porous surfaces provide more surface area to react with tetradecanoic acid.

Figure 4-15 (D) and **Figure 4-16 (D)** show the surfaces of the aminolized PCL/Acetone substrates further reacted with 0.01 M dodecanedicarboxylic acid solution. Comparing **Figure 4-15 (A)** and **(D)**, the aminolized PCL/Dichloromethane surface shows no obvious difference, but tiny pores that appeared on non-modified PCL/Dichloromethane have disappeared after the aminolized surface reacts with dodecanedicarboxylic acid.

Based on these SEM images, **Figure 4.11-17**, we can conclude that the surface morphologies of PCL substrates depend on the solubility of PCL powders in the respective solvent systems. The time required for the solvent to dissolve PCL powders is (from shortest to longest) dichloromethane (about 30-60 minutes) < THF (about 5-8 hours) < acetone (more than 12 hours); the degree of roughness is (from rough to smooth) PCL/acetone > PCL/THF > PCL/dichloromethane and the particle size of fused aggregates comprised of PCL substrate is (from large to small) PCL/dichloromethane > PCL/THF > PCL/acetone (filamentous structure). It means that the sooner the solvent

dissolve PCL powders, the smoother the surface will be. The reason is that the less efficient solvents such as acetone are less mixable with PCL powders than the highly efficient solvents such as dichloromethane so that the less efficient solvent evaporate very fast when PCL substrates are naturally dried in the Teflon dish. Because of the higher evaporation rate, the rough surface and the small fused aggregates (or filamentous structure) will be formed on the surface of PCL substrates.

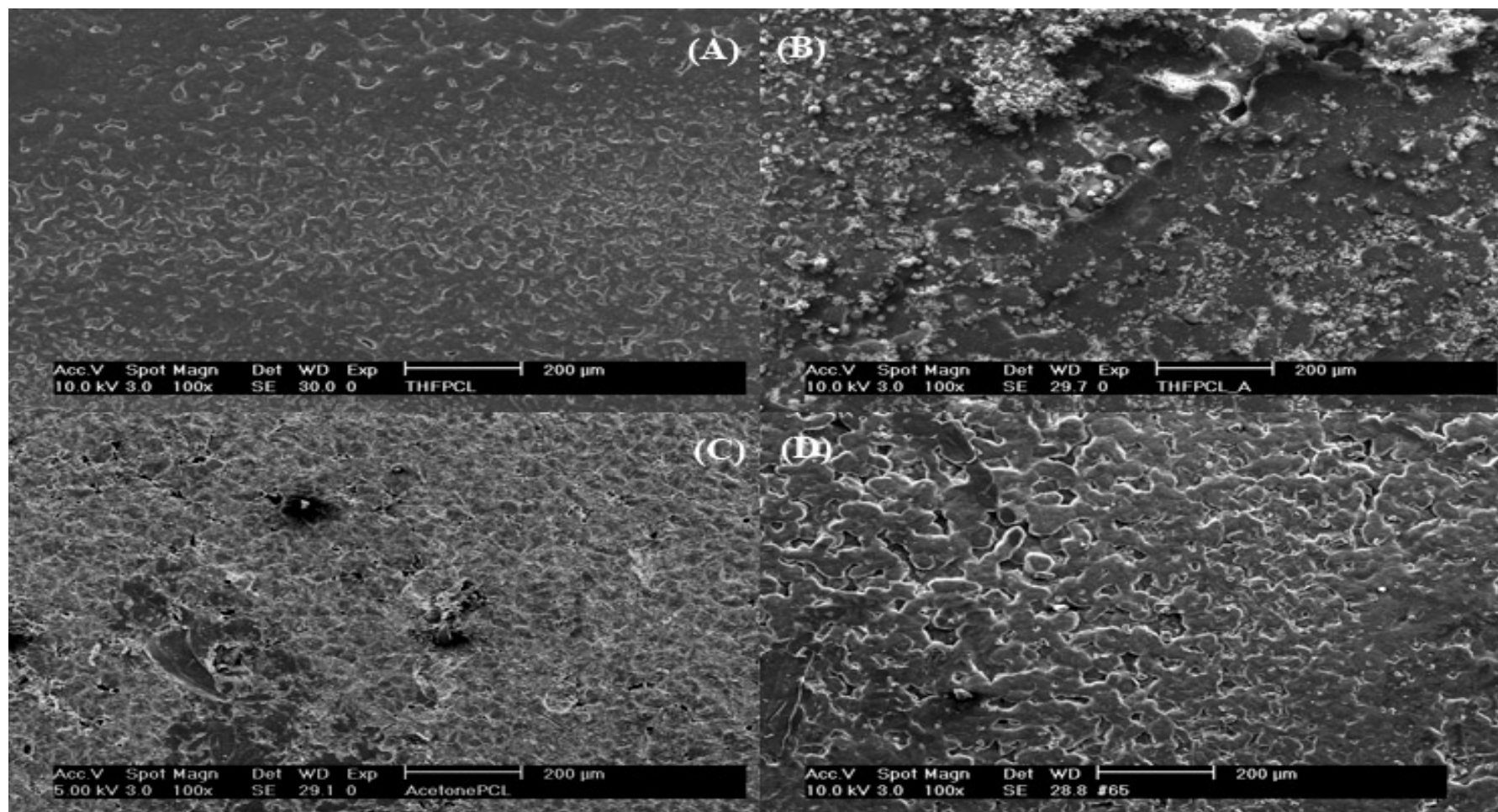


Figure 4-11 SEM images of modified PCL substrates using THF as the solvent (A) non-modified PCL surface; (B) PCL surface after aminolization and PCL surface further reacted with (C) tetradecanoic acid and (D) dodecanedicarboxylic acid at lower magnification.

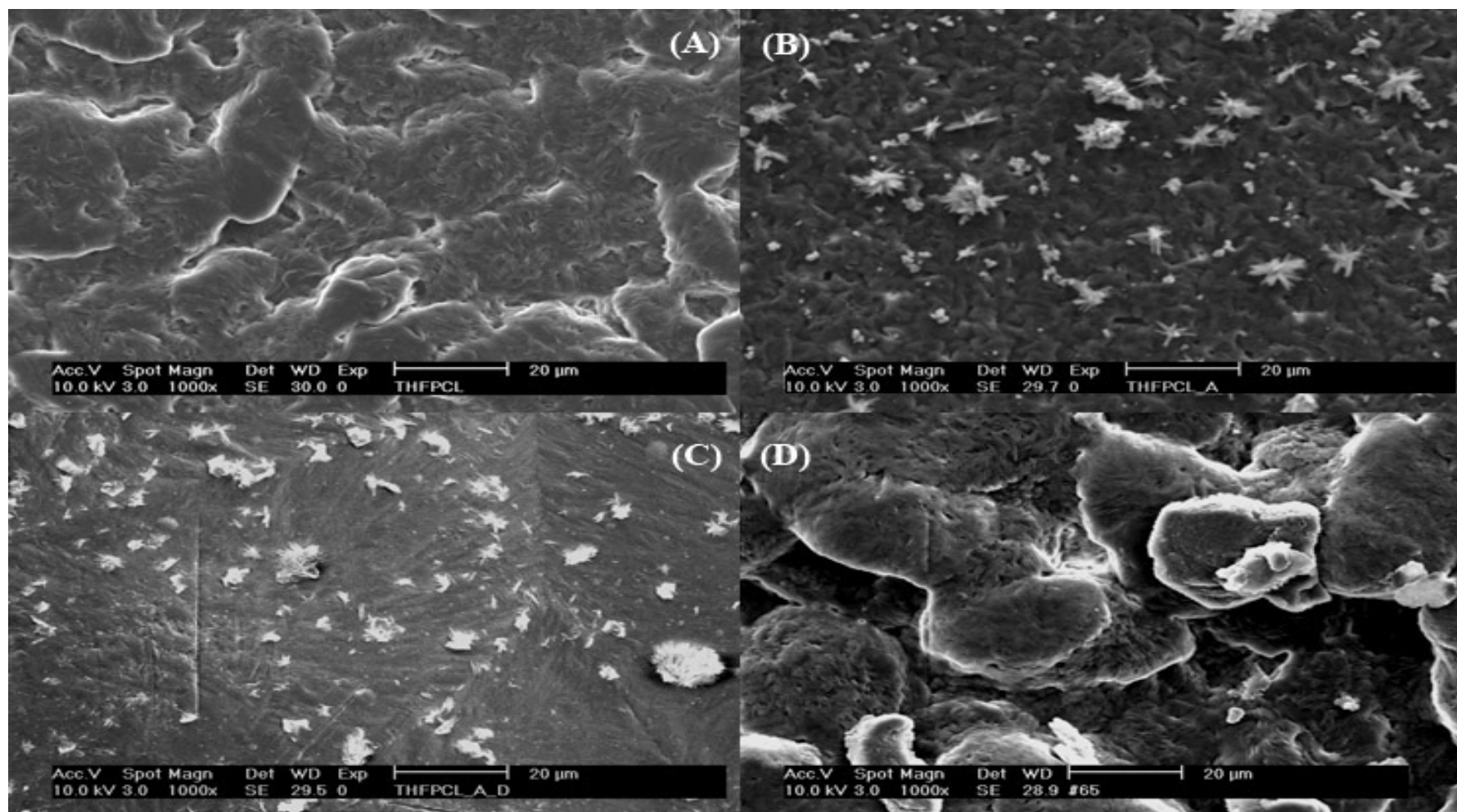


Figure 4-12 SEM images of modified PCL substrates using THF as the solvent (A) non-modified PCL surface; (B) PCL surface after aminolization and PCL surface further reacted with (C) tetradecanoic acid and (D) dodecanedicarboxylic acid at higher magnification.

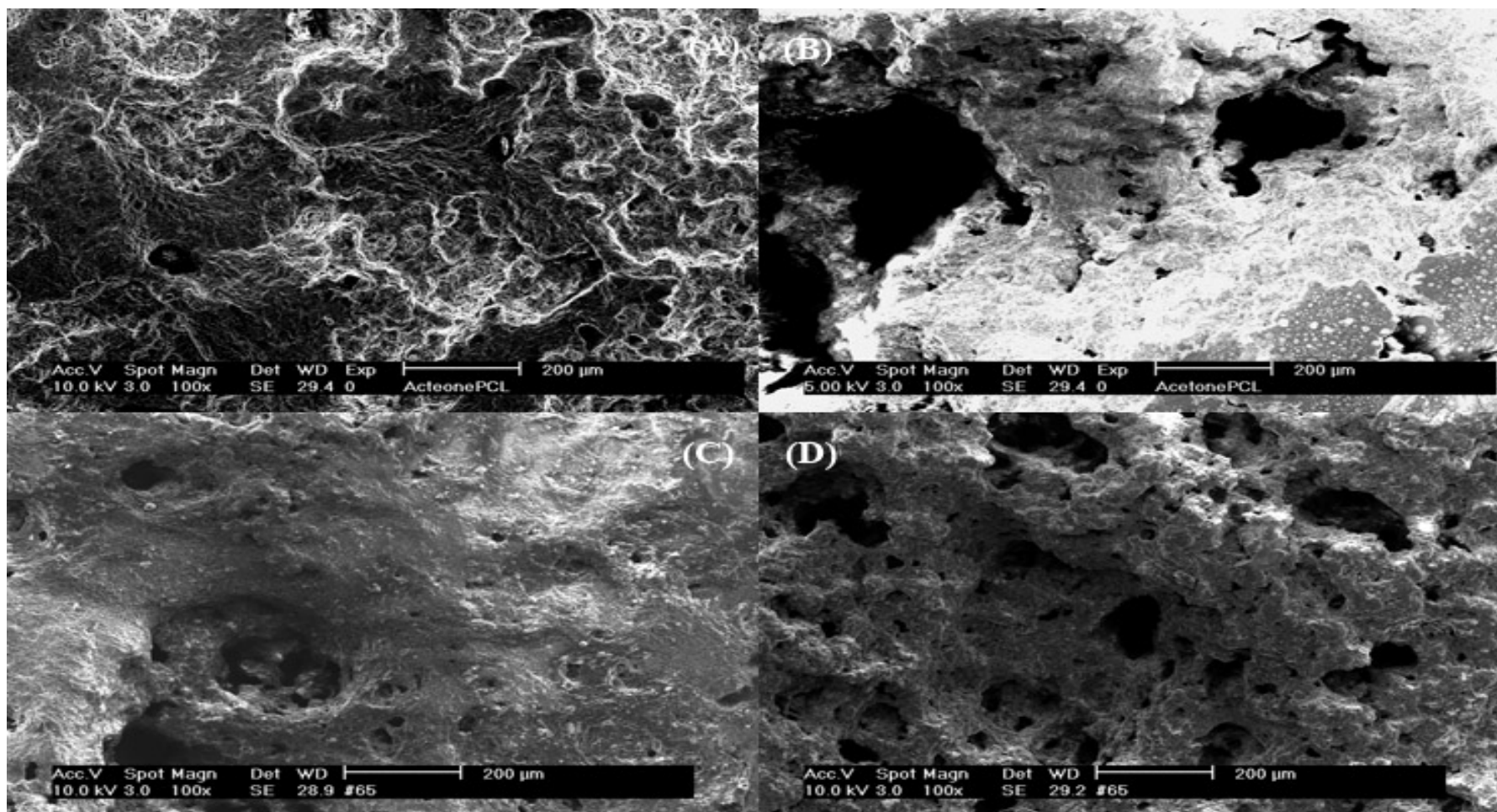


Figure 4-13 SEM images of modified PCL substrates using acetone as the solvent (A) non-modified PCL surface; (B) PCL surface after aminolization and PCL surface further reacted with (C) tetradecanoic acid and (D) dodecanedicarboxylic acid at lower magnification.

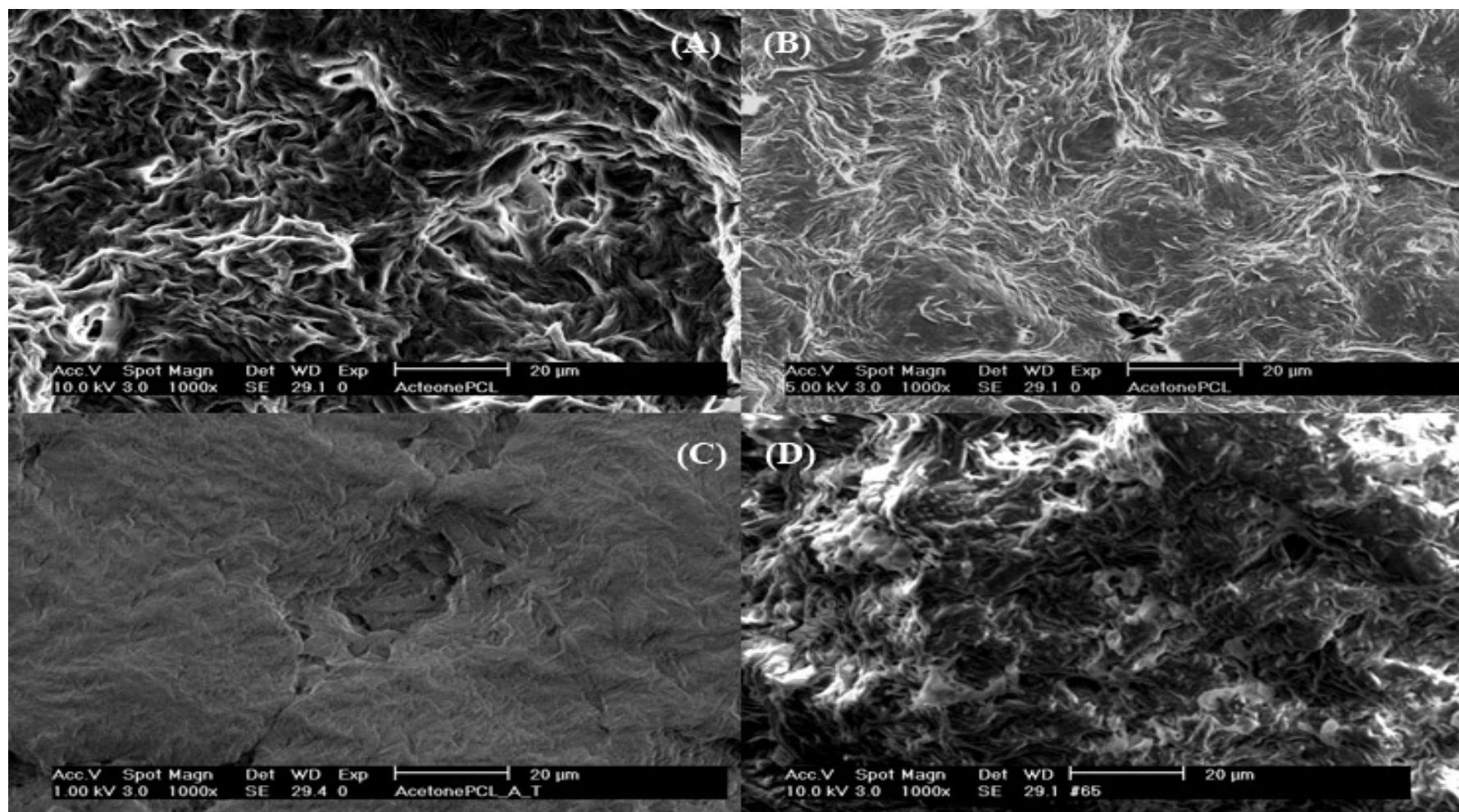


Figure 4-14 SEM images of modified PCL substrates using acetone as the solvent (A) non-modified PCL surface; (B) PCL surface after aminolization and PCL surface further reacted with (C) tetradecanoic acid and (D) dodecanedicarboxylic acid at higher magnification.

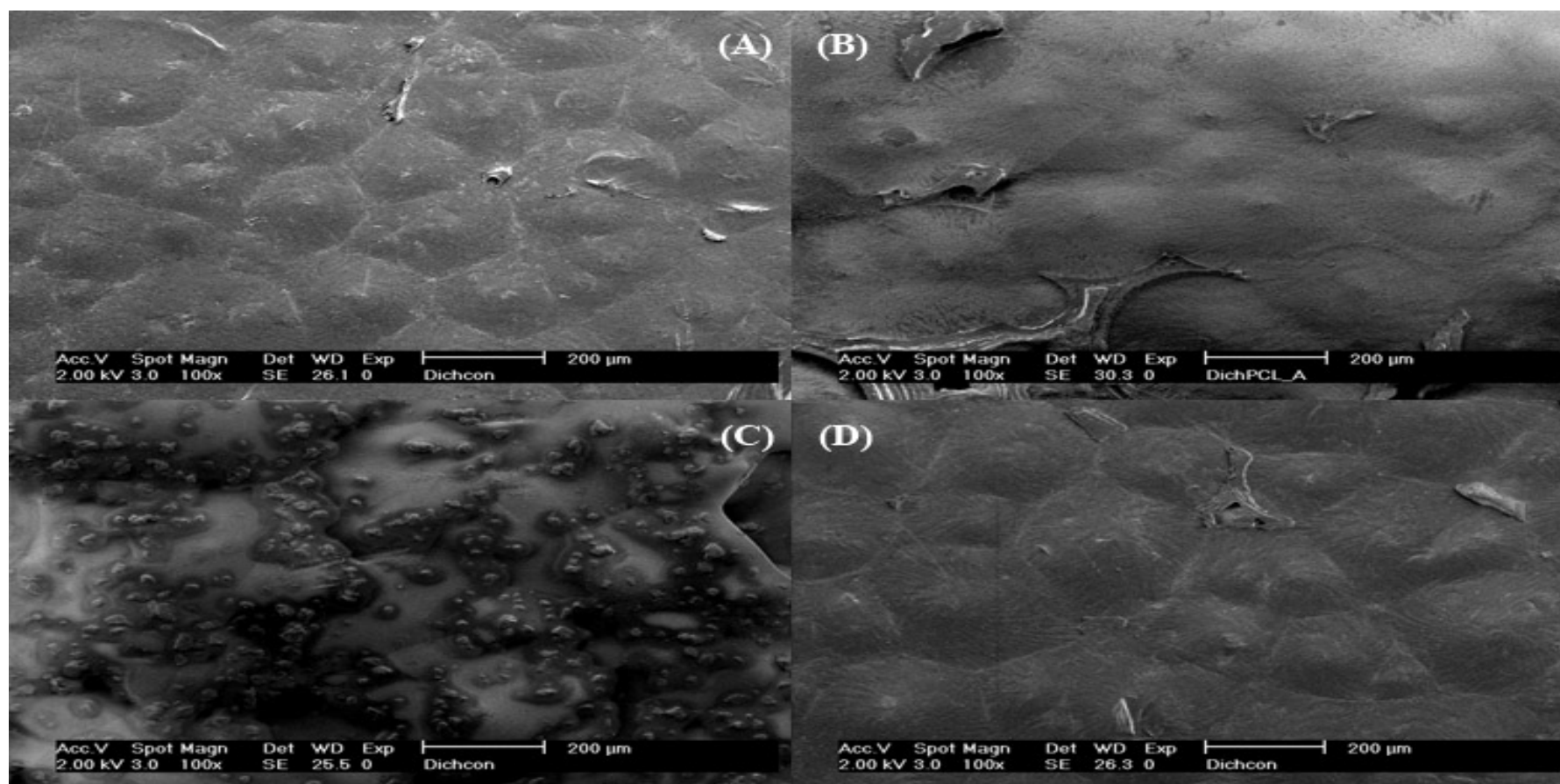


Figure 4-15 SEM images of modified PCL substrates using dichloromethane as the solvent (A) non-modified PCL surface; (B) PCL surface after aminolization and PCL surface further reacted with (C) tetradecanoic acid and (D) dodecanedicarboxylic acid at lower magnification.

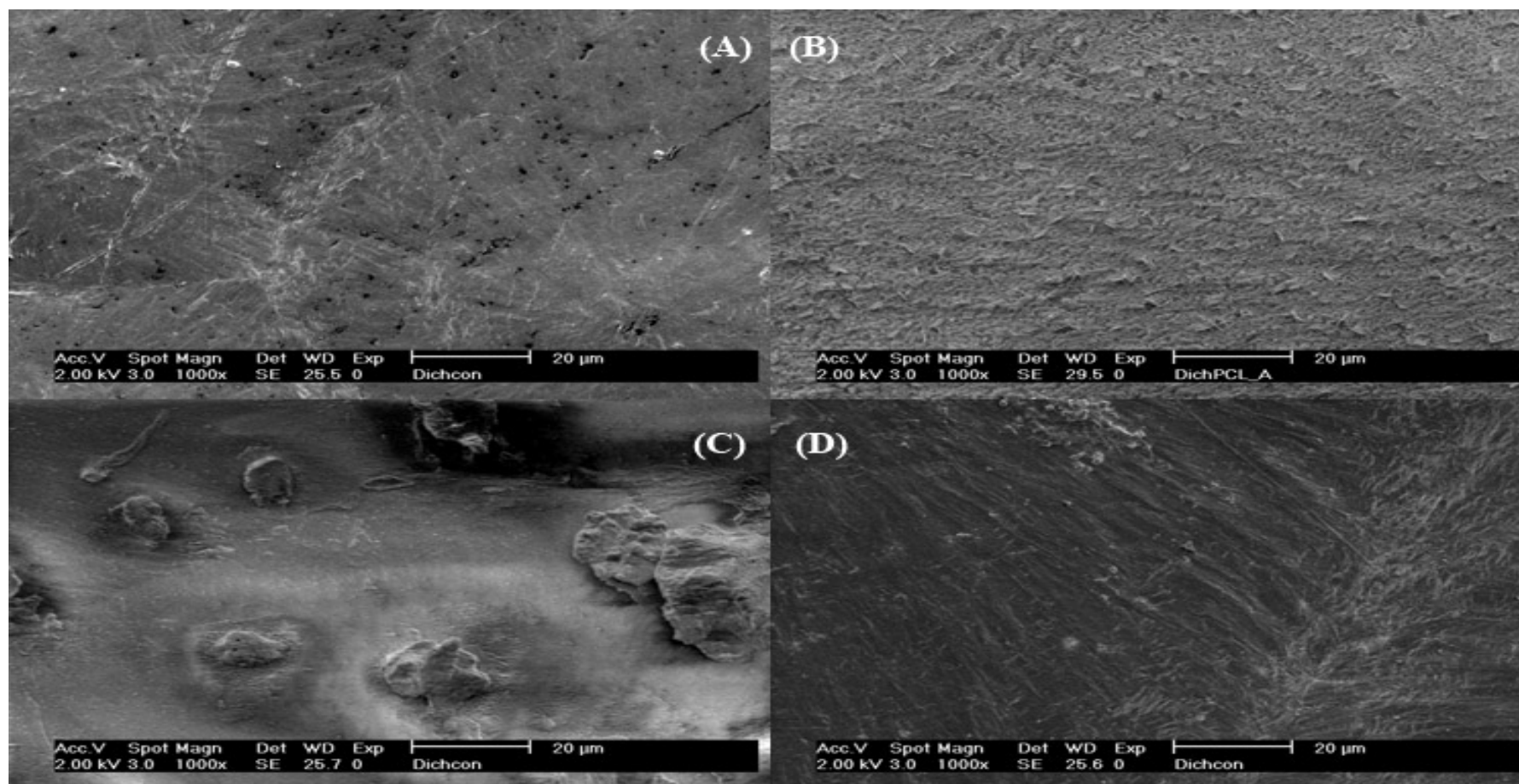


Figure 4-16 SEM images of modified PCL substrates using dichloromethane as the solvent (A) non-modified PCL surface; (B) PCL surface after aminolization and PCL surface further reacted with (C) tetradecanoic acid and (D) dodecanedicarboxylic acid at higher magnification.

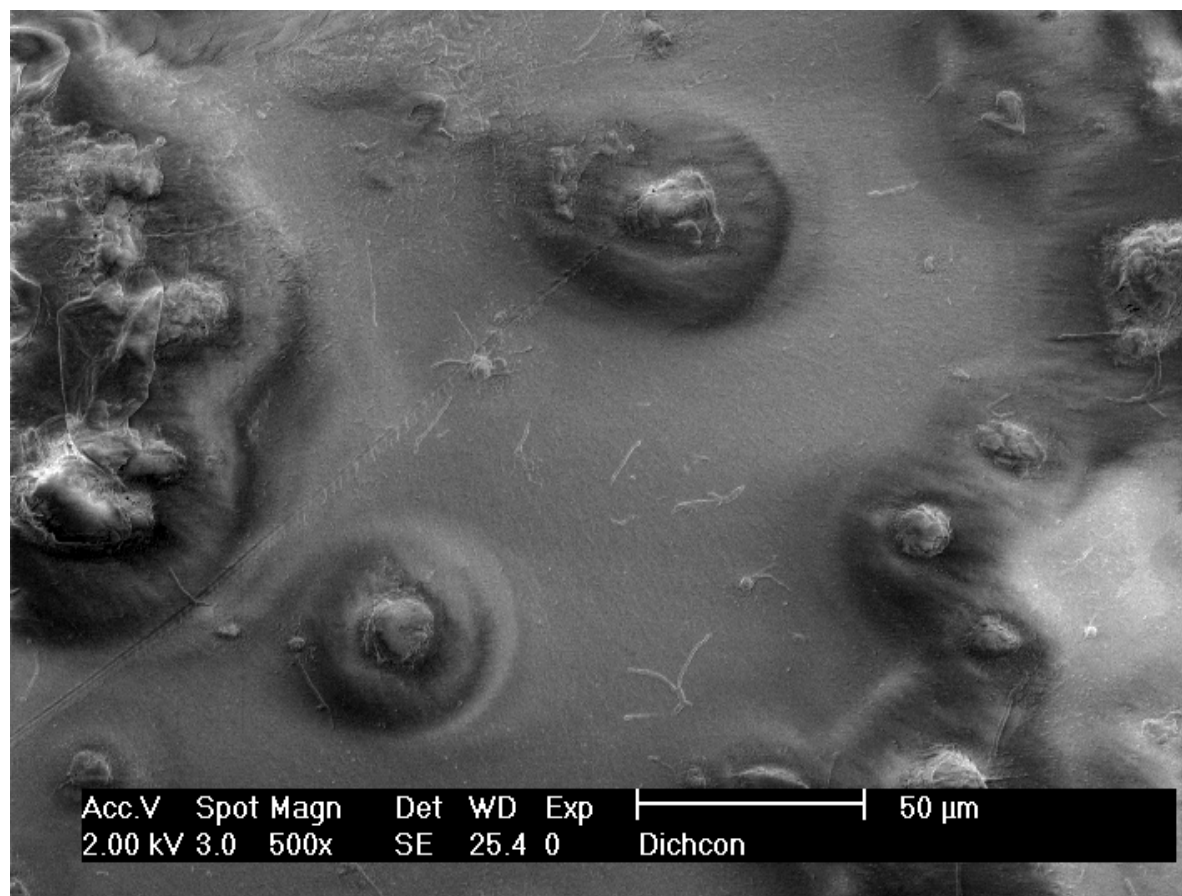


Figure 4-17 SEM images of modified PCL/Dichloromethane surface after the surface aminolization and further react with tetradecanoic acid.

4.3.2 Surface energy analysis

Figure 4-18 shows the surface advancing contact angle (ACA) of PCL/ THF, acetone and dichloromethane substrates. The surface of PCL/acetone substrates presents the highest advancing contact angle among all the non-modified substrates and the similar result can be observed on other modified PCL surfaces. The surface advancing contact angle of non-modified PCL substrates is PCL/acetone ($85.33 \pm 5.3^\circ$) > PCL/THF ($80.2 \pm 2.7^\circ$) > PCL/dichloromethane ($68.3 \pm 1.4^\circ$) which shows the same tendency with the data reported in Tang's paper [49]. Factors responsible for the contact angle of the polymer surface include surface contamination, heterogeneity of the surface structure, reorientation or mobility of the surface segment, swelling and deformation [55,56]. In our case, the density of the hydrophilic functional groups, the degree of surface roughness and the solubility of the solvent should be mainly attributed to the advancing contact angles; however, no reference has been published to explain why different solvents yield different contact angles of PCL surfaces. It would be necessary to further investigate the relationship between the PCL surface contact angle and the solvent used for dissolving PCL powders.

Based on **Figure 4-18**, we can know that advancing contact angle slightly decrease after surface aminolization and both increase after further surface modifications, no matter what solvents that are used for dissolving PCL powders show the same trend. No effect in **Figure 4-18**, the PCL surface modified by dodecanedicarboxylic acid has higher advancing contact angles than the PCL surface modified by tetradecanoic acid. If CONH bonds formed after surface modification, as expected, the PCL surface terminated by $-\text{CH}_3$ should have higher contact angles than the PCL surface terminated by $-\text{COOH}$. Referring to the SEM images (**Figure 4.11 – 4.17**), the reasonable explanations are 1) the

coagulation of tetradecanoic acid surfactants are bound onto PCL surface and form a thin film covered on the surface; 2) the hydrophilic surface area is increased after surface modified by tetradecanoic acid as shown in **Figure 4-21**.

Receding contact angle (RCA) is measured after 10 minutes as shown in **Figure 4-19**. The result of RCA shows the same tendency as the result of ACA (**Figure 4-18**) which is $\text{PCL/Acetone} > \text{PCL/THF} > \text{PCL/Dichloromethane}$.

Figure 4-20 presents the contact angle hysteresis (ACA-RCA). According to Tang et al. [49], PCL/THF and PCL/acetone have higher contact angle hystereses. However, in our case higher contact angle hystereses do not show up on PCL/acetone surface. The reason is that the PCL substrates we made are much thicker than the substrates reported by Tang. In our case, PCL/Acetone substrates look like “a foam” and have very rugged and rough surface. In order to measure the contact angle, the smooth and non-porous part on the surface on which to place the water drop has to be chosen. Therefore, PCL/Acetone shows low contact angle hystereses.

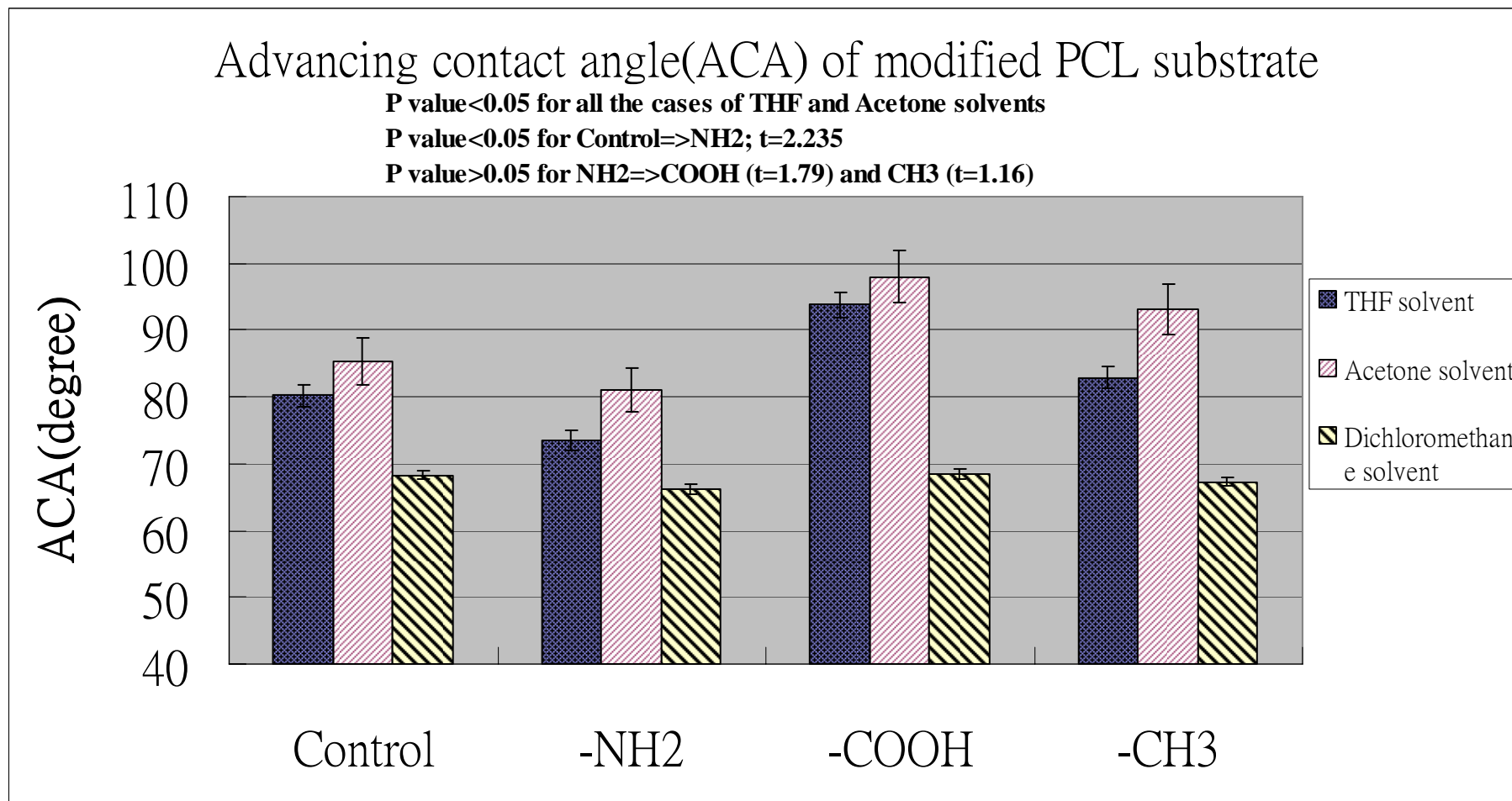


Figure 4-18 The surface advancing contact angle (ACA) of PCL/THF, PCL/ Acetone and PCL/Dichloromethane substrates

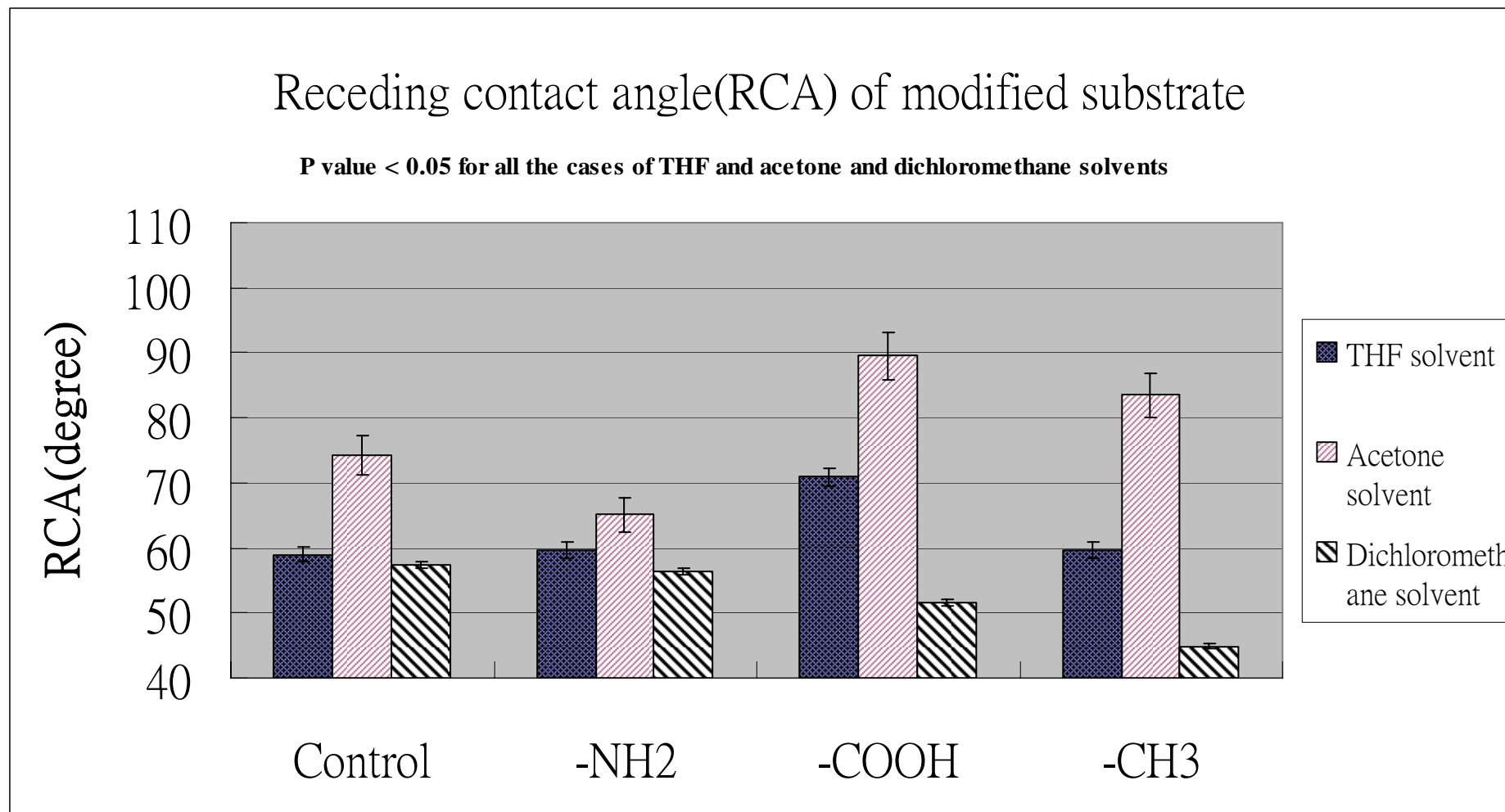


Figure 4-19 The surface receding contact angle (RCA) of PCL/THF, PCL/ Acetone and PCL/Dichloromethane substrates.

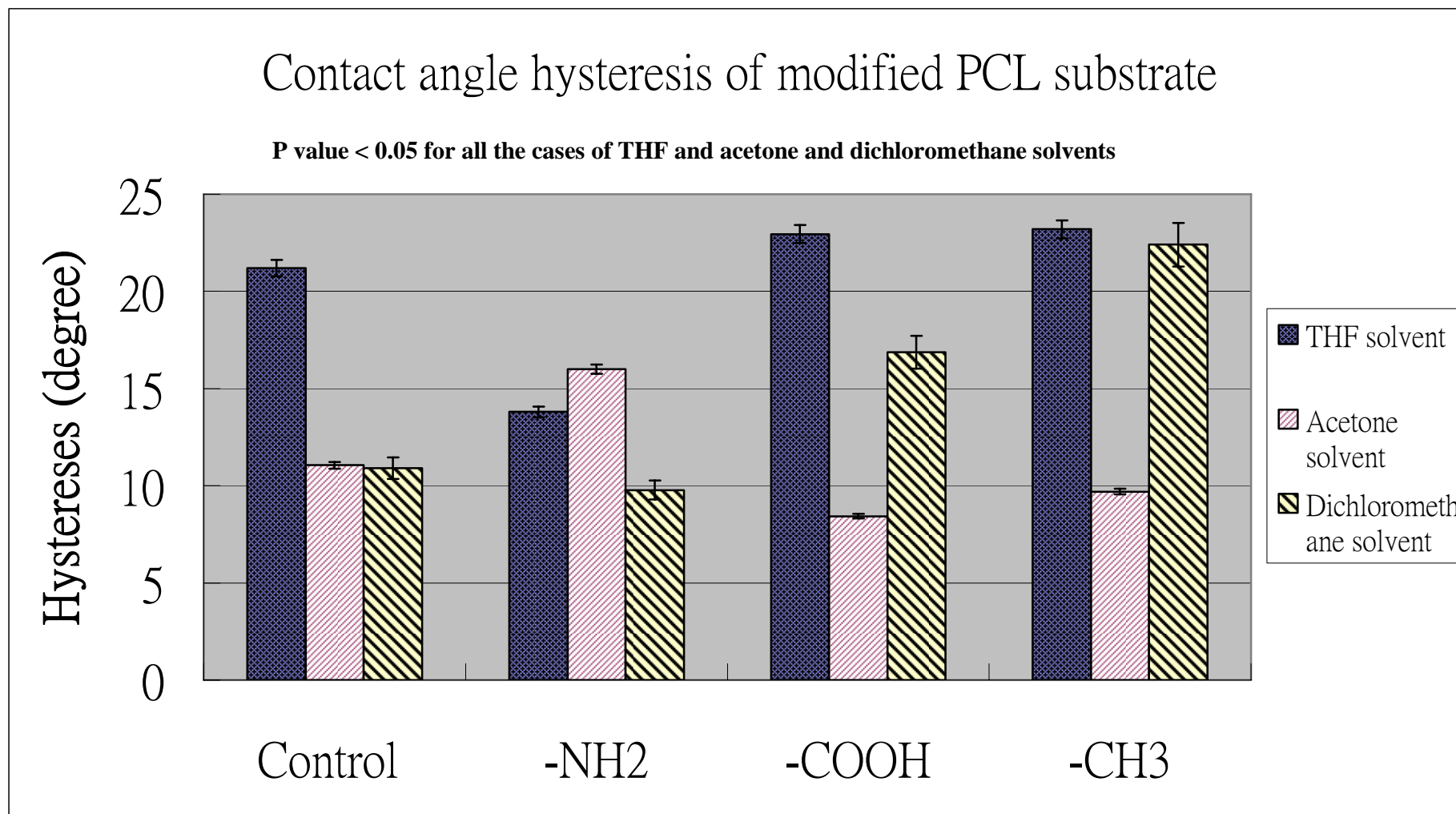
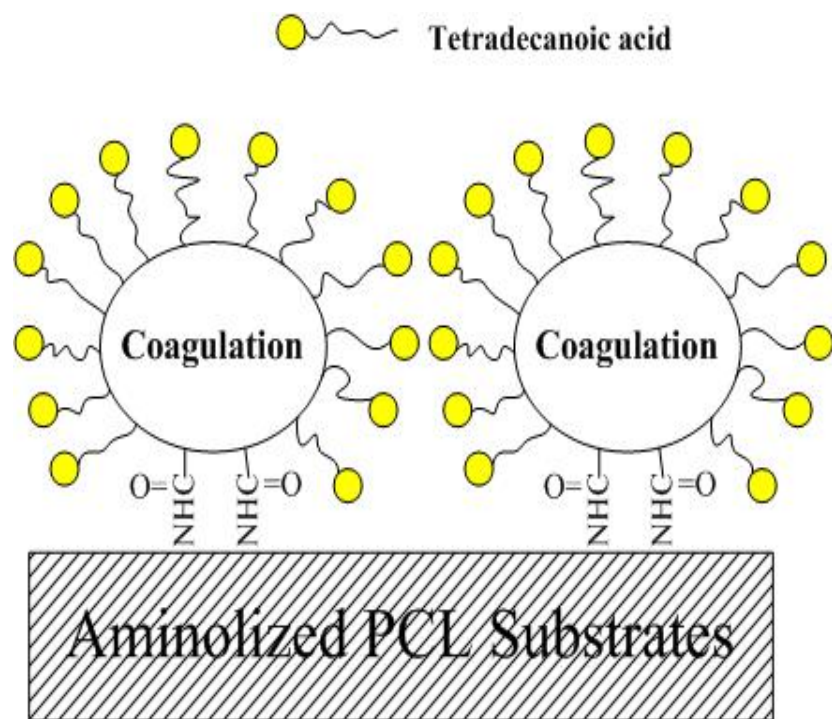
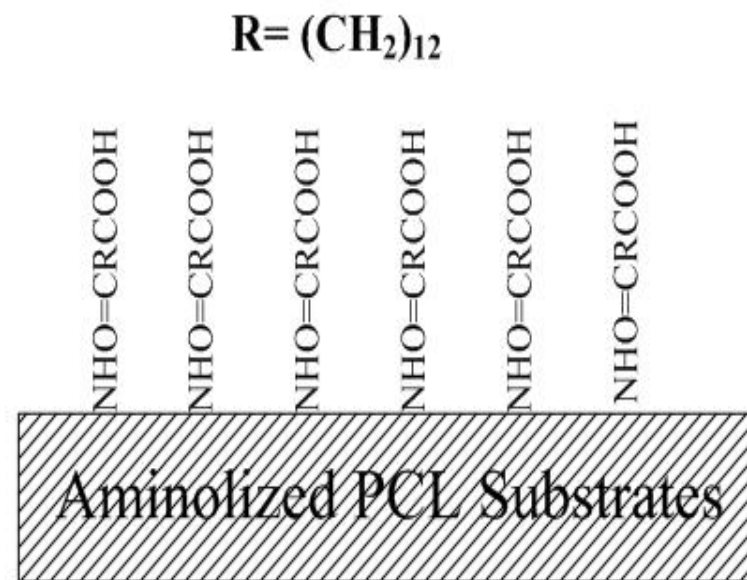


Figure 4-20 The contact angle hystereses (ACA-RCA) of PCL/THF, PCL/ Acetone and PCL/Dichloromethane substrates.



(A)



(B)

Figure 4 -21 Schematic illustration of the possible structure of the PCL surface after the surface reacted with (A) 0.01 M tetradecanoic acid and (B) 0.01 M dodecanedicarboxylic acid

4.3.3 Cell culture analysis

Figure 4-22, Figure 4-23 and **Figure 4-24** show that the numbers of PC12 cells adhere onto the modified PCL/THF, PCL/Acetone and PCL/Dichloromethane substrates, respectively, after 12 hr cell culture. Based on **Figure 4-22, Figure 4-23** and **Figure 4-24**, the results indicate that the non-treated PCL surface is the most conducive to PC12 cell adhesion whereas the PCL surface terminated NH_2 is the least conducive. The numbers of cells adhering to each modified surface after a 12 hr cell culture in an ascending order is as follows: $\text{NH}_2 < \text{COOH} < \text{CH}_3$, Control PCL.

In three different solvent systems, the PC12 cell culture results show that the cell attachment of the aminolyzed PCL substrates is decreased compared with the control PCL substrates, although the water contact angles of these aminolyzed substrates have been decreased (refer to **Figure 4-18**). The same results have been reported by Zhu et al. [18, 24]. In their work, the extent of endothelial cell adhesion slightly decreased after PCL and Poly (L-lactic acid) surface aminolyzeation, but when they further increased the amount of NH_2 groups onto the surface, they found the amount of cell adhesion was not obviously changed. The reason that the NH_2 groups have a negative effect on cell attachment behavior is still unknown.

The negative effect of $-\text{COOH}$ groups on cell adhesion behavior has been reported [11, 12, 60, 61]. It is assumed that this effect comes from the negative charge characteristic of surface $-\text{COOH}$ groups, which causes considerable electrostatic repulsion interaction between the negatively charged cell membranes and negatively charged substrate surface [60]. In our case, this phenomenon can be seen in all three different solvent systems.

Comparing all modified PCL surfaces, we suggest that the aminolyzed PCL surfaces further reacted with tetradecanoic acid have the largest amount of PC12 cell adhesion among all modified PCL surfaces. In the THF solvent system, the surface even has higher PC12 cell adhesion than the blank PCL substrates (Control). Although the data shown in **Figure 4-18** indicate that the aminolyzed PCL substrates reacted with tetradecanoic acid has more hydrophilic surface than the surface further reacted with dodecanedicarboxylic acid, the amount of cell adhesion onto “CH₃ terminated PCL surface” is extraordinarily higher than that onto the COOH terminated PCL surface. The explanations, we suggest, are: 1) the surface area for cell adhesion is increased by the coagulation of tetradecanoic acid surfactants attached to the aminolyzed PCL surface; 2) the coagulation of tetradecanoic acid surfactants are washed out of the PCL surface so that the PCL surface properties are exactly the same as blank PCL. The effect of temperature and pH values on aggregation behavior of surfactants in aqueous solution has been reported [62, 63]. In our case, the surface modification procedure is processed at room temperature and in acid solution (pH<7), however, cell culture have to be processed at 37°C and pH=7 which is consistent with the environment in the human body. The coagulation of tetradecanoic acid surfactants might be dissolved into the aqueous media used for cell culture. The SEM images of modified PCL surfaces after cell culture could provide helpful evidence to understand the change of PCL surface composition and properties.

Figure 4-25 shows that the amount of PC12 cells attached onto modified PCL substrates after 12 hr cell culture. PCL/Acetone substrates adsorb more PC12 cells onto the modified and blank surfaces compared to PCL/Dichloromethane and PCL/THF substrates. From the SEM images (**Figure 4-14** and **Figure 4-15**), PCL/Acetone substrates are more porous so that more surface area can be used for PC12 cells adhesion;

it is also possible that more cell culture media remained in the porous substrates where it is not easy to remove the media.

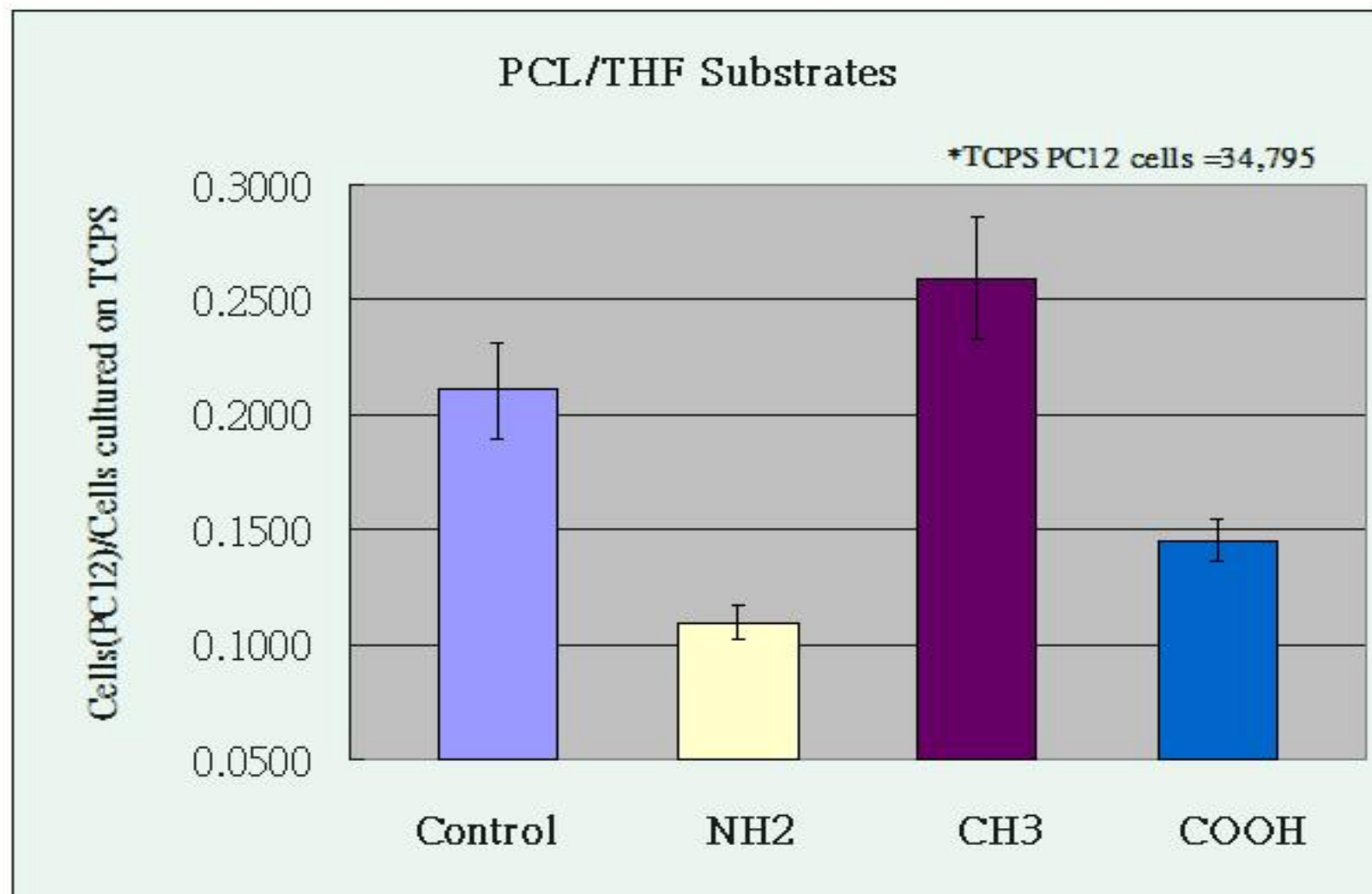


Figure 4-22 PC12 cells attached onto modified PCL/THF substrates for 12 hr.

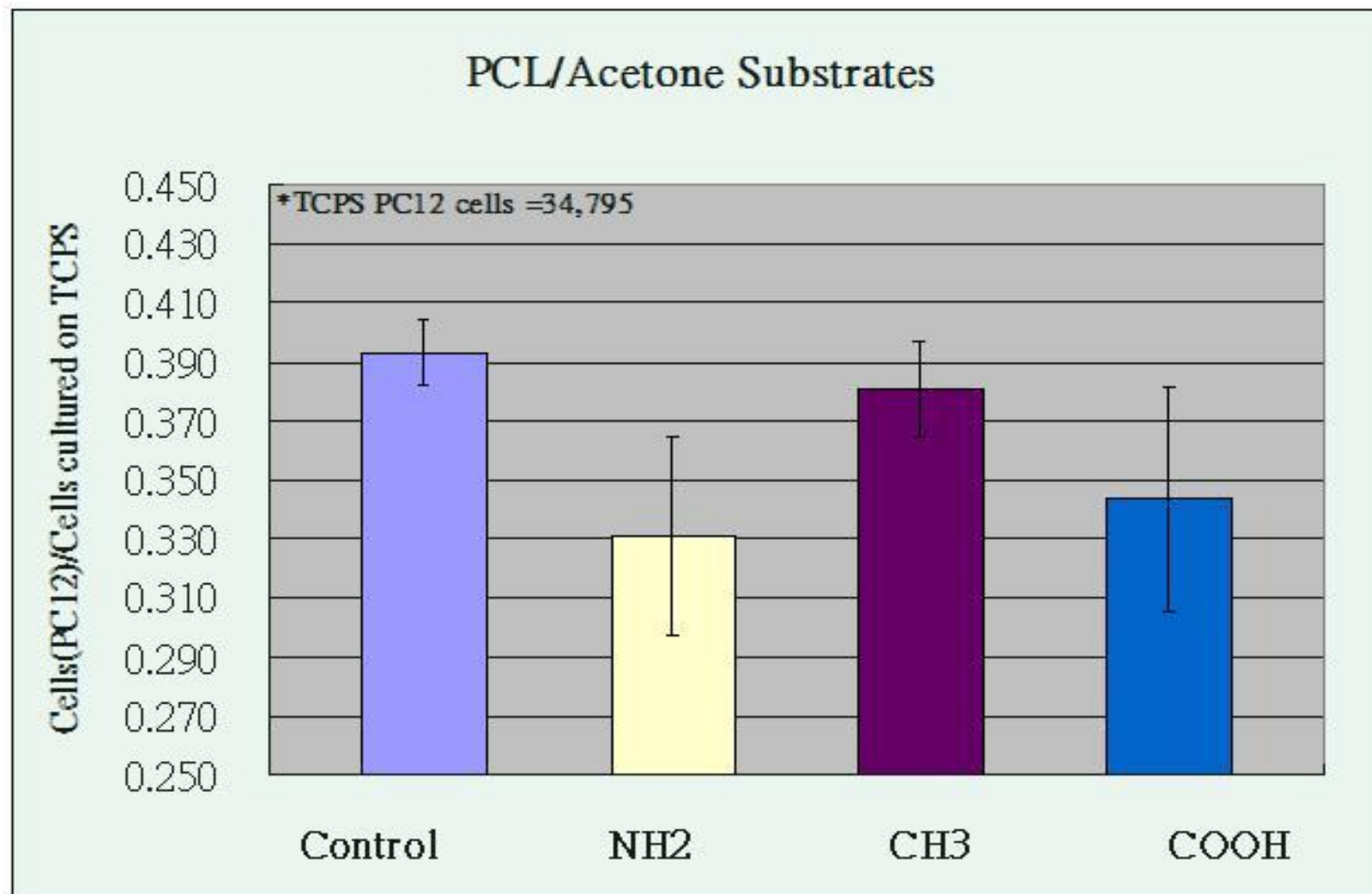


Figure 4-23 PC12 cells attached onto modified PCL/Acetone substrates after 12 hr cell culture.

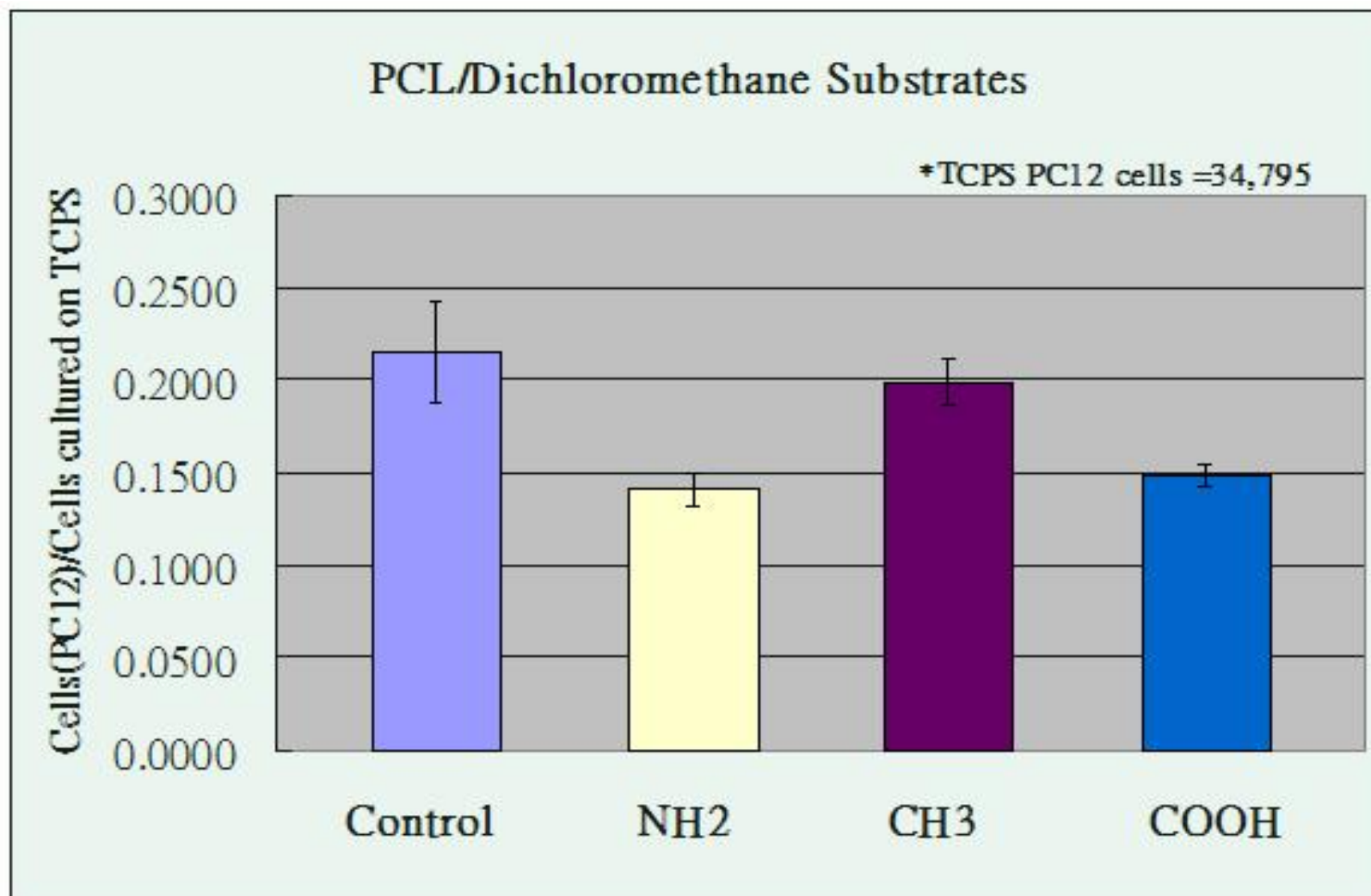


Figure 4-24 PC12 cells attached onto modified PCL/Dichloromethane substrates after 12 hr cell culture.

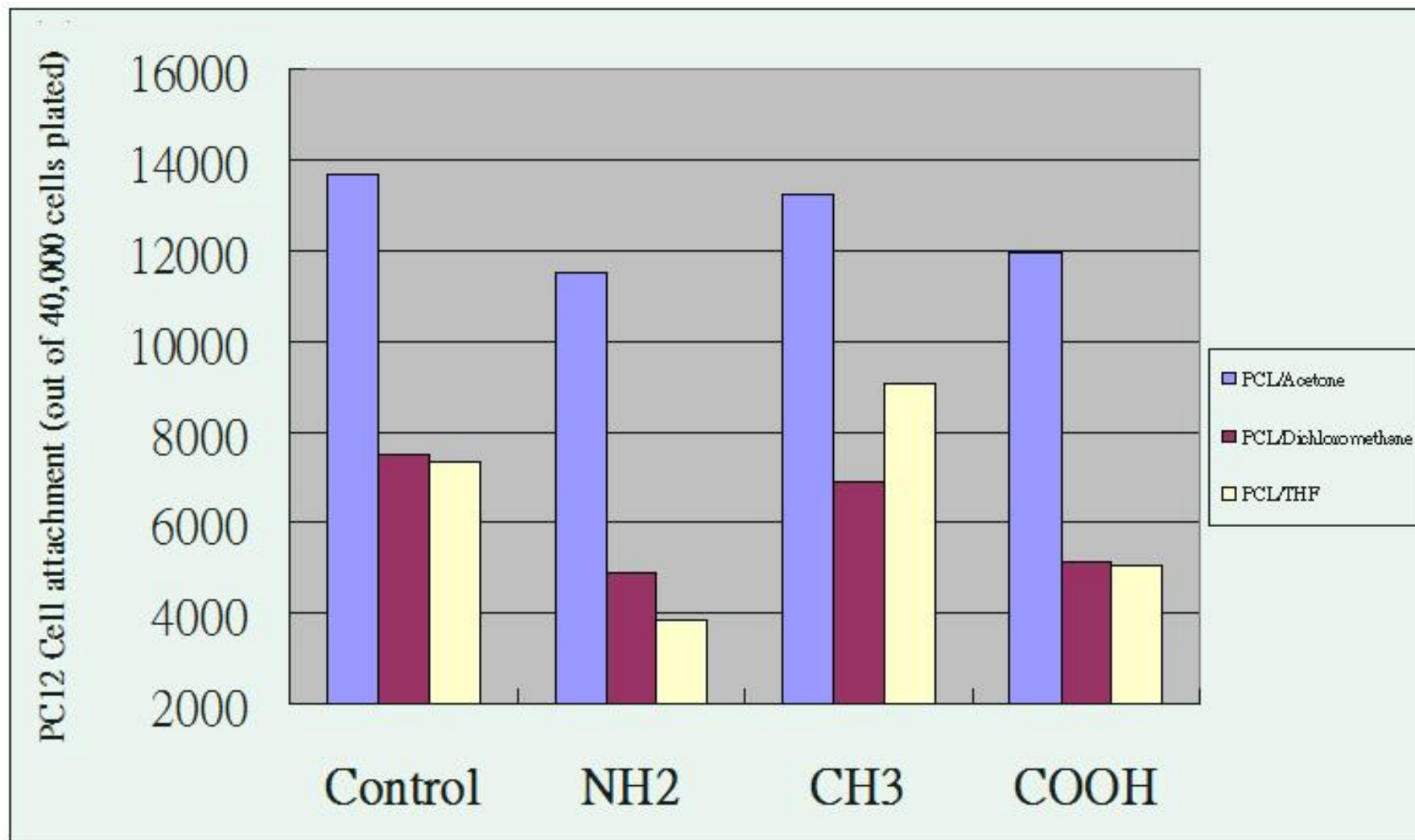


Figure 4-25 PC12 cells attached onto modified PCL substrates after 12 hr cell culture.

5.0 SUMMARY AND CONCLUSIONS

In this research PC12 cell outgrowth and proliferation was examined on the mica substrates coated with monolayer and multilayer dendrimers. Neuron cells outgrowth and the sprout of neurite have been observed on the OM images. This promising result showed that the surface charges from functional groups on the modified surface were capable to enhance cell outgrowth and proliferation.

After the mica substrates, the glass coverslips were chose as a substrate for surface modification because the round glass coverslips could completely fitted the shape of well plate, and the transparent glass coverslips are capable to be used for the observation of cell outgrowth and proliferation via optical microscopy. The glass coverslips were, first, coated with 10nm titanium (bottom layer) which can enhance the adhesion between the gold layer and the substrate, and then the 20 nm gold layer were sputter onto the titanium-coated substrates. Three different thiol chemicals (1- dodecanethiol, 11-mercaptoundecanoic acid and 11-mercapto-1-undecanol) were respectively bonded to the substrates coated with the titanium and gold layer because gold atomic and sulfur atomic would naturally form a chemical bonding. Therefore, the modified surfaces terminated by OH, COOH, or NH₂ were used for cell culture. Form the contact angle measurement, the data indicated that -CH₃ terminated SAMs on gold-coated substrate showed hydrophobic surface on which the average contact angle was $107.43 \pm 4.6^\circ$; -COOH and -OH terminated SAMs on gold-coated substarte were both hydrophilic surface on which the average contact angles were $37.24 \pm 2.2^\circ$ and $28.42 \pm 2.0^\circ$ respectively. According to these data, we can preliminary conjecture that the surfaces were successfully modified as we expected. From the

cell culture analysis, the result showed that the amount of cells adhering onto modified substrates was $\text{COOH} > \text{OH} > \text{CH}_3$ in both female and male adipose-derived stem cells (ASCs). However, the residual ethanol solution on the modified surface would affect the amount of cell attachment. It is hard to be achieved an absence of ethanol environment because ethanol was used to completely dissolve thiol surfactants which is barely dissolved in water and other polar solutions. Also, gold-coated glass substrates are bio-incompatible, so poly (caprolactone) substrates were used to instead of gold-coated glass coverslips.

Three different solutions, THF, acetone and dichloromethane, were used to dissolve PCL powders. Different surface morphologies were formed after solvents were naturally evaporated. The degree of roughness was (from rough to smooth) $\text{PCL/acetone} > \text{PCL/THF} > \text{PCL/dichloromethane}$ and the particle size of fused aggregates comprised of PCL substrate was (from large to small) $\text{PCL/dichloromethane} > \text{PCL/THF} > \text{PCL/acetone}$ (filamentous structure). These PCL substrates were dipped into 1, 6 hexanediamine solution to form a NH_2 terminated surface, and then the aminolyzed PCL surface would further reacted with tetradecanoic acid and dodecanedicarboxylic acid respectively in order to form a COOH and CH_3 terminated PCL surface. The SEM images showed that PCL substrates were covered by many tetradecanoic acid coagulations after the aminolyzed PCL surface reacted with tetradecanoic acid; whereas, the aminolyzed surface reacted with dodecanedicarboxylic acid exhibited a etched-like surface. The contact angle measurement showed that advancing contact angle slightly decrease after surface aminolyzation and both increased after further surface modifications, no matter what solvents that were used for dissolving PCL powders showed the same trend. Because the aminolyzed PCL surface further reacted with tetradecanoic acid was more hydrophilic than the surface further reacted with dodecanedicarboxylic acid in all three solvents system, the reacting mechanism of

tetradecanoic acid bound to aminolyzed PCL surface was not the same as we expected to form a CH_3 terminated PCL surface. The reasonable mechanisms were a) the coagulation of tetradecanoic acid surfactants bound onto the aminolyzed PCL surface and form a thin film covered on the surface; b) the hydrophilic surface area is increased after surface modified by tetradecanoic acid as shown in **Figure 4-22**. From cell culture analysis, the numbers of cells adhering to each modified surface after a 12 hr cell culture in an ascending order is as follow: $\text{NH}_2 < \text{COOH} < \text{CH}_3$, Control PCL. The result of cell culture on NH_2 and COOH terminated PCL surface were similar to the result reported from Zhu's papers [18, 24] and Lee's paper [60]. However, the numbers of cell adhering onto CH_3 terminated surface were extraordinarily higher than that onto the COOH terminated surface. The reasonable explanations were: a) the surface area for cell adhesion was increased by the coagulation of tetradecanoic acid surfactants attached to the aminolyzed PCL surface; b) the coagulation of tetradecanoic acid surfactants were washed out of the PCL surface so that the PCL surface properties were exactly the same as blank PCL.

6.0 Suggestion for future work

1. In order to understand the mechanism of PCL surface modifications, further research such as ATR-FTIR analysis is needed.
2. Cells outgrowth and proliferation on the modified PCL surfaces are necessary to be examined in order to know the effect of functional groups on cell proliferation and outgrowth.
3. Except -NH_2 , -COOH and -CH_3 terminated PCL surface, more other functional groups such as -OH terminated PCL surface should be used to verify the surface modification effect on cell culture.
4. The surface composition of the aminolyzed PCL substrates further reacted with tetradecanoic acid surfactants has to be fully understood.
5. Other biocompatible substrates such as PVDF, PLGA and PMMA can be used to do surface modifications.
6. Corona charging is another way to lead the permanent surface charge.

APPENDIX A

GLOSSARY

<The table is listed alphabetically.>

Advancing contact angle(ACA), Receding contact angle (RCA) and contact angle hysteresis

The value of static contact angles are found to depend on the recent history of the interaction. When the drop has recently expanded the angle is said to represent the ‘advanced’ contact angle. When the drop has recently contracted the angle is said to represent the ‘receded’ contact angle. These angles fall within a range with advanced angles approaching a maximum value and receded angles approaching a minimum value. The difference between the maximum (advanced/advancing) and minimum (receded/receding) contact angle values is called the contact angle hysteresis.

Allogeneic Schwann cells (homologous Schwann cells)

Schwann cells are a variety of neuroglia that wrap around axons in the peripheral nervous system, forming the myelin sheath. The nervous system depends crucially on this sheath for insulation and an increase in impulse speed. They are the peripheral nervous system analogues of the central nervous system oligodendrocytes.

ATR-FTIR

ATR-FTIR is an abbreviation of **A**ttenuated **T**otal **R**eflection **F**ourier **T**ransform **I**nfra**R**ed Spectroscopy. It provides a unique configuration in which the infrared spectrum of a liquid phase can be obtained in a slurry in-situ without phase separation.

Axon

The **axon** is a long extension of a nerve cell and takes information away from the cell body. Bundles of axons are known as nerves or, within the CNS (central nervous system), as nerve tracts or pathways. Dendrites bring information to the cell body.

Cell differentiation

Cell differentiation is the process during which young, immature (unspecialized) cells take on individual characteristics and reach their mature (specialized) form and function.

Enantiomeric isomers

Enantiomeric isomers are molecules which exist in two nonsuperimposable mirror images, analogous to human hands. Chiral molecules are perfect physical and chemical models of each other with the exception of their rotation of polarized light and those interactions that involve other chiral systems, such as chiral molecular recognition. A racemic mixture contains equal amounts of two enantiomers and thus produces no rotation of the plane of polarization of light.

Endothelial cells

Endothelial cells are the cells that line the inner surface of the cornea in a single layer (endothelium). They are responsible for pumping fluid out of the cornea to keep it clear. These cells gradually decrease in number over a lifetime. They can die off faster than normal from damage during surgery or after surgery. If the number of endothelial cells becomes too low, your cornea becomes cloudy, you lose vision and may require a corneal transplant.

Gastrocnemius muscles (mGC)

Gastrocnemius muscles are the muscles in the back part of the leg that forms the greater part of the calf; responsible for the plantar flexion of the foot.

Fibronectin (Fn)

Fibronectin (Fn) is a high molecular weight glycoprotein containing about 5% carbohydrate that bind to receptor proteins spanning the cell membrane called integrins and to the extracellular matrix. It can also specifically bind to other molecules such as collagen, fibrin and heparin.

Homopolymer

Homopolymer is a macromolecule consisting of only one type of building unit.

Human articular chondrocytes

Human articular chondrocytes are cells in human articular folds.

Isograft

Bones or muscles transferred between animals that are identical in histocompatibility antigens.

Mineralization

Mineralization is a normal biological process which takes place during the life of an organism such as the formation of bone tissue or egg shells.

Motoneurons

In vertebrates, motoneurons (also called motor neurons) are efferent neurons that originate in the spinal cord and synapse with muscle fibers to facilitate muscle contraction and with muscle spindles to modify proprioceptive sensitivity.

Mouse neuroblastoma(Nb2a) cells

Neuroblastoma cells are fast-growing cancers that develop from nerve cells and typically arise in the adrenal glands.

Myelinated axon

A nerve fiber encased in a sheath of myelin. Consisting of segmented, multilayered wrappings of myelin, a whitish protein, myelin sheaths wrap around certain nerve fibers, providing electrical insulation and serving to speed the transmission of nerve signals.

Osteoblasts

Osteoblasts are bone-forming cells that synthesize and secrete non-mineralized bone matrix, participate in the calcification and resorption of bone, and regulate the flux of calcium and phosphate in and out of bone. Bone formation occurs in two stages, matrix formation, and mineralization. When osteoblasts stop synthesizing matrix and become embedded within bone, they are called osteocytes.

Osteoconductive materials

Osteoconductive materials include the inorganic bioceramics, calcium phosphate and calcium sulfate as well as the hydroxyapatites. These materials are available in many forms, including powders, granules, blocks and morsels.

Phosphate buffered saline (PBS)

Phosphate buffered saline (PBS) is a buffer solution commonly used in biochemistry. It is a salty solution containing sodium chloride, sodium phosphate and potassium phosphate. The buffer helps to maintain a constant pH. The concentration usually matches the human body (isotonic).

Plantar muscles (mPL)

Plantar muscles are the muscles in the bottom of the foot.

PC12 Cell

PC12 cell is a cell line from rat pheochromocytoma, which alters in morphology to neuron-like cells in response to nerve growth factor (NGF) by stopping cell division and extending long and branching neurites. This capacity to undergo neuronal differentiation in response to NGF stimulation makes the PC12 cell line an extremely valuable neuronal model system and has been

widely used to investigate the cellular and molecular mechanisms underlying neuronal differentiation

Poly[50/50(85/15 L/D)LA/ ϵ -CL]

The biodegradable synthetic polymer contains biodegradable copolymer consists of 50% PLA (85% L-lactide (PLLA) and 15% D- lactide (PDLA)) and 50% poly (ϵ -caprolactone).

The compound muscle action potential (CMAP)

The compound muscle action potential (CMAP) is a measure of the muscle response to pudendal nerve stimulation. CMAP represents the total number of muscle fibers supplied by the nerve and may be a more sensitive measurement of the denervation of the external anal sphincter.

Tibialis anterior muscles (mTA)

Tibialis anterior muscles originate from the lateral condyle on the upper half of the tibia and the interosseous membrane.

APPENDIX B

FUNDAMENTAL PROCEDURES AND KNOWLEDGE FOR CELL CULTURE

(Provided by Dr. Marra and Candace, Brayfield)

1. Preparation

- a. Turn the UV light on in the hood for 20 min
- b. Turn on the 37 °C water bath
- c. Warm up media and PBS in the 37 °C water bath for ~20 min
- d. Gather all tissue cultures needed supplies. Remember to always clamp or close with tape the opened packages (e.g., tubes and pipettes)

2. Switch the hood controller from UV to normal operation and turn on the fluorescent light.

Wipe the wood down thoroughly with 70% ethanol.

3. Sterility: Use only sterile pipettes, disposable test tubes and autoclaved pipettes tips for cell culture. All culture vessels, test tubes, pipette tip boxes, stock of sterile eppendorfs, etc. should be opened only in the laminar flow hood. If something is opened elsewhere in the lab by accident, always assume that it is contaminated. If something does become contaminated, immediately discard in biohazard box.

4. Biohazard Box: Anything that comes into contact with cells, cell media, or human tissue is contaminated and should be placed into the biohazard box. This includes contaminated flask, plates, tubes, tips and gloves. Avoid placing uncontaminated paper into the box. Contaminated glassware is to be placed into bleach water, washed in Alconox water and then autoclaved. No glassware is to go into the biohazard box.
5. Feed cells,
 - a. Remove old media with a 1 ml pipette connected to the vacuum.
 - b. Add fresh media with Drummond
 - c. Return flask to the incubator; remember to loosen the lid to allow airflow.
6. Split cells,
 - a. Remove media
 - b. Add enough trypsin-EDTA solution to cover the bottom of the culture vessel (~2mL)
 - c. Place culture dish in the incubator for ~2 min
 - d. Monitor cells under microscope. Cells are beginning to detach when they appear rounded.
 - e. As soon as cells are in suspension (<1min), immediately add culture medium containing serum. Wash cells once with serum containing medium and dilute as appropriate (generally 4-20 fold).

Cell counting using a hemacytometer

The most widely used method of counting chamber is called a hemacytometer (since it was originally designed for performing blood cell counts). This method is based on the principle that live cells do not take up certain dyes, whereas dead cells do.

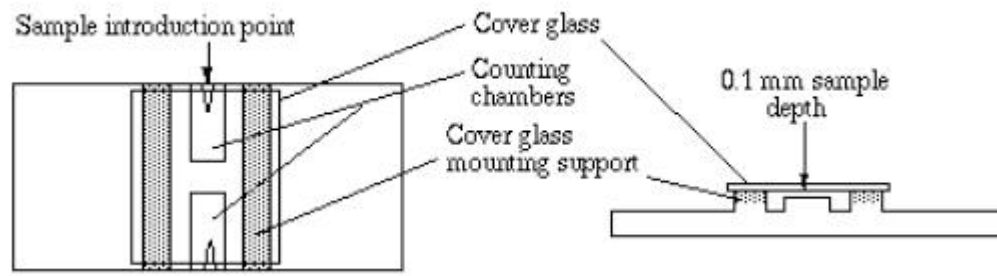


Figure B-1 Hemacytometer method [65]

To prepare the hemacytometer, the mirror-like polished surface is carefully cleaned with lens paper and ethanol. The coverslips (which is thicker than those for conventional microscopy) should also be cleaned. The coverslip is placed over the counting surface prior to adding the cell suspension as **Figure B-1** shown above.

The cell suspension is introduced into one of the V-shaped wells using a pasteur pipet. Allow the area under the coverslip to fill by capillary action. Enough liquid should be introduced so that the mirrored surface is just covered. The counting chamber is then placed on the microscope stage and the counting grid is brought into focus at low power.

One entire grid on standard hemacytometers with Neubauer rulings can be seen at 40x (4x objective). The main divisions separate the grid into 9 large squares. Each square has a surface area of 1mm^2 , and the depth of the chamber is 0.1mm as shown in **Figure B-2**. Each square of the hemacytometer (with cover slip in place) represents a total volume of 0.1 mm^3 or 10^{-4} cm^3 .

Since $1 \text{ cm}^3 = 1 \text{ ml}$, the subsequent cell concentration per ml will be determined using the following calculations.

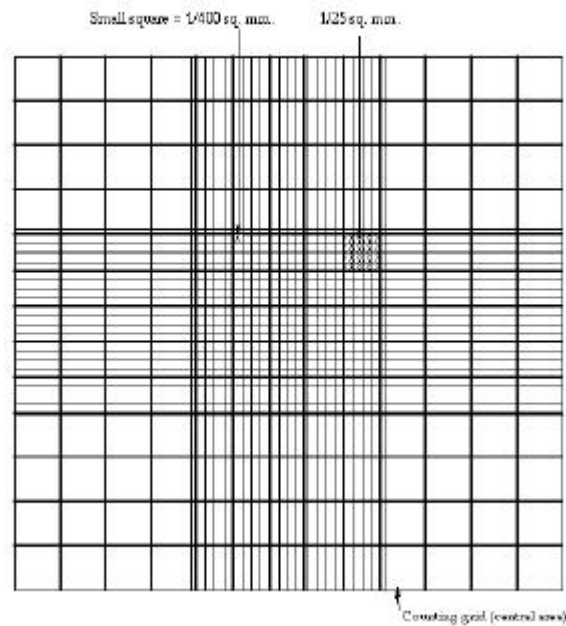


Figure B-2 Counting chamber [65]

Cell suspensions should be dilute enough so that the cells do not overlap each other on the grid, and should be uniformly distributed as it is assumed that the total volume in the chamber represents a random sample. This will not be a valid assumption unless the suspension consists of individual well separated cells. Cell clumps will distribute in the same way as single cells and can distort the result. Unless 90% or more of the cells are free from contact with other cells, the count should be repeated with a new sample. Also, the sample will not be representative if the cells are allowed to settle before a sample is taken. Mix the cell suspension thoroughly before taking a sample to count.

It is best to systematically count the cells in selected squares so that the total count is approximately 100 cells (number of cells needed for a statistically significant count). For large

cells this may mean counting the four large corner squares and the middle one. For a dense suspension of small cells you may count the cells in the four 1/25 sq. mm corners plus the middle square in the central square. Additionally, a common convention is to count cells that touch the middle lines (of the triple lines) to the left and top of the square, but do not count cells similarly on the right or bottom of the square (to avoid double-counting). For cells that overlap a line, count a cell as "in" if it overlaps the top or right line, and "out" if it overlaps the bottom or left line.

To get the final count in cells/ml, first divide the total count by 0.1mm (chamber depth) then divide the result by the total surface area counted (each large square is 1 mm²). For example, if you counted 125 cells total in the four large corner squares plus the middle, divide 125 by 0.1mm, and then divide the result by 5 mm².

$125\text{cells}/0.1\text{mm} = 1250\text{ cells/mm}$ ($1250\text{ cells/mm})/ 5\text{mm}^2 = 250,000\text{ cells/ mm}^3 = 250,000\text{ cells/ml}$

Cells per ml = the average count per square x the dilution factor x 10⁴

Sometimes you will need to dilute a cell suspension to get the cell density low enough for counting. In that case you will need to multiply your final count by the dilution factor. For example, if you take an aliquot and dilute it 10-fold and obtain a final count of 250,000 cells/ml, then the count in the original (undiluted) suspension is 10 x 250,000 which is 2,500,000 cells/ml. The cell suspension should be diluted so that each square has between 20 - 50 cells (2-5 x 10⁵

cells/ml). A total of 300 - 400 cells should be counted since the counting error is approximated by the square root of the total count.

To count most mammalian cells on a ~80-90% confluent 100mm TC plate:

- a. Rinse cells in 1x PBS.
- b. Add 2ml 1xtrypsin and put in incubator ~5min.
- c. Add 8 ml of media, pipet up and down to mix cells then transfer to a 15ml conical tube.
- d. Centrifuge at 2000rpm for 2 min.
- e. Aspirate off media to the desired level
- f. Gently resuspend pellet with the remaining media. Mix well to separate clumps, but be Gentle with the cells and avoid bubbles.
- g. Remove a small drop with a Pastuer pipet and count cells using the hemacytometer.

Histological assessment

The colorimetric method, called CellTiter 96® AQueous One Solution Cell Proliferation Assay, was used for determining the number of viable cells in proliferation. The CellTiter 96® AQueous reagent contains a novel tetrazolium compound [3-(4,5-dimethylthiazol-2-yl)-5-(3-carboxymethoxyphenyl)-2-(4-sulfophenyl)-2H-tetrazolium, inner salt; MTS(a)] and an electron coupling reagent (phenazine ethosulfate; PES). PES has enhanced chemical stability, which allows it to be combined with MTS to form a stable solution. The MTS tetrazolium compound is bio-reduced by cells into a colored formazan product that is soluble in tissue culture medium. This conversion is presumably accomplished by NADPH or NADH (NADPH and NADH are reducing agents that supply hydrogen atoms or electrons in chemical reactions) produced by

dehydrogenase enzymes in metabolically active cells. Assays are performed by adding a small amount of the CellTiter 96® AQueous One Solution Reagent directly to culture wells, incubating for 1-4 hours and then recording the absorbance at 490nm with a 96-well plate reader.

The quantity of formazan product as measured by the absorbance at 490nm is directly proportional to the number of living cells in culture. Because the MTS formazan product is soluble in cell culture medium, the CellTiter 96® AQueous One Solution Assay requires fewer steps than procedures that use tetrazolium compounds such as MTT or INT. The formazan product of MTT reduction is a crystalline precipitate that requires an additional step in the procedure to dissolve the crystals before recording absorbance readings at 570nm.

General protocol:

- a. Thaw the CellTiter 96® AQueous One Solution Reagent. It should take approximately 90 minutes at room temperature on the bench top, or 10 minutes in a water bath at 37°C, to completely thaw the 20ml size.
- b. Pipet 20µl of CellTiter 96® AQueous One Solution Reagent into each well of the 96-well assay plate containing the samples in 100µl of culture medium.

Note: Repeating pipettes, digital pipettes or multi-channel pipettes are used for convenient delivery of uniform volumes of CellTiter 96® AQueous One Solution Reagent to the 96-well plate.

- c. Incubate the plate for 1.4 hours at 37°C in a humidified, 5% CO₂ atmosphere.

Note: To measure the amount of soluble formazan produced by cellular reduction of the MTS, proceed immediately to Step 4. Alternatively, to measure the absorbance later, add 25µl of 10% SDS to each well to stop the reaction. Store

SDS-treated plates protected from light in a humidified chamber at room temperature for up to 18 hours. Proceed to Step 4.

- d. Record the absorbance at 490nm using a 96-well plate reader.

APPENDIX C

FORMULAS AND PARAMETERS APPEARED IN AFM IMAGES

$$Z_i = f(x, y)$$

$$Z_0 = \frac{1}{Q} \int_{Y_T}^{Y_B} \int_{X_L}^{X_R} f(x, y) dx dy$$

$$R_a = \frac{1}{Q} \int_{Y_T}^{Y_B} \int_{X_L}^{X_R} |f(x, y) - Z_0| dx dy$$

$$R_{ms} = \left[\frac{1}{Q} \int_{Y_T}^{Y_B} \int_{X_L}^{X_R} \{f(x, y) - Z_0\}^2 dx dy \right]^{1/2}$$

$$R_z = \frac{\sum_{i=1}^N (Z_{i,p} - Z_{i,v})}{N}$$

(R_a) : average plane roughness

(R_{ms}) : square mean plane roughness

(R_z) : 10 point mean plane roughness

Q : the area of the specific plane

$Z_i = f(x, y)$: the high of the plane

Z_0 : the mean high of the specific plane

BIBLIOGRAPHY

1. Jason S. Belkas, Molly S. Shoichet and Rajiv Midha, *Peripheral nerve regeneration through guidance tubes*, **Neurological Research**, 2004, Volume 26, P151- 160
2. Millesi H, Ganglberger J, Berger A., *Erfahrungen mit der Mikrochirurgie peripherer Nerven*. **Chir. Plast.** 1967, 3: 47
3. Evans GR, Brandt K, Niederbichler AD, Chauvin P, Herrman S, et al., *Clinical long-term in vivo evaluation of poly(L-lactic acid) porous conduits for peripheral nerve regeneration*. **J. Biomater. Sci. Polym. Ed.**, 2000, 11: 869- 78
4. Evans GR, Brandt K, Katz S, Chauvin P, Otto L, et al. *Bioactive poly (L-lactic acid) conduits seeded with Schwann cells for peripheral nerve regeneration*. **Biomaterials**, 23: 841- 48
5. Molander H, Olsson Y, Engkvist O, Bowald S, Eriksson I., *Regeneration of peripheral nerve through a polyglactin tube*. **Muscle Nerve**, 1992, 5: 54- 57
6. den Dunnen WF, Meek MF, Grijpma DW, Robinson PH, Schakenraad JM., *In vivo and in vitro degradation of poly[(50)/(50) ((85)/(15)(L)/(D))LA/epsilon-CL], and the implications for the use in nerve reconstruction*. **J. Biomed. Mater. Res.** 1998, 51: 575- 85
7. Valero-Cabre A, Tsironis K, Skouras E, Perego G, Navarro X, et al., *Superior muscle reinnervation after autologous nerve graft or poly-L-lactide-epsilon- caprolactone (PLC) tube implantation in comparison to silicone tube repair*. **J. Neurosci. Res.** 2001, 63: 214- 23
8. Christine E. Schmidt, Venkatram R. Shastri, Joseph P. Vacati, and Robert Langer., *Stimulation of neurite outgrowth using an electrically conducting polymer.*, **Proc. Natl. Acad. Sci.** 1997, 94: 8948- 8953
9. Kishida A, Iwata H, Tamada Y, Ikada Y., *Cell behaviour on polymer surfaces grafted with non-ionic and ionic monomers*. **Biomaterials**, 1991, 12: 786- 92
10. Lee JH, Jung HW, Kang IK, Lee HB. *Cell behaviour on polymer surfaces with different functional groups.*, **Biomaterials**, 1994, 15: 705- 11
11. Bin L., Yuexia M., Shu W., Peter M. M. *A technique for preparing protein gradients on polymeric surfaces: effects on PC12 pheochromocytoma cells*. **Biomaterials**, 2005, 26: 1487- 95

12. Bin L., Yuexia M., Shu W., Peter M. M., *Influence of carboxyl group on neuron cell attachment and differentiation behavior: Gradient-guided neurite outgrowth.*, **Biomaterials**, 2005, 26: 4956- 63
13. Keselowsky, B. G., Collard, D. M., Garcia, A. J., *Surface chemistry modulates fibronectin conformation and directs integrin binding and specificity to control cell adhesion.*, **J. Biomed. Mater. Res.** **66A**, 247- 259
14. Keselowsky, B. G., Collard, D. M., Garcia, A. J., *Integrin binding specificity regulates biomaterials surface chemistry effects on cell differentiation.* **PNAS** **17**, 102, 5953- 57
15. Kacy G. Marra, *Biodegradable Polymers and Microspheres for Tissue Engineered Therapies*, **Bone Tissue Engineering**. 149- 165.
16. David J. Bryan, Jin Bo Tang, Stephen A Doherty, David D Hile, Debra J Trantolo, Donald L Wise and Ian C Summerhayes, *Enhanced peripheral nerve regeneration through a poled bioresorbable poly(lactic- co- glycolic acid) guidance channel*, **J Neural Eng.**, **1**, 2004, 91- 98.
17. David J. Bryan, Antonia H. Holway, Kai-Kai Wang, Alyson E. Silva, Debra J. Trantolo, Donald Wise and Ian C. Summerhayes, *Influence of Glial Growth Factor Schwann cells in a Bioresorbable Guidance Channel on Peripheral Nerve Regeneration*, **Tissue Engineering**, **6**, 2000, 129- 138
18. Y. Zhu, C. Gao, X. Liu, J. Shen (2002). *Surface modification of polycaprotone membrane via aminolysis and biomacromolecule immobilization for promoting cytocompatibility of human endothelial cells.* **Biomacromolecules**, 2002, 3: 1312- 1319
19. Christine E. Schmidt and Jennie Baier Leach, *Neural Tissue Engineering: Strategies For Repair and Regeneration.*, **Annu. Rev. Biomed. Eng.**, 2003, 5: 293- 347
20. David J. Bryan, Jin Bo Tang, Stephen A. Doherty, David D. Hile, Debra J. Trantolo, Donald L. Wise and Ian C. Summerhayes, *Enhanced peripheral nerve regeneration through a poled bioresorbable poly (lactic-co-glycolic acid) guidance channel*, **J. Neural Eng.** **1**, 2004, 91– 98
21. Aebischer, P., Valentini, R. F., Dario, P., Domenici, C. and Galletti, P. M., *Piezoelectric guidance channels enhance regeneration in the mouse sciatic nerve after axotomy.* **Brain. Res.** 1987, 436: 165- 168
22. Valentini RF, Vargo TG, Gardella Jr. JA, Aebischer P., *Electrically charged polymeric substrates enhance nerve fibre outgrowth in vitro.* **Biomaterials**, 1992, 13: 183- 190.
23. Valentini RF, Sabatini AM, Dario P, Aebischer P., *Polymer electret guidance channels enhance peripheral nerve regeneration in mice.* **Brain. Res.**, 1989, 480: 300- 304.

24. Yabin Zhu, Changyou Gao, Xingyu Liu, Tao He and Jiacong Shen, *Immobilization of Biomacromolecules onto Aminolyzed Poly(L-lactic acid) toward Acceleration of Endothelium Regeneration.*, **Tissue Engineering**, 2004, 10: 53- 61
25. Valentini RF, Vargo TG, Gardella JA Jr., Aebischer P. , *Patterned neuronal attachment and outgrowth on surface modified, electrically charged fluoropolymer substrates.* **J. Biomater. Sci. Polym. Ed.**, 1993, 5: 13- 36
26. Soldani G, Varelli G, Minnocci A, Dario P., *Manufacturing and microscopical characterization of polyurethane nerve guidance channel featuring a highly smooth internal surface.* **Biomaterials**, 1998, 19: 1919- 1924
27. Nicoli Aldini N, Fini M, Rocca M, Giavaresi G, Giardino R., *Guided regeneration with restorable conduits in experimental peripheral nerve injuries.*, **Int. Orthop.** 2000, 24: 121- 125
28. Dalton PD, Flynn L, and Shoichet MS, *Manufacture of poly (2-hydroxyethyl methacrylate-co- methyl methacrylate) hydrogeltubes for use as nerve guidance channels.* **Biomaterials**, 2002, 23: 3843- 3851
29. Young RC, Wiberg M, Terenghi G., *Poly- 3- hydroxybutyrate (PHB): a restorable conduit for long-gap repair in peripheral nerves.*, **Br. J. Plast.**, 2002, 55: 235- 240
30. Hadlock T, Elisseeff J, Langer R, Vacanti J, Cheney M., *A tissue-engineered conduit for peripheral nerve repair.*, **Arch. Otolaryngol. Head Neck Surg.**, 1998, 124 :1081- 1086
31. Tong XJ, Hirai K, Shimada H, MizutaniY, and Izumi T. *Sciatic nerve regeneration navigated by laminin-fibronectin double coated biodegradable collagen grafts in rats.* **Brain Res.**, 1994, 663: 155- 162
32. Lundborg G, Dahlin L, Dohi D, Kanje M, and Terada N. *A new type of “bioarti- ficial” nerve graft for bridging extended defects in nerves.*, **J. Hand Surg.**, 1997, 22: 299- 303
33. Matsumoto K, Ohnishi K, Kiyotani T, Sekine T, and Ueda H., *Peripheral nerve regeneration across an 80-mm gap bridged by a polyglycolic acid (PGA)- collagen tube filled with laminin- coated collagen fibers: a histological and electrophysiological evaluation of regenerated nerves.* **Brain Res.**, 2000, 868: 315- 328
34. Toba T, Nakamura T, Shimizu Y, Matsumoto K, and Ohnishi K, *Regeneration of canine peroneal nerve with the use of a polyglycolic acid-collagen tube filled with laminin-soaked collagen sponge: a comparative study of collagen sponge and collagen fibers as filling materials for nerve conduits.*, **J. Biomed. Mater. Res.**, 2001, 58: 622- 630
35. Ceballos D, Navarro X, Dubey N, Wendelschafer-Crabb G, and Kennedy WR., *Magnetically aligned collagen gel filling a collagen nerve guide improves peripheral nerve regeneration.*, **Exp. Neurol.**, 1999, 158: 290- 300

36. Dubey N, Letourneau PC, and Tranquillo RT., *Guided neurite elongation and Schwann cell invasion into magnetically aligned collagen in simulated peripheral nerve regeneration.* **Exp. Neurol.**, 1999, 158: 338- 350
37. Dubey N, Letourneau PC and Tranquillo RT. *Neuronal contact guidance in magnetically aligned fibrin gels: effect of variation in gel mechano-structural properties.*, **Biomaterials**, 2001, 22: 1065- 1075
38. Hadlock T, Sundback C, Hunter D, Cheney M, and Vacanti JP. *A polymer foam conduit seeded with Schwann cells promotes guided peripheral nerve regeneration.*, **Tissue Eng.**, 2000, 6: 119- 127
39. Sundback C, Hadlock T, Cheney M, and Vacanti J., *Manufacture of porous polymer nerve conduits by a novel lowpressure injection molding process.*, **Biomaterials**, 2003, 24: 819- 830
40. Teng YD, Lavik EB, Qu X, Park KI, and Ourednik J., *Functional recovery following traumatic spinal cord injury mediated by a unique polymer scaffold seeded with neural stem cells.* **Proc. Natl. Acad. Sci. USA**, 2002, 99: 3024- 3029
41. Friedman JA, Windebank AJ, Moore MJ, Spinner RJ, and Currier BL., *Biodegradable polymer grafts for surgical repair of the injured spinal cord.* **Neurosurgery**, 2002, 51: 742- 751
42. M. Charbonnier, M. Romand, M. Alami and Tran Minh Duc, *Surface modification of poly(tetrafluoroethylene) in RF glow-discharge (H₂, He, Ar, O₂, N₂, NH₃) plasmas. XPS characterization*, **Polymer Surface Modification: Relevance to Adhesion, Vol. 2**, Mittal, K. L., ed., 2000, 3- 28, VSP.
43. S. Yuan, G. Szakalas- Gratzl, G., N. P. Ziats, D. W. Joacobsen, K. Kottke- Marchant and R. E. Marchant, *Immobilization of High-affinity Heparin Oligosaccharides to Radiofrequency Plasma- Modified Polyethylene*, **J. Biomed. Mat. Res.**, 1993, 27: 811.
44. M. S. Sheu, A. S. Hoffman and J. Feijen, *A Glow- Discharge Treatment to Immobilize Poly (ethylene Oxide)/Poly(propylene Oxide) Surfactants for Wettable and Non- fouling Biomaterials.*, **J. Adhesion Sci. & Tech.**, 1992, 6: 995.
45. M. S. Sheu, D. M. Hudson and I. H. Loh, *Biomaterials Surface Modification Using Plasma Gas Discharge Processes*, **Encyclopedic Handbook of Biomaterials and Bioengineering, Part A. Materials**, edited by D. L. Wise, D. J. Trantolo, D. E. Altobelli, M. J. Yaszemski, J. D. Gresser and E. R. Schwartz, Marcer Dekker, NewYork, 1995, 1: 865- 894.
46. Miller C, Shanks H, Witt A, Rutkowski G and Mallapragada S., *Oriented Schwann cell growth on micropatterned biodegradable polymer substrates.* **Biomaterials**, 2001, 22: 1263- 1269.

47. Ishaug-Riley SL, Okun LE, Prado G, Applegate MA. and Ratcliffe A., *Human articular chondrocyte adhesion and proliferation on synthetic biodegradable polymer films*. **Biomaterials**, 1999, 20: 2245- 2256.
48. Calvert J. W., Marra K. G., Cook L, Kumta P. N., DiMilla P. A., and Weiss L. E., *Characterization of osteoblast-like behaviour of cultured bone marrow stromal cells on various polymer surfaces*. **J. Biomed. Mater. Res.**, 2000, 52: 279- 284.
49. Tang Z. G., Black R. A., Curran J. M., Hunt J. A., Rhodes N. P., and Williams D. F., *Surface properties and biocompatibility of solvent-cast poly[e-caprolactone] films*. **Biomaterials**, 2004, 25: 4741- 4748
50. Young T., *An Essay on the Cohesion of Fluids*, **Philosophical Transactions of the Royal Society of London**, 1805, 95: 65- 87.
51. Xu F. T., Street S. C., and Barnard J. A., *Coverage Dependent Evolution of Two-Dimensional Dendrimer/Mica Domain Patterns.*, **J. Phys. Chem. B**, 2003, 5- 8
52. Xu F. T., Street S. C., and Barnard J. A., *Pattern Formation in Aerosol-Deposited Dendrimer Films.*, **Langmuir**, 2003, 19: 3066- 3070
53. Sergey Rozhok, Clifton K. F. Shen, Pey-Lih H. Littler, Zhifang Fan, Chang Liu, Chad A. Mirkin, and Richard C. Holz, *Methods for Fabricating Microarrays of Motile Bacteria.*, **small**, 2005, 4: 445 –451
54. Hyo-Sok Ahn, Pham Duc Cuong, Sangkwon Park, Yong-Wook Kim, and Jong-Choo Lim, *Effect of molecular structure of self-assembled monolayers on their tribological behaviors in nano- and microscale.*, **Wear**, 2003, 255: 819– 825
55. Xiao G., *Solvent-induced changes on corona-discharge-treated polyolefin surfaces probed by contact angle measurement*. **J Colloid Interface Sci.**, 1995, 4: 171- 200.
56. Otsuka H, Nagasaki Y, and Kataoka K., *Dynamic wettability study on the functionalised PEGylated layer on a polylactide surface constructed by coating of aldehyde- ended poly (ethylene glycol) (PEG)/ polylactide (PLA) block copolymer*. **Sci Technol Adv Mater.**, 2000, 9: 21– 29.
57. Khorasani M. T., Mirzadeh H. and Sammes P. G., *Laser induced surface modification of polydimethylsiloxane as a super-hydrophobic material.*, **Radiat. Phys. Chem.** 1996, 47: 881- 888.
58. Khorasani M. T., Mirzadeh H and Sammes P. G., *Laser surface modification of polymers to improve biocompatibility: HEMA grafted PDMS, in vitro assay- III.*, **Radiat. Phys. Chem.**, 1999, 55: 685- 689.

59. K. S. Tiaw, S. W. Goha, M. Hong, Z. Wangb, B. Lan and S. H. Teoh, *Laser surface modification of poly (ε-caprolactone) (PCL) membrane for tissue engineering applications.*, **Biomaterials**, 2005, 26: 763- 769
60. Lee J. H., Juang H. W., Kang I. K., Lee H. B., *Cell behaviour on polymer surfaces with different functional groups.*, **Biomaterials**, 1994, 15: 705- 711
61. Bet M. R., Goissis G., Vargas S., and Selistre-de-Araujo H. S., *Cell adhesion and cytotoxicity studies over polyanionic collagen surfaces with variable negative charge and wettability.* **Biomaterials**, 2003, 24: 33- 41
62. Ya Cao and Huilin Li, *Effect of Temperature and pH Values on Aggregation Behavior of Polymeric Surfactants in Aqueous Solution*, **J. of Applied Polymer Science**, 2005, 98: 945- 949
63. Valfredo A. Lemos, Juracir S. Santos and Patrícia X. Baliza, *Me-BTABr Reagent in Cloud Point Extraction for Spectrometric Determination of Copper in Water Samples*, **J. Braz. Chem. Soc.**, 2006, 17: No. 1, 30- 35.
64. Buddy D. Ratner, Allan S. Hoffman and Frederick J. Schoen, *Biomaterials Science: An introduction to Materials in Medicine* 2nd Edition, 2004, Elsevier Inc., p. 67- 80
65. Enchanted learning,
<http://www.enchantedlearning.com/subjects/anatomy/brain/Neuron.shtml>
66. Cheol Park, Zoubeida Ounaies, and Kristopher E. Wise, *In Situ Poling and Imidization of Amorphous Piezoelectric Polyimides*, NASA/CR- 2002- 211948, ICASE Report No. 2002- 39